

**Deliverable D6.5: *Mid-term report on scientific outputs from
EUROCHAMP-2020***

**Author(s): *Christian George, Jean-François Doussin (CNRS), all
partners***

Work package no	6
Deliverable no.	6.5
Lead beneficiary	CNRS
Deliverable type	<input checked="" type="checkbox"/> R (document, report) <input type="checkbox"/> DEC (websites, patent filings, videos, etc.) <input type="checkbox"/> OTHER: please specify
Dissemination level	<input checked="" type="checkbox"/> PU (public) <input type="checkbox"/> CO (confidential, only for members of the Consortium, including the Commission)
Estimated delivery date	M22
Actual delivery date	08/10/18
Version	1
Comments	<p>The content of this deliverable has largely been reported by the consortium through the 1st periodic report, submitted in month 20. Indeed, in the technical part, all scientific activities and the related achievements have been described in detail. This document collects the descriptions of the periodic report about the most science-focused Work Packages i.e., WP 2, 7, 9, 10 and 11. The focus on the impact of such activities on the research world and on the wide society, is underlined in the very beginning of the document.</p>

Table of content

Main scientific Achievements	3
Scientific achievements impacting research communities	3
Scientific achievements related to technology and innovation	4
Scientific achievements impacting societal services	5
Scientific Outputs	8
Scientific achievements of the EUROCHAMP-2020 project by work-packages	9
Work Package 2: Atmospheric simulation chamber characterization and interoperability (NA2) 9	
Work Package 7: Physical access to the chambers (TNA1).....	13
Work Package 10: Evolution of atmospheric simulation chamber infrastructure to address broader scientific and societal needs (JRA1)	18
Work Package 11: Model development and evaluation to enhance and optimally exploit the chamber infrastructure (JRA2)	45
Annex 1: details about scientific outreach activities	63

Main scientific Achievements

The largest uncertainties in our current knowledge on atmospheric processes and their impact on air quality and climate change are associated with complex feedback mechanisms in the Earth System. Understanding and quantifying feedback mechanisms, that are just becoming measurable, will only be possible through a synergistic approach which combines atmospheric observations, detailed simulation experiments and modelling. Simulation chambers are the best research tools for obtaining a quantitative understanding of physic-chemical transformations in the atmosphere and provide a lot of the parameters used in atmospheric models.

Scientific achievements impacting research communities

EUROCHAMP-2020 offers an integrated suite of state-of-the-art simulation chambers which provides unprecedented opportunities for atmospheric scientists to perform experiments that address important questions on air quality and climate research.

In parallel, EUROCHAMP-2020 incorporates a range of chamber platforms that are both diverse and highly versatile. EUROCHAMP-2020 is thus a basis for engaging the wider scientific community in more trans-disciplinary approaches to better understand the impacts of atmospheric processes in an integrated manner. This opens up to exciting opportunities for researchers working in a range of areas such as health and cultural heritage, as well as in the broader environmental domain, to seek and provide solutions for key scientific and societal problems.

While being at the first third of the project, some of the joint research activities performed within WP10 have already had some impact on the research community.

For example, the investigations performed at **CNRS-LISA** of the variability of the mineral dust long wave (LW) refractive index as a function of its mineralogical composition and size distribution have been published in Di Biagio et al. (2017). The available data have allowed other groups worldwide to improve the **dust aerosol radiative forcing** (Meloni et al., 2018; Li and Sokolik, 2018; Song et al, 2018) and also to **improve the satellite retrieval** of desert dust plume (Liuzzi et al., 2017; Xu et al., 2017; Banks et al., 2018).

Within the TNA project AIDA-002-2017 at the **AIDA** chamber, the INUIT 09 campaign “Ice nucleation of mineral dust” allowed the assessment of the role of mineralogy in the ice nucleating (IN) efficiency of several natural desert dust samples from Africa. This chamber campaign is bringing new important insights in a potentially very important climatic feedback linking the extension of desert area and the resulting increase of the atmospheric dust load to the cloud cover and water cycle perturbation.

A combination of TNA research projects took advantage of the Roland von Glasow Air-Sea-Ice Chamber (**RvG-ASIC**) unique features – being the only large-scale chamber of its kind – to address the issue of so-called Arctic amplification of global warming. *RvG-ASIC-001-2017* investigated how temperature changes in the Arctic may quickly enhance methane emissions, due to large natural sources. *RvG-ASIC-002-2017* aimed to provide novel quantitative data on poorly characterized micro-ecosystems with potential global significance and provided also a

mechanistic understanding of colonization processes through various stages of sea-ice. *RvG-ASIC-003-2017* is addressing the issue of retreating Arctic sea-ice and its impact on the Earth's energy balance.

On a more methodological point of view, the characterization of particles' wall losses under various electrostatic states of Teflon chambers performed by **FORTH** has not only led to more robust protocols that can now be shared with the global community, but it also shines a new light on the secondary aerosol yield studies performed in Teflon chambers which are the most common type worldwide. Published in Wang et al. (2018) this work will be certain to have a strong impact on the chamber methodology applied far beyond the EUROCHAMP-2020 consortium.

Capacity development constitutes one of the strategic priorities of EUROCHAMP-2020. With the combination of the training session held in January 2017 at **OGTAC CC** with the inter-laboratory comparison (ILC) organised three months later, 18 international users (from Germany, France, Spain, Poland, Ireland, Romania and Denmark) coming from both the chamber and field measurement communities were trained with advanced analytical techniques for the analysis of atmospherically relevant particulate products at the molecular level, for a high level of QA/QC. With this first session (that will be repeated during RP2) more than 10 different groups across Europe were taught how to measure highly oxygenated components and atmospheric tracers. They were hence driven to optimally use the available instrumentation at their institutes for the greatest benefit of future observations including both field campaigns and chamber experiments.

The strong development of the EUROCHAMP DC during RP1 is notable not only for the services provided to the users, but also the concept of the DC itself. The DC is making a step further now as EUROCHAMP-2020 has committed during RP1 in the ENVRI-FAIR within ACTRIS-ESFRI. This strategic project will ensure that a clear and coherent catalogue of services will be proposed by ENVRI as part of their contribution to European Open Science Cloud. It is expected that developments towards higher maturity data and service levels will be addressed within this project. This will ensure that data from measurements performed for ACTRIS-ERIC at Exploratory Platforms are made available to users through the ACTRIS-ERIC Data Centre (DC) and has certainly an impact on the research communities.

The development of the EUROCHAMP DC has inspired similar initiatives beyond Europe. The presentation of our project during the ACM meeting in Davis, California has triggered a similar project in the US. The *NSF ICARUS* proposal was prepared in 2017 to build a comparable data centre for the US community of simulation chambers. It was supported by EUROCHAMP and has been eventually funded. It is now developing a similar concept in good coordination with EUROCHAMP (Spyros Pandis as a member of the two consortia acting as a link) and discussion are on-going for the sharing of data formats and routines.

Scientific achievements related to technology and innovation

EUROCHAMP-2020 has devoted substantial efforts towards innovation and transfer of knowledge to SMEs in WP4 but also through the work performed within WP7, WP8 and WP10.

During RP1, **KIT** has developed, in close collaboration with the **NCAS-Leeds**, a new and innovative mobile instrument for fully automated atmospheric measurements of ice nucleating particle (INP) concentrations and laboratory studies of ice nucleation processes. This new instrument called PINE (Portable Ice Nucleation Experiment) will be the first instrument of its kind for fully-automated long term INP measurements at high sensitivity and time resolution. A commercial version of PINE is developed together with Bilfinger Noell GmbH and will be available in early 2019. This accomplishment demonstrates not only the impact of EUROCHAMP-2020 on the private sector but also its contribution to the current atmospheric monitoring system. It also demonstrates how the future ACTRIS-ERIC, integrating both ACTRIS-2 and EUROCHAMP, will have the potential for an end-to-end control of the atmospheric short-lived species monitoring activities.

The work carried within TNAs during RP1 has also contributed to the development of new technologies. For example, within *PACS-C3-003-2018* an advanced mass spectrometric method developed by the Ionicon Analytik GmbH, a SME located in Innsbruck, Austria was used together with two state-of-the-art instruments developed at **PSI** to study the chemical composition of SOA. In addition to the current state-of-the-art high resolution time-of-flight aerosol mass spectrometer (HR-TOF-AMS), the Paul Scherrer Institute has deployed their recently developed extractive electro-spray ionization TOF-MS (EESI-TOF) complemented by Ionicon's modular "Chemical Analysis of Aerosol Online" (CHARON) particle inlet, coupled to a new-generation proton-transfer-reaction time-of-flight mass spectrometer (PTR-TOF 6000 X2).

During RP1, *Blue Industry and Science*, a French SME involved in advanced laser spectrometers for trace gas monitoring has been advised by our *Innovation Platform* (WP4) and guided among the available facilities until when eventually a dedicated TNA has been organized at **EUPHORE** to better characterize their tuneable diode laser trace gas analysers.

Finally, during the preparation phase of this proposal, a list of more than 40 potential industry users was prepared leading to the involvement of 19 European SMEs and companies as potential Associated Partners of EUROCHAMP-2020 and showing the strong link between the simulation chamber community and the private sector. During RP1, 7 of them have completed the associated partnership process, with additional ones being in contact or applied for TNA.

Scientific achievements impacting societal services

EUROCHAMP-2020 continues to liaise with other relevant actors (space agencies, environmental agencies, research networks) both in Europe and worldwide (WP5). Because the work carried out within EUROCHAMP-2020 concern processes and properties within the atmosphere, the EUROCHAMP-2020 progress is relevant not only for Europe but also for other regions in the world.

As the public debate on the impact of car emissions on air quality and even on climate change drivers is strong over the whole society, many EUROCHAMP-2020 partners (**UMAN, PSI, UEF, CNRS-LISA**) have started the adaptation of simulation chambers protocols to enable the robust study of the adverse effects of these sources. An example reported within WP10, the

NCAS-UMAN chamber has been coupled to a light duty diesel engine. Using this setup, a comprehensive set of experiments has been conducted at realistic engine speed and load conditions and under a range of dilution ratios. The use of the chamber proved effective at enabling measurements of diesel exhaust using long sample times, even during unstable engine conditions. A further advantage is the effect of a wide range of exhaust dilution on the particles and gases can be studied; published data on the resulting variability in VOC and IVOC compounds across conditions is available.

Research projects through physical access to simulation chambers (WP7), resulted in improvements of the general understanding of how air pollution processes and climate change drivers contribute to the general well-being and to the economy, by reducing financial and social risks and by creating new opportunities, as many economic sectors and public and private activities are affected by these phenomena. Improving the quantification of atmospheric compounds transformation and properties, strengthens the accuracy of air pollution forecasts and climate predictions; therefore, it benefits the society, in its economic and societal sectors. Specifically, some TNA projects are particularly remarkable:

QUAREC-002-2017: This TNA project carried out during RP1 aimed at investigating the atmospheric fate of halogenated substances that are massively involved in the CFC replacement protocols. The kinetics studies performed at different temperatures allows us to define the lifetime of these compounds and therefore the extent of their impacts. The product analysis opens the way to the assessment of the toxicological impacts of these species in all the biosphere compartments.

A series of TNAs focusing on the adverse effects of wood burning and coal on air quality were conducted during RP1. *ILMARI-003-2017* is a multidisciplinary research project concerning the variations in the health impact of aged mixtures of pollutants. Lung cells were exposed to emissions from logwood fire and from a gasoline generator (gas and particulate matters). In parallel, *PACS-C3-002-2018* has focused on understanding secondary organic aerosol formation from biomass burning and coal combustion. Coal- and wood-burning aerosols revealed complex composition and their chemical transformation (aging) trajectories during photo-oxidation were visualized. These studies are of importance as they will eventually lead to improved air quality forecasts and sources assessments in Northern European regions and Alpine valleys, where these combustion processes are often important.

Other impacts on societal services are linked to support of the manufacturing industry, the developers, the instrument integrators and the societal services that require operational instruments that can be developed/characterized in chambers. Some of them needs also diagnostic about the impact of their technologies on the atmospheric environments (adverse effects, pollutant removal efficiencies, etc.).

References

Banks, J. R., Schepanski, K., Heinold, B., Hünerbein, A., and Brindley, H. E.: The influence of dust optical properties on the colour of simulated MSG-SEVIRI Desert Dust infrared imagery, *Atmos. Chem. Phys.*, 18, 9681-9703, , 2018.

Di Biagio C., P. Formenti, Y. Balkanski, L. Caponi, M. Cazaunau, E. Pangui, E. Journet, S. Nowak, S. C., M. O. Andreae, K. Kandler, T. Saeed, S. Piketh, D. Seibert, E. Williams, and J.-F. Doussin. Global scale variability of the mineral dust longwave

refractive index: a new dataset of in situ measurements for climate modelling and remote sensing, *Atmospheric Chemistry and Physics*, 17, 3, pp: 1901-1929; 2017a.

Li, L., & Sokolik, I. N. (2018). The dust direct radiative impact and its sensitivity to the land surface state and key minerals in the WRF-Chem-DuMo model: A case study of dust storms in Central Asia. *Journal of Geophysical Research: Atmospheres*, 123, 4564–4582.

Liuzzi, G., G. Masiello, C. Serio, D. Meloni, C. Di Biagio, and P. Formenti, Consistency of dimensional distributions and refractive indices of desert dust measured over Lampedusa with IASI radiances, *Atmos. Meas. Tech.*, 10, 599-615, d, 2017.

Meloni, D., di Sarra, A., Brogniez, G., Denjean, C., De Silvestri, L., Di Iorio, T., Formenti, P., Gómez-Amo, J. L., Gröbner, J., Kouremeti, N., Liuzzi, G., Mallet, M., Pace, G., and Sferlazzo, D. M.: Determining the infrared radiative effects of Saharan dust: a radiative transfer modelling study based on vertically resolved measurements at Lampedusa, *Atmos. Chem. Phys.*, 18, 4377-4401, 2018.

Song, Q., Zhang, Z., Yu, H., Kato, S., Yang, P., Colarco, P., Remer, L. A., and Ryder, C. L.: Toward an Observation-Based Estimate of Dust Net Radiative Effects in Tropical North Atlantic Through Integrating Satellite Observations and In Situ Measurements of Dust Properties, *Atmos. Chem. Phys. Discuss.*, in review, 2018.

Wang N., S. D. Jorga, J. R. Pierce, N. M. Donahue, and S. N. Pandis (2018) Particle wall-loss correction methods in smog chamber experiments, *Atmos. Meas. Tech.*, submitted for publication.

Xu, X., J. Wang, Y. Wang, D. K. Henze, L. Zhang, G. A. Grell, S. A. McKeen, and B. A. Wielicki (2017), Sense size-dependent dust loading and emission from space using reflected solar and infrared spectral measurements: An observation system simulation experiment, *J. Geophys. Res. Atmos.*, 122, 8233–8254, 2017.

Scientific Outputs

<i>Typology</i>	<i>2017</i>	<i>2018</i>
Scientific articles	17	13
Oral in an international conference	10	22
Oral in a national conference	6	12
Poster in an international conference	12	13
Poster in a national conference	3	9
PhD thesis	3 still in progress	
Master thesis	0	3

Scientific achievements of the EUROCHAMP-2020 project by work-packages

Work Package 2: Atmospheric simulation chamber characterization and interoperability (NA2)

The main objective of WP2 is focused on maintaining and improving the quality, robustness and comparability of the experiments carried out in the simulation chambers through high level characterization of chamber capabilities, quality assessment, and experiment inter-comparisons.

WP2 activities have been designed to establish the basis for improving interoperability of the chambers. Even if this goal may sound rather technical, important scientific achievements are underlying much progress in this field.

The main tasks carried out within WP2 during the first 18 months are described below.

Directory of each chamber's detailed characteristics

Collecting, maintaining and disseminating the detailed characteristics of the EUROCHAMP-2020 simulation chamber is a very important activities and it has been achieved via the project website (<http://www.eurochamp.org/Facilities/SimulationChambers.asp>).

Overview of chamber-dependent parameters affecting chemistry

Determination of chamber dependent parameters affecting radical chemistry (2.1.2)

Photolysis frequencies

Understanding how the fundamental properties of specific chambers influence their scientific results is crucial in order to achieve a better interpretation of the measurements and data inter-comparability between different chambers, providing enhanced datasets for use by mechanism developers and modellers.

This is why *in-situ* wavelength dependent chamber irradiance and actinic flux data have/are being determined for all chambers. This is being carried out using spectral radiometers (c.a. 290 – 800 nm range). Example sets of radiation measurements from the UAIC *ESC-Q-UAIC chamber*, the NCAS-UEA *RvG-ASIC* and the *CESAM* chambers are shown in Figure 1.2.2-2.

The photolysis frequency of NO₂, J_{NO₂}, is a very important parameter both because of its atmospheric interest and because it provides a total integrated measure of UV-intensity and as a useful comparison to the wavelength dependent irradiance/actinic flux point measurements. Following a standard protocol (see. Table 1.2.2-1 and WP3 report). Chemical actinometry experiments have hence been carried out in each indoor chamber in order to give access to this parameter and to allow robust scaling of the lamp emission spectra. J_{NO₂} measurements range from $1.17 \times 10^{-3} \text{ s}^{-1}$ (*ILMARI@UEF*), $2.9 \times 10^{-3} \text{ s}^{-1}$ (*CERNESIM@IASI*), $6.4 \times 10^{-3} \text{ s}^{-1}$ (*CESAM@CNRS-LISA*) to $9.8 \times 10^{-3} \text{ s}^{-1}$ (*ASC@FORTH*).

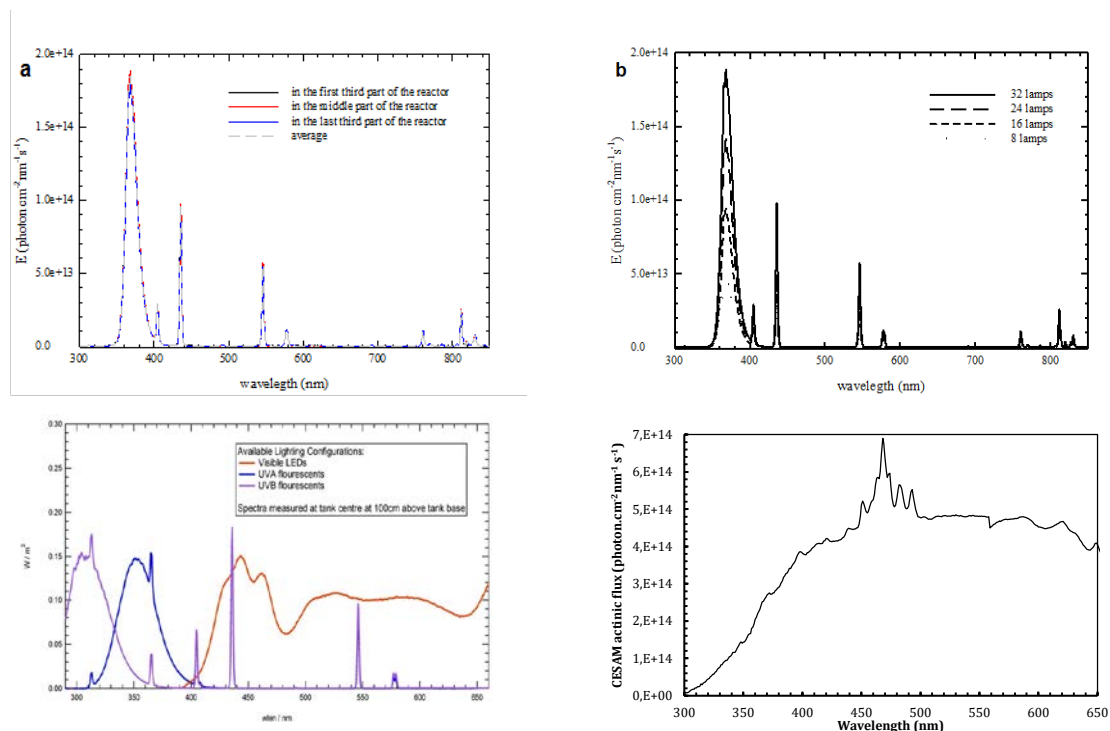


Figure 1.2.2-1 Top - Irradiation spectra in the ESC-Q-UAIC chamber: a – for all lamps at different points in the reactor; b - for a limited number of lamps. Bottom - light field characterization of the NCAS-UEA RvG-ASIC facility (1 m above the tank base in centre, full illumination). Both using LICOR LI-1800 spectral radiometer (CNRS-LISA)

New chamber characterization for the gas-phase studies:

The first objective for the newly developed Environmental Simulation Chamber made of Quartz from the “Alexandru Ioan Cuza” University of Iasi, Romania (*ESC-Q-UAIC*) was to validate the chamber for atmospheric gas-kinetic experiments. The first set of experiments was focused on the OH kinetics with some aromatic compounds (Figure 1.2.2-3) (by relative kinetic technique) and the second one on the determination of the gas-phase absorption cross sections of selected aromatic hydrocarbons in the IR spectral ranges. The preliminary average rate coefficients showed good agreement with literature values (Calvert et al., 2002).

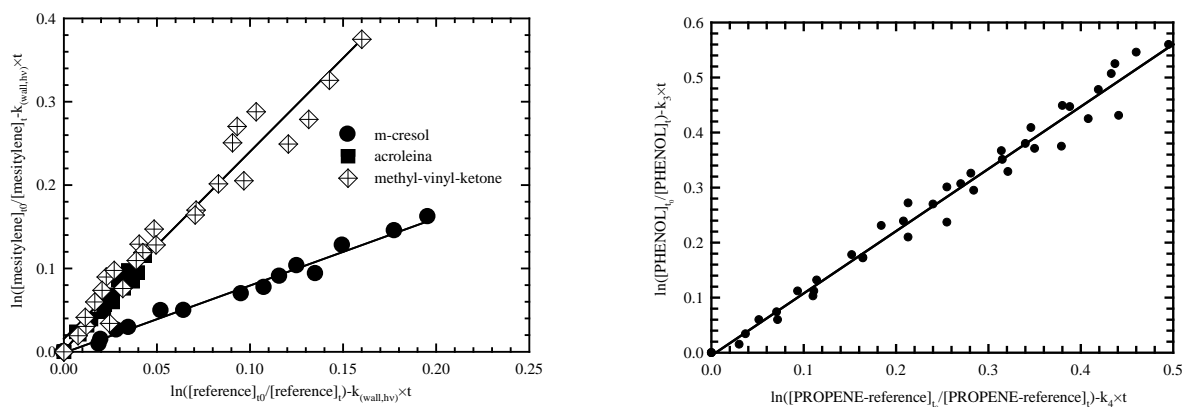


Figure 1.2.2-2: Kinetic data plotted for the reaction of OH radicals with mesitylene (left; using m-cresol, acrolein and methyl-vinyl ketone as reference hydrocarbons) and for the reaction of OH radicals with phenol (right; using propene as reference hydrocarbon).

Determination of chamber dependent parameters affecting SOA formation (task 2.1.3)

Non-volatile particle physical wall losses and Semi-volatile vapour wall losses:

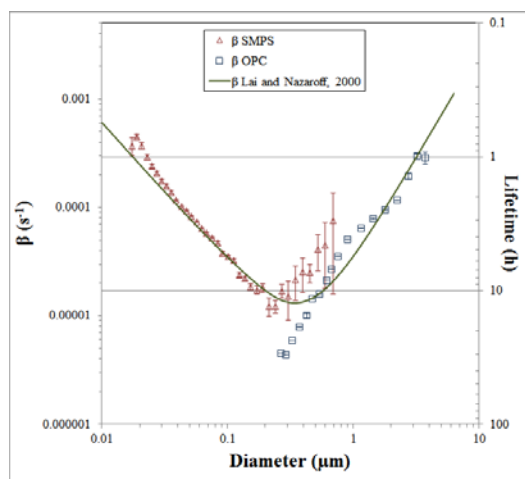


Figure 1.2.2-3: Particle loss coefficient (β) and life time right axis), versus aerosol size by NaCl salt injection in ChAMBRé.

For the newly set-up INFN chamber (*ChAMBRé*) size dependent particle wall loss was determined (see Figure 1.2.2-3). The protocol to perform experimental studies on primary biological aerosol particles and bacteria in particular, has been quantitatively assessed. The injection and extraction phases have been thoroughly tested both with Gram positive and Gram negative bacterial strains. With a clean atmosphere maintained inside ChAMBRé, the ratio between injected and extracted viable bacteria turned out to be reproducible at a 10 % level (Massabò et al., 2018), assessing this way the chamber sensitivity for systematic studies on bacterial viability vs. environmental conditions.

Overall, size dependent physical wall losses were studied in most of the chambers of the consortium such as *CESAM* (CNRS-LISA), *ISAC* (CNRS-Lyon), *AIDA* (KIT), *ILMARI* (UEF), *FORTH*, *MAC* (NCAS-UMAN) and *ChAMBRé* (INFN) and made available on-line in the directory of chamber during this first reporting period.

For complex experiments such as chemical aging of SOA, the results of the SOA quantification analysis can be quite sensitive to the adopted correction method due to the evolution of the particle size distribution and the duration of these experiments. These loss rates depend on the chamber material, flows inside the chamber and other parameters such as size, shape, and charge of particles. One example of studies related to particle physical wall losses is provided by the FORTH team in collaboration with Carnegie Mellon University which have evaluated the performance of several particle wall-loss correction methods for aging experiments of α -pinene ozonolysis products (Wang et al, 2018).

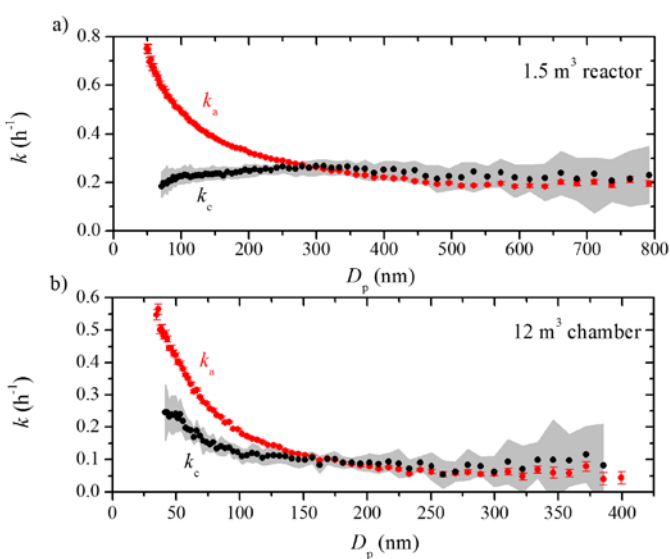


Figure 1.2.2-4: The apparent (k_a) (red symbols) and coagulation-corrected (k_c) (black symbols) particle wall-loss rate constants as a function of particle size for a) a 1.5 m³ Teflon chamber and b) a 12 m³ smog chamber after the two systems have been left undisturbed in the lab for weeks. The particle loss rate constants were derived based on SMPS measurements

Particle number losses in chamber experiments due to coagulation can be significant for small particles (< 150 nm under conditions in this work). It is thus important to correct for this coagulation effect when calculating the particle wall-loss rate constants especially for experiments in which the behaviour of the nanoparticles is important (e.g., when they carry a significant fraction of the total particle mass). The impact of coagulation on the particle wall-loss rate constant is shown in Figure 1.2.2-4 for a typical small and large Teflon reactor.

Semi-volatile vapour wall losses:

With respect to semi-volatile vapour wall losses determination activities, the exact species to

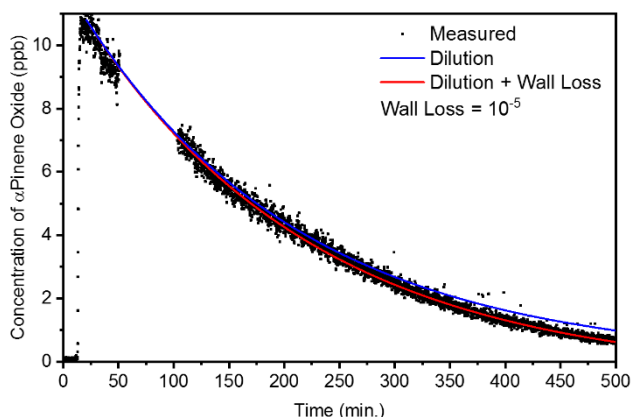


Figure 1.2.2-5: Decay of α -pinene oxide during chamber dilution in the dark.

be measured need to be decided within the next months, as it is not clear that the state-of-the-science is sufficiently developed and in most cases, the development of some instrumentation/technologies foreseen within WP10 is still needed. Certainly, common procedures need to be defined taking into account results from WP10 to guarantee high quality and reproducible data. Nevertheless, some previous experiments are being carried out by some partners. For example, as a preliminary experiment PSI injected α -pinene oxide ($C_{10}H_{16}O$) into the cool chamber and observed its decay as a function of time while diluting the chamber at 40 L min^{-1} . The decay of α -pinene oxide was monitored with a proton transfer-reaction mass spectrometer. Figure 1.2.2-5 demonstrates the decay of α -pinene oxide over 8 hours. While the initial decay fits well with the expected decay from pure dilution, the discrepancy becomes obvious at long times and to make up the difference a wall loss rate of 10^{-5} min^{-1} was used.

References for WP2

Etzkorn, T., Klotz, B., Sørensen, S., Patroescu, I., Barnes, I., Becker, K.H., Platt, U., Atmos. Environ., 33, 525-540, 1999

Massabò D., Danelli S.G., Brotto P., Comite A., Costa C., Di Cesare A., Doussin J.F., Ferraro F., Formenti P., Gatta E., Negretti L., Oliva M., Parodi F., Vezzulli L., Prati P., ChAMBRé: a new atmospheric simulation

Chamber for Aerosol Modelling and Bio-aerosol Research, Atmos. Meas. Tech. Discuss., <https://doi.org/10.5194/amt-2018-147>, in review, 2018.

Wang N., S. D. Jorga, J. R. Pierce, N. M. Donahue, and S. N. Pandis (2018) Particle wall-loss correction methods in smog chamber experiments, Atmos. Meas. Tech. Discuss., doi.org/10.5194/amt-2018-175.

Work Package 7: Physical access to the chambers (TNA1)

Through WP7, transnational access activities (TNA), the EUROCHAMP-2020 infrastructure offers hands-on experience and training in sixteen world-class atmospheric simulation chamber facilities across Europe, three more than previously within the FP6 and FP7 funded Integrating Activities projects EUROCHAMP (2004-2009) and EUROCHAMP-2 (2009-2013).



Figure 1.2.7-1: Overview of simulation chamber offered to physical access through TNA

From January 1st, 2017 - when the call for applications was launched accomplishing the milestone 42 - until May 31st, 2018 a total of **34 TNA proposals** were submitted to the Project Office. Four proposals were rejected based on eligibility (non-compliance with the TNA rules) or selection (decision of the TUSP) criteria. One should mention that, at the beginning of the project, the rate of submission was lower than expected. Thanks to a proactive communication strategy, this induction time has ended and a significant increase of the rate of submission has been recorded by the Project Office: in fact, half of the applications has been submitted during the last seven months of RP1.

Short description of TNA projects

An overview on the TNA situation, including the users' detailed reports, is published on the project website at <https://www.eurochamp.org/Project/Documentation/TNAdocuments.aspx> and is continuously updated by the Project Office.

[Access provided by CESAM \(CNRS\)](#)

CESAM-001-2017 dealt with the aqueous formation of Brown Carbon in aerosols and was a combined training and mobility activity. The scientific report shows that the goals of the TNA at CESAM were fulfilled; further processing of the results are required before publication.

CESAM-002-2018 was a border interdisciplinary activity (experts' mobility) addressing the origin of particulate matters that reach remote regions of the Earth, previously considered "pristine", such as the Polar regions. The user group proposed to investigate the trace elements and the isotopic compositions of dust from Namibia. To do so, the CESAM chamber was used, which is equipped with a state-of-the-art generation system for mineral dust generation and protocols for suspension and multi-parametric analysis.

[Access provided by HELIOS \(CNRS\)](#)

HELIOS-002-2017 made use of a particular feature allowing experiments to be conducted under true solar light conditions. The large range of analytical instruments present at HELIOS provided comprehensive data on the atmospheric fate of methyl ethyl ketone and facilitated training on use of state-of-the art instrumentation.

[Access provided by QUAREC \(BUW\)](#)

Gas-phase chemistry of organic compounds known to be released from plants into the atmosphere was studied within *QUAREC-001-2017*. The study included both use of instruments provided by the host, and the collection of samples of the reaction mixtures to be analysed at the guests' laboratory.

QUAREC-002-2017 investigated the photooxidation of halogenated substances emitted from various industrial processes and waste disposals. Kinetics and product analyses were performed at different temperatures. The final results will be included in a PhD thesis and also published.

The environmental chamber QUAREC has been disassembled and relocated within the University of Wuppertal into a new building successfully. Currently the chamber is subject to maintenance an up-grading work. Accordingly, the chamber is closed for TNA activities from May 2018 to November 2018.

[Transnational Access provided by AIDA \(KIT\)](#)

Within *AIDA-001-2017* an experience exchange occurred between the guests' expertise in generating proxy sea spray aerosol and the unique opportunities to study aerosol-cloud interactions at the AIDA facility, thus a mixed training-experts' mobility activity that benefited both parties. Various experiments were successfully performed to determine the ice nucleating efficiency of seawater/phytoplankton culture samples during 20 access days.

AIDA-002-2017 was a mobility activity that ran for 14 days at the AIDA chamber. A guest LAAP-TOF instrument took part in the INUIT 09 campaign "Ice nucleation of mineral dust". It was used to evaluate the single particle composition of several natural desert dust samples from Africa in order to assess the role of mineralogy in the ice nucleating (IN) efficiency of natural desert dust samples.

The campaign *AIDA-003-2017* addressed the SOA formation from anthropogenic and biogenic

precursors. It was a combined experts' mobility and training activity that took advantage of the manifold investigation possibilities at AIDA to investigate chemical kinetics, aerosol chemistry, aerosol physics, and cloud microphysics in a wide range of atmospheric conditions, crucial for the scientific objectives of the study, e.g. pressure (1 to 1000 hPa), temperature (40 °C to -90 °C), and relative humidity (from extremely dry to super saturations).

AIDA-004-2018 was an interdisciplinary campaign focusing on improving knowledge about the role of volcanic ash as ice nuclei (IN) in the atmosphere.

Transnational Access provided by SAPHIR (FZJ)

The *SAPHIR-001-2017* activity investigated over 18 access days, detailed aspects of the photochemistry of forest emitted isoprene. These chemical processes can be investigated at *SAPHIR* under realistic conditions with respect to both VOC concentration ranges and oxidant levels. The guest group got training to perform experiments at the chamber. Time series of trace gases and radicals were measured during the campaign by a PTR brought from Harvard University and with instrumentation provided by the host.

Transnational Access provided by PACS-C3 (PSI)

Through *PACS-C3-001-2018* an interdisciplinary investigation was conducted upon characterization of VOC emission from cell cultures as a diagnostic tool for metabolic processes. During a 10 days campaign a PTR-TOF 8000 instrument from the University of Oslo was successfully coupled to a cell exposure chamber at PSI to study emissions from bronchial cell cultures subjected to oxidative stress and SOA.

Apart from the unique features of the *PACS-C3* installation, the study benefited also from the well-established research collaboration between host and an air toxicology group at the University of Bern (http://www.ana.unibe.ch/research/group_geiser/index_eng.html) which is a necessary prerequisite for conducting front-end-research at the interface between atmospheric chemistry and life sciences.

PACS-C3-002-2018 focuses on understanding SOA formation from biomass burning and coal combustion through the application of ultra-high performance investigative techniques as UHPLC coupled to electrospray ionization ultra-high resolution mass spectrometry. Through this activity, undergraduate and postgraduate students from both guest and host research groups were trained in the use of state-of-the-art analytical techniques.

Within *PACS-C3-003-2018* an advanced mass spectrometric method developed by the Ionicon Analytik GmbH, a SME located in Innsbruck, Austria was used together with two state-of-the-art instruments developed at PSI to study the chemical composition of SOA. The objectives are to reduce the gaps of knowledge on the chemical composition and photochemical transformation of complex systems and to test the instruments. In this project, ten chamber studies of SOA formed from α -pinene, toluene, cresol and a mixture of α -pinene and toluene were performed at the PACS-C3 chamber. In addition to the current state-of-the-art high resolution time-of-flight aerosol mass spectrometer (HR-TOF-AMS), the Paul Scherrer Institute has deployed their very recently developed extractive electro-spray ionization TOF-MS (EESI-TOF). These two instruments were complemented by Ionicon's modular "Chemical Analysis of Aerosol Online" (CHARON) particle inlet coupled to a new-generation proton-

transfer-reaction time-of-flight mass spectrometer (PTR-TOF 6000 X2).

Transnational Access provided by EUPHORE (CEAM)

EUPHORE-001-2017 took advantage of the natural solar irradiation combined with a wide range of analytical techniques provided at CEAM to investigate the photolysis of oxygenated compounds under natural irradiation.

The study aims at providing accurate photolysis frequencies for atmospheric chemistry models like MCM or GECKO-A, in order to improve the consistency and robustness of atmospheric chemistry models. The report acknowledges that the campaign was successful in achieving new data on the significance of atmospheric photolysis for multifunctional oxygenated compounds.

EUPHORE-003-2018 is an experts' mobility activity granting access to a guest SIFT instrument to take part in the EUROCHAMP2020 "Inter-comparison of instruments for measurements of small oxygenated organics". Work involved establishing whether a new state of the art commercially available Selected Ion Flow Tube Mass Spectrometer (SIFT-MS, Syft technologies) had adequate mass resolution and sensitivity for atmospheric applications. The SIFT-MS results from this project will be compared to other OVOC measurement techniques such as PTR-MS and FTIR.

Transnational Access provided by LEAK-LACIS (TROPOS)

In the actual reporting period one TNA was granted at *LACIS*, *LEAK-LACIS-001-2017* covering 10 access days. The activity aimed at exploring the limits of the holographic system "HoloPi" developed at the Michigan Technological University, USA, when applied to the investigation of cloud droplets and ice particles. Apart from testing the instrument, both guest and host researchers benefited from hands-on training on operating the cloud simulation chamber and a new technology respectively.

Transnational Access provided by ILMARI (UEF)

Through *ILMARI-003-2017*, 25 access days were granted to a multidisciplinary research project concerning the variations in the health impact of mixtures of pollutants when aging. Lung cells were exposed to emissions from logwood fire and from a gasoline generator (gas and particulate matters).

Transnational Access provided by FORTH-ASC (FORTH)

FORTH-ASC-002-2017 is a combined training and mobility activity aiming at understanding the atmospheric relevance of aerosol formation in the photooxidation of α -pinene aged products.

Within *FORTH-ASC-003-2017*, a mobility activity, the chemical aging of ambient organic aerosol was investigated as it is exposed to OH. The FORTH-ASC facility offers the unique possibility to use 2 identical chambers simultaneously, one as reference and one in which a perturbation factor is added.

Transnational Access provided by RvG-ASIC (NCAS)

RvG-ASIC-001-2017 addressed the issue of so-called Arctic amplification of global warming (i.e., warming feeds warming). In the Arctic, temperature changes may quickly enhance methane emissions, due to large natural sources. The study investigates the methane pathways

during sea ice formation and melts under laboratory conditions under special consideration of the kinetic isotopic fractionation effect on the $\delta^{13}\text{C}$ signature of methane along these pathways, i.e. into, within and out of sea ice in both directions from sea water to sea ice and from sea ice back into sea water or into air. It supplies a first data set about the effect of kinetic fractionation on methane along pathways coupled to various sea ice formation conditions.

Through *RvG-ASIC-002-2017* the guest researchers made use of the RvG-ASIC unique features – being the only large-scale chamber of its kind - to study biological and chemical air-sea-ice-frost flower interactions.

RvG-ASIC-003-2017 addressed the issue of retreating Arctic sea-ice and its impact on the Earth's energy balance. The project aims to gain important insights into the physics of radiation transfer within young sea ice and to test newly developed instruments for light measurements in sea ice for their potential use in the field. The guest researcher received support and training on using the installation from the experienced facility staff.

**Work Package 10: Evolution of atmospheric simulation chamber infrastructure to address
broader scientific and societal needs (JRA1)**

The overall aim of this Work Package is to bring the capacity of simulation chambers to a new level by widening the range of applications in response to research questions linked to atmospheric science and related fields.

Evolution of atmospheric simulation chamber infrastructure to enable the study of climate change drivers (Task 10.1)**Improved protocols and tools for the investigation of aerosol-radiation interaction (sub-task 10.1.1)**

Laboratory and modelling studies have shown that the addition of non-black-carbon materials to black-carbon particles may enhance the particles' light absorption by 50 to 60% by refracting and reflecting light (known as the lensing effect). NCAS-UMAN performed a set of experiments measuring the total mass of individual black carbon containing particles and the mass of the refractory black carbon emitted by a diesel engine running at different speed and load conditions (Liu et al., 2017). This was achieved through a novel coupling of a Centrifugal Particle Mass Analyser (CPMA, Cambustion), which selects particles of known and quantifiable charge-to-mass ratios across a narrow and well-defined distribution, and a single-particle soot photometer (SP2, DMT), which is introduced downstream of the CPMA and determines the mass of refractory black carbon and the intensity of scattered light for each BC particle sampled. This combination enabled, for the first time, the quantification of the mixing state of individual BC particles from a variety of laboratory and field experiments. NCAS-UMAN showed that particles with a mass ratio of non-black carbon to black carbon of less than 1.5, which is typical of fresh traffic sources, are best represented as having no absorption enhancement. In contrast, black carbon particles with a ratio greater than 3, which is typical of biomass-burning emissions, are best described assuming optical lensing leading to an absorption enhancement (Liu et al., 2017). These findings enabled the introduction of a generalised hybrid model approach for estimating scattering and absorption enhancements based on laboratory and atmospheric observations.

PSI has worked towards the Deliverable D10.3 (**Protocols for an artefact free determination of the mass absorption cross section**: document about optimal combination of filter based instruments such as aethalometers as well as in-situ absorption measurements with instrumentation that is based on mass or refractory black carbon mass), due in Month 24. Artefact free measurement of the mass absorption cross section (MAC) of a specific aerosol component (e.g. BC) requires isolation of that component (physically or virtually) to determine its absorption coefficient and mass concentration (e.g. refractory black carbon mass quantified with laser-induced incandescence) as illustrated in Figure 1.2.10-1.

Looking at Figure 1.2.10-1, it follows that accurate measurements of MAC_x are therefore only achieved if the appropriate (artefact free) methods are used for the measurements of $b_{abs,x}$ and m_x . This means methods selective

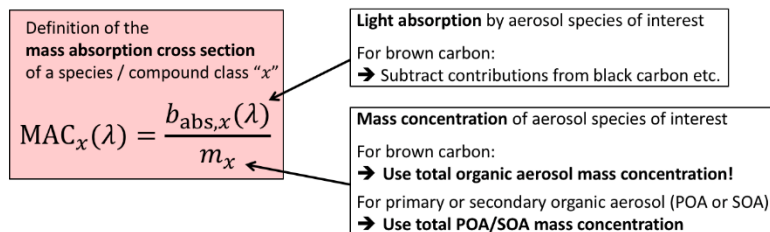


Figure 1.2.10-1: Definition of the mass absorption cross section for species x.

to contributions from "x" (without interference), proportional to total contribution by "x", and with absolute calibration (discussed below). Traceable mass concentration measurements of a component such as BC are only possible if the BC is available in pure form, and traceable standards must be used (both substance and instrumentation alike). Traceability to an absolute mass measurement is not always possible for a variety of reasons, in which case harmonization between different measurement techniques and/or instruments becomes the minimal goal.

In the case of quantifying black carbon mass using the thermo-optical OCEC (organic carbon / elemental carbon) method for example, which provides operationally defined elemental carbon mass, such instrument and protocol harmonization is controlled through the corresponding ACTRIS Central Facility. Absolute traceability is also not possible for black carbon mass measurements using laser-induced incandescence ((LII) e.g. single particle soot photometer, SP2), which is addressed in this activity and provides operationally defined refractory black carbon mass, because the proportionality constant between LII signal and true BC mass depends on the optical properties of the BC under investigation. For harmonization purposes PSI recommend the use of AquaDAG as a common "refractory black mass carbon" reference for all instruments, since AquaDAG is a readily available material with good consistency across batches. This harmonization does include a correction factor to account for the known difference in SP2 sensitivity to AquaDAG and to typical BC found in atmospheric particles.

At present there exists no standard technique for measuring aerosol absorption coefficients, nor a material that could be used as an absorption standard. However, our results indicate that despite the limitations of each technique, consistent results can be obtained between carefully performed measurements with the multi-angle absorption photometer (MAAP), an extinction-minus-scattering absorption photometer (CAPS PM_{SSA}), and a photoacoustic spectrometer (PAX). Work is still in progress to develop robust methods for calibrating the PAX, and characterizing the truncation correction and cross-calibration factors associated with the CAPS PM_{SSA} .

CNRS-LISA has worked on providing estimates of the Aethalometer multiple scattering correction C for mineral dust aerosols. The C at 450 and 660 nm was obtained from the combination of Aethalometer data (Magee Sci. AE31) with Cavity Attenuated Phase Shift Extinction analyser (CAPS PM_{ex}), a nephelometer and a MAAP. Measurements were performed on seven dust aerosol, pure kaolinite and pollution aerosol. Results have been published in Di Biagio et al, 2017b.

At CNRS-LISA the variability of the mineral dust long wave (LW) refractive index as a function of its mineralogical composition and size distribution is explored by *in situ* long path FTIR measurements in the **CESAM chamber**. Mineral dust aerosols were generated from 19 natural soils from different regions worldwide, chosen to represent the diversity of sources from arid and semi-arid areas and to account for the heterogeneity of the soil composition. Aerosol samples generated from soils were re-suspended in the chamber (protocol in preparation for WP3). The generated aerosol exhibits a very realistic size distribution and mineralogy,

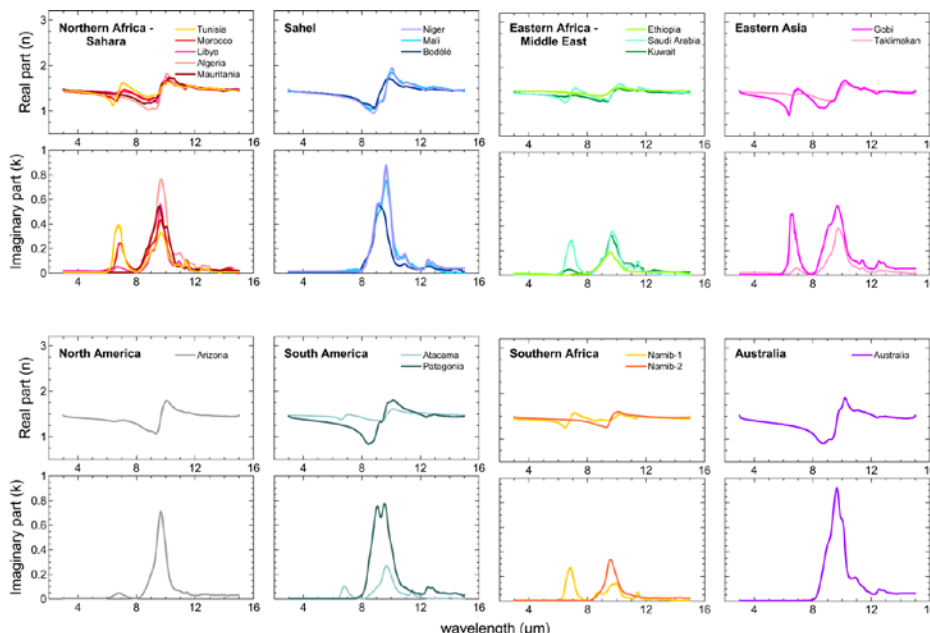


Figure 1.2.10-2: Real (n) and imaginary (k) parts of the dust complex refractive index obtained for the 19 aerosol samples generated in the CESAM chamber (CNRS-LISA). Data correspond to the time average of the 10 min values obtained between the peak of the injection and 120 min later.

including both the sub- and super-micron fractions. The complex refractive index of the aerosol is obtained by an optical inversion based upon the measured extinction spectrum and size distribution. Results (see Figure 1.2.10-2) show that the imaginary LW refractive index (k) of dust varies greatly both in magnitude and spectral shape from sample to sample. The work have been published in Di Biagio et al, 2017 and the data will be submitted to the LADP pillar of the EUROCHAMP-2020 DC when becomes operational.

To expand this approach from the LW domain to the UV-visible range, a high resolution large band (300-1000 nm) spectrometer is under development at **CNRS-LISA** and will be interfaced



Figure 1.2.10-3: Schematic view of the new large band UV-vis spectrometer interfaced to CESAM.

to **CESAM chamber** for *in situ* measurements of aerosol optical properties (Figure 10.1.5). This instrument will allow derivation of optical properties of particles such as mass extinction cross sections. This work has been taken in charge by an optical engineer appointed on this specific assignment. The spectrometer consists of a wide-band source (Hg(Xe)), an enhanced sensitivity spectrometer and a custom-designed multi-reflection white cell based on high-reflectivity broad-band mirrors. The delivery of the mirrors, currently under way, was delayed by several weeks. This has provoked the current delay in the

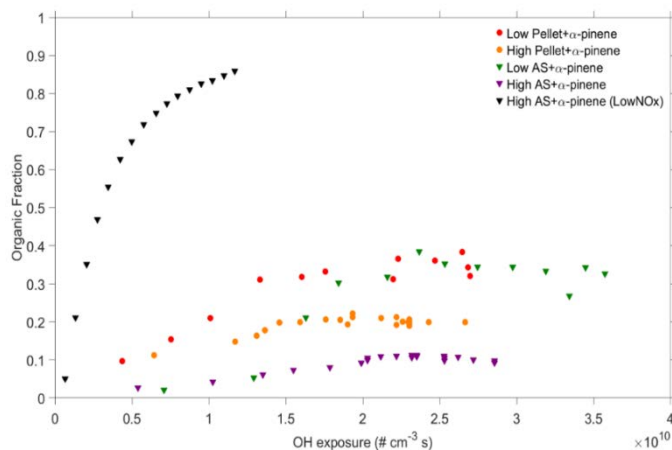


Figure 1.2.10-4: Organic mass fraction for each studied OH systems presented as a function of OH exposure. “Low Pellet” or “High Pellet” in series name refers to the seed concentration. Ammonium sulphate (AS) experiments were also performed for comparison.

provision of a demonstration case, which however should be completed in the course of July 2018.

As the structure and coating properties of particles affects their aerosol-radiation interaction properties, UEF performed a series of experiments in the *ILMARI chamber* to investigate how the seed particle coating thickness and properties can be controlled when real combustion emission sources are used to facilitate the controlled radiation interaction studies in ILMARI.

Improved protocols and tools for the investigation of aerosol-cloud interaction (sub-task 10.1.2)

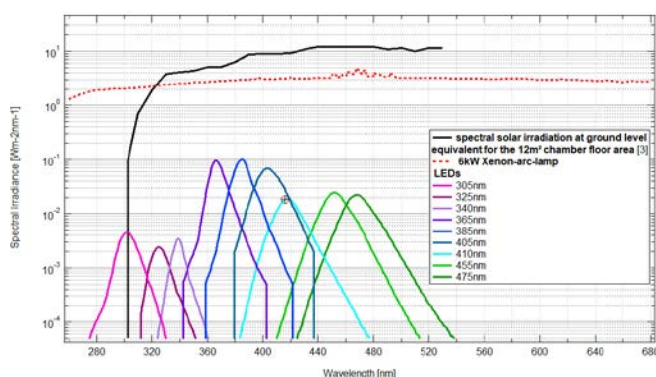


Figure 1.2.10-5: Spectra of commercially available LEDs in the UV-VIS spectral range compared to emissions of a Xenon arc lamp and the typical solar irradiation at ground level.

The *AIDA chamber* at KIT is among the best facilities in the world to study aerosol-cloud interaction but until now this unique facilities was not equipped with light sources preventing the users from studying the effects of photochemistry on cloud involving systems: With the installation of a new light source in the AIDA chamber, reaching from the UV into the visible spectrum KIT aims to simulate daylight conditions of different intensities and corresponding to different altitudes in the

atmosphere and thus facilitating studies on photochemical processes including trace gases, aerosol particles and clouds. The design for the new **UV light source** for the AIDA chamber in order to initiate photo-chemical processes has been completed and the first components have been tested successfully.

In order not to disturb the excellent temperature homogeneity within the AIDA chamber a combination of different high power light emitting diodes (LEDs) (Figure 1.2.10-5) will be used. Since the LEDs will be located in the temperature controlled housing of the AIDA chamber with temperatures ranging from 303 K to 183 K, the influence of temperature on the light emission characteristics of different LEDs was tested showing increasing intensities for lower temperatures.

The AIDA aerosol and cloud chamber of **KIT** is equipped with an instrument (SIMONE) measuring the forward and backward scattering intensities as well as the depolarization of backscattered light for aerosol particles, cloud droplets and ice crystals. SIMONE has now been

upgraded for higher sensitivity of scattered light detection and for reduced crosstalk in the depolarization measurement. Calibration measurements revealed that the residual crosstalk depolarization signal could be reduced to about 1%.

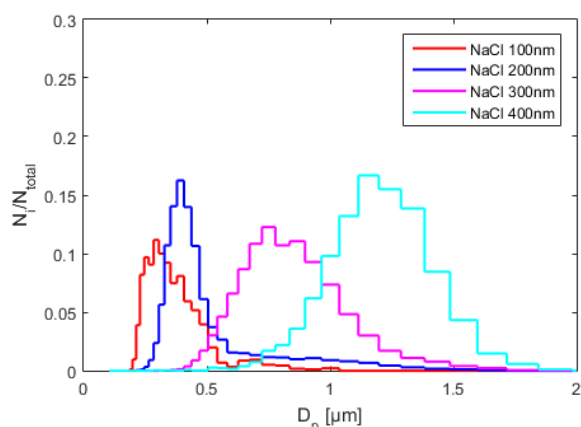


Figure 1.2.10-6: Size distributions of hygroscopically grown and activated droplets for different seed particle diameters

depicts size distributions of hygroscopically grown and/or activated droplets using sodium chloride particles as seeds. The distributions were measured with a WELAS 2300 optical particle spectrometer (Palas GmbH, Germany). Possible influences of turbulence manifest in the observed size distribution by the occurrence of larger droplets at the upper end of the distribution for the initially 200 nm seed particles.

The **FORTH** team has been continuing the development of an experimental approach for the measurement of organic aerosol hygroscopicity, oxidation levels, and volatility distributions (Cain and Pandis, 2017). The experimental setup utilizes a cloud condensation nuclei (CCN) counter to quantify hygroscopic activity, an aerosol mass spectrometer to

measure the oxidation level, and a thermodenuder to evaluate the volatility of OA in the simulation chamber. A data analysis technique has also been developed to convert the results of the experiments to parameters that can be used by chemical transport models based on the Volatility Basis Set. The system was tested for α -pinene SOA and provided distributions of SOA O:C and the hygroscopic parameter kappa as a function of its effective volatility C^* (Figure 1.2.10-8). Ongoing FORTH work involves the application of the approach to other SOA systems, addition of an isothermal dilution measurement to decrease the uncertainty of the corresponding estimated parameters, and application of the method to the dual mobile chamber system.

TROPOS has extended the **Leipzig Aerosol Cloud Interaction Simulator's (LACIS)** capabilities to enable investigation of the interactions between cloud microphysical processes (e.g., particle activation to droplets and droplet freezing) and turbulence under well-defined turbulence and thermodynamic conditions. The flow and thermodynamic fields inside the setup have been characterized. First investigations with respect to the activation of aerosol particles to cloud droplets under turbulent conditions have been performed and are continued. Figure 1.2.10-7

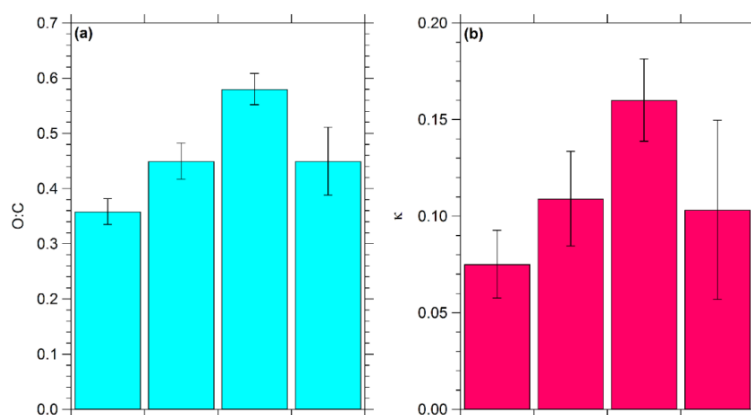


Figure 1.2.10-7: The (a) O:C ratio and (b) κ distributions for the volatility bins characterized in this study for α -pinene ozonolysis SOA. The error bars represent one standard deviation of the mean obtained from the parameter estimation algorithm.

NCAS-UMAN has coupled the **Manchester Aerosol Chamber (MAC)** to the **Manchester Ice and Cloud Chamber (MICC)**, which enabled direct measurements of the cloud condensation and ice nucleation potential of secondary organic aerosol particles from biogenic and anthropogenic origins under atmospherically representative conditions. Using this combined chambers setup, NCAS-UMAN conducted a series of experiments investigating the ice nucleating ability of photochemically produced SOA particles (Frey et al., 2018). Three SOA systems were studied resembling biogenic/anthropogenic particles and particles of different phase states. These are namely α -pinene, heptadecane, and 1,3,5-trimethylbenzene. After the aerosol particles were formed, they were transferred into the cloud chamber where subsequent quasi-adiabatic cloud activation experiments were performed. Furthermore, the ice forming abilities of ammonium sulphate and kaolinite were investigated as a reference to test the experimental setup. Clouds were formed in the temperature range of -20°C to -28.6°C . Only the reference experiment using dust particles showed evidence of ice nucleation (Figure 1.2.10-9, top right panel). No ice particles were observed in any of the SOA experiments (e.g. Figure 1.2.10-9, top left panel). NCAS-UMAN concluded that SOA particles produced under the conditions of these experiments were not efficient ice nucleating particles starting at liquid saturation under mixed-phase cloud conditions.

Evolution of atmospheric simulation chamber infrastructure to enable the studies of the impact of air quality on health and culture heritage (Task 10.2)

Our goal in this task is to further develop the operational modes and characteristics of EUROCHAMP chambers so that they can be used as controlled, reproducible and realistic air pollution sources. This will enable toxicological studies using a variety of biological systems from simple cell cultures to in-vivo murine models, as well as studies on the effects of air pollution on cultural heritage such as building materials.

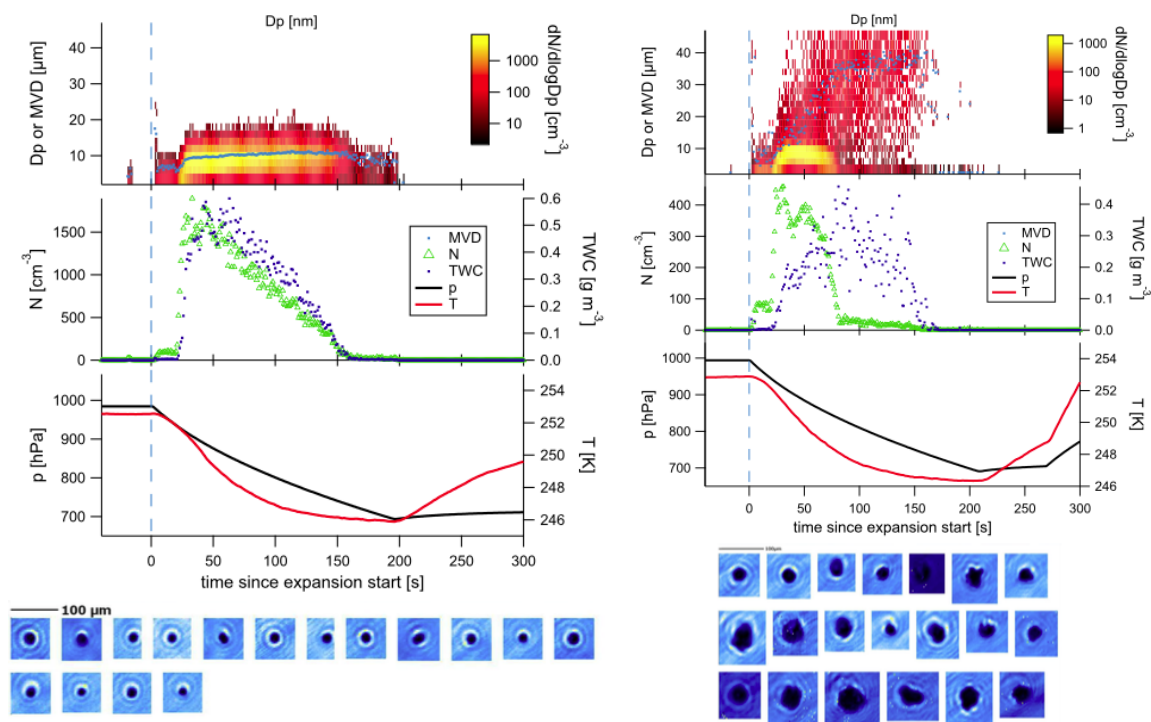


Figure 1.2.10-8: Example of a cloud evacuation performed on heptadecane SOA (left side) and reference dust particles (right side). Time series of cloud droplet size distributions are shown in the top panels. Cloud droplet number concentration (N), mean volume diameter (MVD) and total water content (TWC) are shown in the middle panels. Chamber temperature and pressure during evacuation are shown in the bottom panel. The images shown above the panels are for cloud droplets or ice particles as captured by the Cloud Particle Imager. Unlike the SOA case, dust shows the formation of ice in a second large mode (top panel), and the decrease and almost disappearance of particle numbers of smaller drops over time (Wegener-Bergeron-Findeisen process).

To enable studies of the impact of air quality on health and culture heritage, controlled, reproducible and realistic air pollution sources need to be provided. For this purpose, selected chambers are coupled to a range of combustion sources (engines and biomass burning) to enable the generation of primary aerosol samples at atmospherically representative and realistic conditions. In the following these activities are described first, followed by studies on the impact of such aerosols on air quality, health, and culture heritage.

PSI has developed procedures for an artefact free sampling of exhaust samples from different combustion processes. Using these procedures, eight combustion devices with different technologies were tested, including a pellet boiler, a moving grate boiler equipped with electrostatic precipitator, an updraft combustion pellet stove, a two-stage combustion downdraft log wood boiler, two advanced two-stage combustion log wood stoves, and two conventional

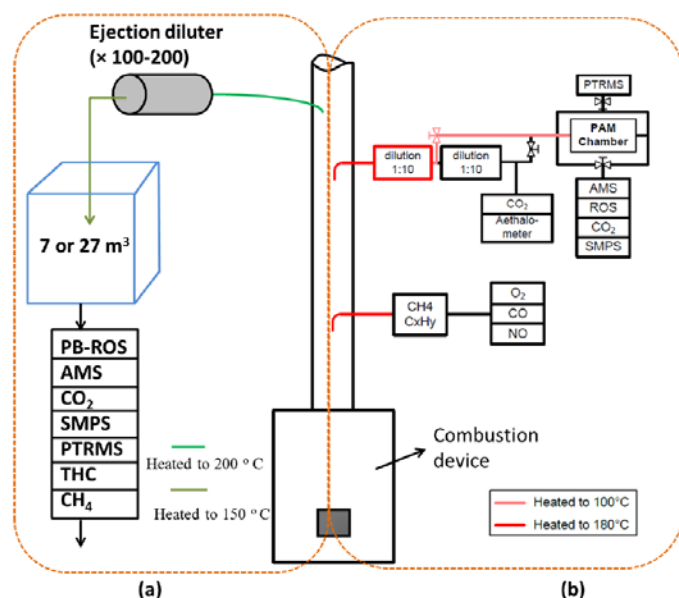


Figure 1.2.10-9: Schematic of wood combustion emissions aged by a) smog chamber and b) a potential aerosol mass (PAM) chamber (Zhou et al., 2018)

single-stage combustion log wood stoves (Zhou et al., 2018). The emissions were sampled through a heated line (473 K), diluted by a factor of 100–150 using two ejector diluters in series (VKL 10, Palas GmbH), and then injected into the aging devices. These experiments were performed in the PSI mobile smog chamber (~7 m³) at temperatures of 263 and 288 K, the PSI stationary smog chamber (27 m³) at 295.5 K, or in a potential aerosol mass (PAM) chamber. An overview of the experimental setup is shown in Figure 1.2.10-10. More details are found in Zhou et al. (2018).

Improved methods to study impacts of AQ on health: Diagnostics (sub-task 10.2.1)

Several chambers investigated the preparation of representative aerosol samples, e.g., from a variety of combustion emission processes, to enable the preparation of the chamber with an aerosol that e.g. represents atmospheric conditions. Moreover, several chambers have performed studies with health relevant properties, such as reactive oxygen species (ROS), as well as exposition of aerosol samples processed in a smog chamber or a flow reactor to human respiratory cells and to living organisms.

Reactive oxygen species (ROS) are oxidizing compounds present in aerosol particles, which are potentially key in describing the toxicity of atmospheric aerosol particles. **NCAS-UCAM** showed in earlier studies (Fuller et al., 2014) that ROS in organic model aerosol have a lifetime of only a few minutes, which demonstrates that conventional analyses of ROS using offline filter sampling where the time delay between aerosol sampling and quantification is often hours to days are not suitable for a reliable quantification of ROS in aerosol because most ROS components would have decayed. Therefore, fast online methods are required to quantify ROS in aerosol particles. NCAS-UMAN developed the first compact online instrument to quantify ROS in aerosols and characterized the formation and lifetime of ROS in SOA generated from limonene ozonolysis in the Cambridge Atmospheric Simulation Chamber (CASC) (Gallimore et al., 2017). These studies showed that there are short-lived and a long-lived ROS components in SOA and that short-lived ROS have a lifetime of about 15-20 min and comprise about 25-40% of the total SOA mass

PSI combined smog chamber PACS-C3 ageing experiments to a cellular deposition chamber, in order to determine the effects of PM related oxidative stress onto human respiratory cells. These studies are motivated by the fact that PM concentration does not seem to be the only parameter responsible for these diseases. One of the main hypotheses is that PM components (e.g. transition metals, quinones, organic peroxides, etc...) can cause oxidative stress within the respiratory tract; however the underlying biological and chemical processes are yet not

fully characterized. The PSI cell chamber was slightly modified to apply either aerosol flow or suspension of aerosols via an injection system, the later allowing deposition of higher PM concentration onto the cellular monolayer, shown in Figure 1.2.10-11. A PTR-ToF-MS was used to perform an online measurement of volatile compounds emitted from bronchial cells before and after treatment. The treatment consisted in using either model compounds present in ambient PM, and known to induce oxidative stress while combined (copper and 1,4-naphthoquinone), or PM obtained from the oxidation of anthropogenic (wood burning) or biogenic sources (α -pinene) in the smog chamber and the volatile organic species measured for different concentration were then compared. In parallel, the cytotoxicity of these treatments was assessed.

Using this innovative method combining biology and aerosol chemistry, PSI determined in the cellular headspace promising markers for oxidative stress that might be helpful to understand the mechanism of PM toxicity.

Long term exposure within methods to study impacts of AQ on health and culture heritage: long term exposure (sub-task 10.2.1 and sub-task 10.2.2)

Several partners have successfully tested the provision of constant test air samples over long time periods as especially in the case of cultural heritage long exposure time are required where the properties of the tested air should be maintained as precisely as possible.

Most of the EUROCHAMP simulation chambers are usually operated in batch mode: reactants are introduced in the beginning of the experiment and the reactions take place in a closed system. While this approach is simple and has provided valuable results, it limits the use of atmospheric simulation chambers for other applications that require exposure to constant concentrations of pollutants for long periods of time. The use of atmospheric simulation

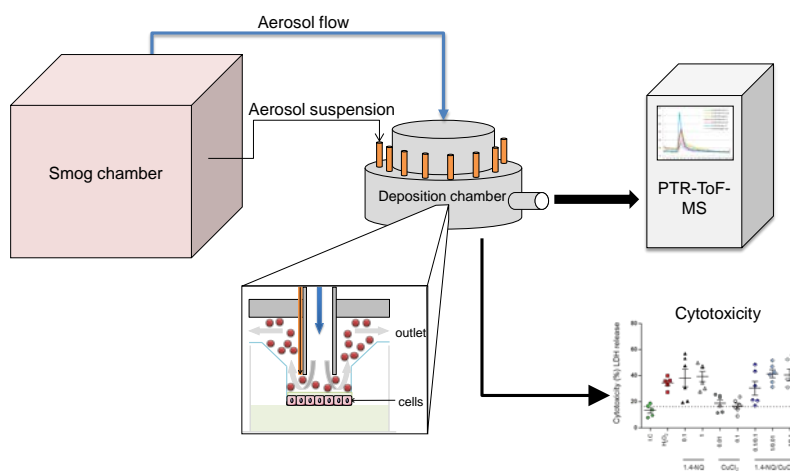


Figure 1.2.10-10: Schematic drawing of the setup. The first part consists in the smog chamber from which the aerosols are either: a) injected onto the cell chamber (blue arrow) or b) collected on filters and extracted before injection onto the cells (thin black arrow). Inside the cell chamber (insert) the aerosols reaches the surface of the cells which, in reaction to this stress, will emit volatile compounds (red dots) that exit the cell chamber following the flow through the outlet. This outlet is connected to a PTR-ToF-MS measuring these volatile compounds released by the aerosol and the cells. The cells are later analysed to determine the cytotoxicity of the PM.

chambers to study air pollution effects on health, cultural heritage, and materials has been limited in the part by the difficulties in achieving appropriate exposure. The EUROCHAMP team has developed experimental approaches that allow operation of the chambers for extended periods of time to simulate the effects of realistic air pollution mixtures. These joint efforts are described in the following sections.

CNRS-LISA developed an original protocol for the characterization of health impacts on living organisms by realistically simulating in *CESAM chamber* the atmospheric mixture in all its complexity. For that purpose,

the myriad of products arising from the atmospheric oxidation of primary organic compounds was generated under controlled conditions. The experimental protocol consists in the continuous injection of relevant mixtures of primary pollutants at low concentrations (ppb levels) in air in the CESAM chamber operated as a slow flow reactor. The residence time of simulated air parcels in the experimental volume is fixed to 4 hours, in order to represent air masses of regional scale.

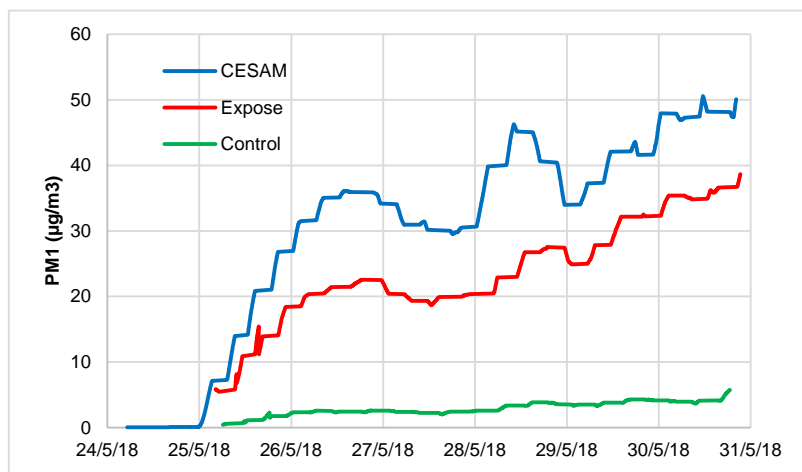


Figure 1.2.10-11: The evolution of the total particles number and concentration as a function of time, successively measured through different compartments of exposure. The highest concentrations are those inside CESAM. The lowest concentrations are those from an "unexposed" reference compartment while the medium level concentrations are those associated with the compartments with exposed living organisms.

During this time the synthetic mixture is exposed to an artificial solar irradiation, allowing secondary pollutants to be produced and to reach their chemical steady state (Figure 1.2.10-12). Living organisms are exposed to constant flows of such a mixture during time scales of week to test their effect on living organisms. To support this protocol, CNRS-LISA ran a predictive model in order to scale the pollutant concentrations in the initial mix. This model estimated the concentrations of all gaseous and particulate species in CESAM, after a residence time of 4 hours in the chamber.

The ability of the **FORTH** simulation chamber to operate at continuously has been tested. The overall design of the system involves the continuous injection of the reactants (precursors, NO_x, oxidants) and seed aerosol, the continuous removal of the products at a flowrate equal to that of the injections, and the

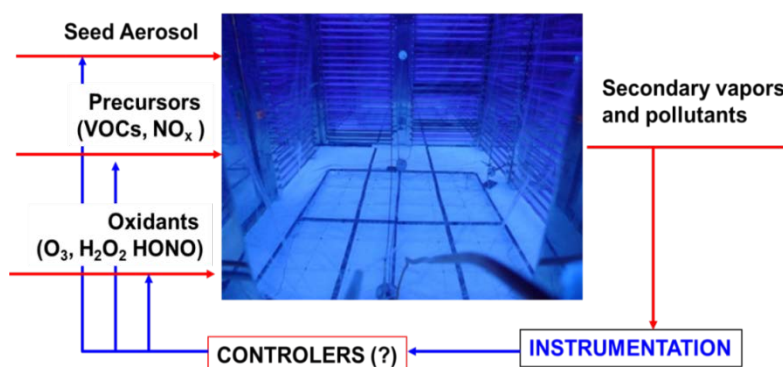


Figure 1.2.10-12: Schematic of a system for the continuous operation of a smog chamber.

monitoring of the concentrations of both the reactants and the products (Figure 1.2.10-13). Additional active controllers may be used for either the various components or the overall system. Our emphasis at this stage of the work was on keeping the system simple so that it may be used in the future in other EUROCHAMP simulation chambers. More details are found in the submitted Deliverable D10.2, which was due in Month 18. The continuous seed generation in the FORTH chamber is based on the continuous atomization of a solution of the desired seed (ammonium sulfate was used in these experiments but other compounds can also be used) using a TSI Model 3076 atomizer. A peristaltic pump (Rainin, Model RP-1) is used to supply the solution (concentrations of 0.1-10 g L⁻¹ were used) instead of the syringe pump that has been used in batch experiments. The peristaltic pump draws the solution from a bottle and can operate continuously at constant rates for several days without for example the need to refill the syringe of the syringe pump. The droplets are dried in a silica gel dryer and are then injected into the simulation chamber. FORTH tried to establish the stability of the system without the use of any additional controllers. The results are quite encouraging. Stability (one standard deviation of the concentrations) of 10% or better could be established for both the ammonium sulphate number and mass concentration in the system for a wide range of concentrations.

TROPOS performed experiments using the **LEAK simulation chamber** in continuous mode as a Continuously Stirred Tank Reactor (CSTR). The mean residence time in the CSTR experiments was in the range of 1.5 to more than 2 hours. The experiment duration was 48- 96 hours, which allows to insert the educts in atmospherically relevant mixing ratios on one side and to produce sufficient mass on the sampled filters for a detailed analysis of the formed particulate products on the other side. A typical result of a α -pinene ozonolysis experiment in LEAK used in the CSTR mode is shown in Figure 1.2.10-16.

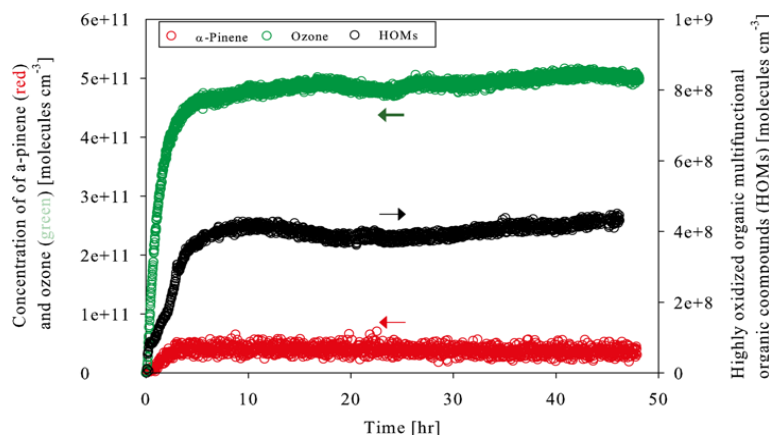


Figure 1.2.10-13: Concentration of α -pinene (red) ozone green and Highly Oxidized Molecular Species formed in the ozonolysis of α -pinene. The concentration of α -pinene was measured with a PTR-MS and the HOMs concentration was determined with an NO₃-CI-API-TOFMS.

Evolution of atmospheric simulation chamber infrastructure to enable process studies of increasing realism and complexity (Task 10.3)

Chamber studies that represent more realistic and more complex conditions are required in order to close the gap between well controlled but simplified laboratory experiments and observations in the real atmosphere. To date, most chamber studies have focused on chemical processes occurring in the gas and aerosol phases. However, under real conditions, processes also take place at the interfaces that connect two environmental compartments (e.g., air-sea or cryosphere-atmosphere interface). This task aims to establish and advance capability in these areas by developing new experimental protocols and performing detailed investigations of

processes relevant for atmospheric interfaces and bioaerosols.

Several chambers have made progress in characterizing process as interfaces, such as the air – sea or air – sea ice interfaces or to act as test beds where the photocatalytic activity of materials to diminish air pollutants. Other chambers report progress on the preparation of complex aerosol mixtures, e.g. aerosol particles from various combustion processes coated with different aerosol material representative of secondary aerosol. Also, links between secondary organic aerosol formation and the specific composition of complicated precursor gas mixtures such as emission exhausts were evaluated. A protocol to study primary biological aerosol particles and bacteria was established, and a 50 m high tower was built to provide real atmospheric air samples with minimized local contamination.

Enabling the study of the atmospheric chemistry at the interfaces (sub-task 10.3.1)

The *Roland von Glasow Air-Sea-Ice Chamber* at NCAS-UEA has carried out a pilot study on the release of NO_x from sea-ice. The hypothesis was that sea-ice photochemistry might be relevant for the NO_x budget over the ice-covered Arctic ocean, similar to the photolytic release of NO_x from snowpack (France et al., 2011). In the latter case, it was found that photolysis can remove up to 80 % of surface snow nitrate over the course of 1 year, with additional losses caused by evaporation. However, in the case of sea-ice, the less porous ice structure might act as a "cap" to any photolysis products formed within the ice.

For the experiments, NCAS-UEA team spiked seawater in the tank with nitrate prior to ice formation. The chamber was isolated and sea-ice allowed to form at -20°C to 15 cm thickness (Figure 1.2.10-17). The nitrate-spiked ice was then illuminated with UV light and the NO_x and

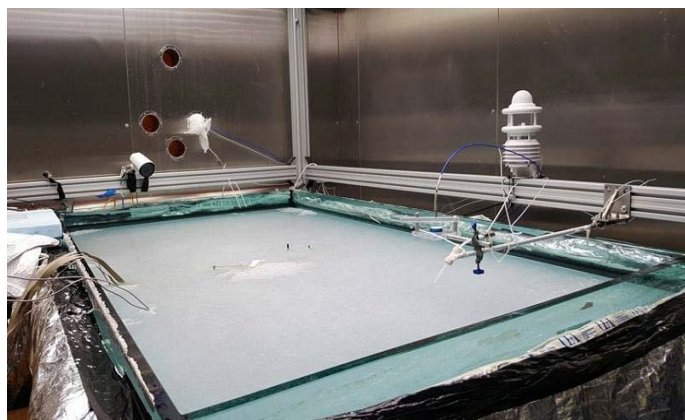


Figure 1.2.10-14: Sea-ice grown to 15 cm thickness.

O_3 mole fractions measured continuously just above the sea-ice (Figure 1.2.10-18). Following the UV irradiation phases, the ice underwent a fast melt over the course of 2 to 3 hours, while the trace gas measurements continued. In-ice salinity and temperature probes as well as meteorological weather station and optical sensors provided auxiliary measurements to monitor the progress of the experiments.

The results showed no NO_x emission under UV-A illumination. A small peak in the NO_x mole fraction was observed during the first UV-B experiment, but not reproduced during a subsequent repeat, for reasons that are yet to be established. However, a very strong NO_x increase above the ice was found during initial melting and coincident O_3 depletion, presumably due to release of photochemical products trapped in the ice. It can be concluded from these pilot studies that sea-ice is likely to act as "cap" for nitrate photolysis products, but further experiments are needed to reproduce and analyse the results in detail.

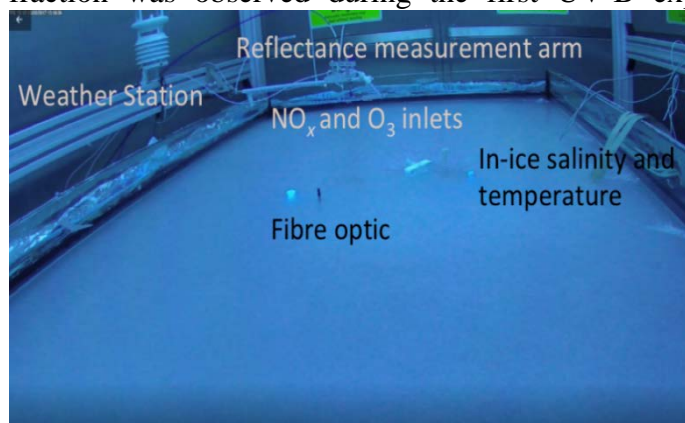


Figure 1.2.10-15: Image of sea-ice bathed in UV-A and UV-B light, taken by remote camera.

CNRS-IRCELYon investigated photosensitized chemistry at the air-sea interface (Figure 10.3.3). This chemistry is a source of SOA. The experimental chamber contained water, humic acid as a proxy for dissolved organic matter, and nonanoic acid, a fatty acid proxy, which formed an organic film at the air-water interface and was used to mimic the sea surface microlayer. While in the dark, no chemistry was observed, upon irradiation, in the actinic region, a rich and complex processing of those chemicals was evidenced. This led to the formation of numerous gas products, including unsaturated ones. Those led to SOA formation upon ozonolysis. From these results, **CNRS-IRCELYon** derived a dependence of SOA numbers on nonanoic acid surface coverage and dissolved organic matter concentration.

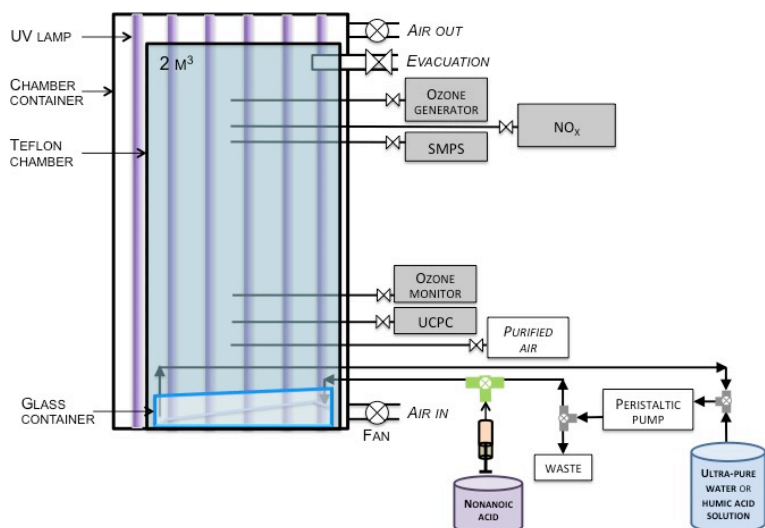


Figure 1.2.10-16: Scheme of the multiphase atmospheric simulation chamber used for the investigation of chemical processes at the air-sea interface.

CEAM has adapted the *EUPHORE chambers* to act as test beds where the photocatalytic activity of materials to diminish air pollutants can be assessed under near-natural atmospheric concentrations and conditions. These processes can be investigated as a function of concentration, light conditions, temperature, etc. For this purpose, the chambers have been provided with the following systems:

Structures to host different photocatalytic materials

Control RH, to maintain the relative humidity constant or apply specific profiles

Control NO_x , to simulate NO_x or NO conditions: constant values or specific profiles

At **TROPOS**, a variety of chamber studies were performed to investigate the efficiency of a photocatalytically active cement based coating material to depollute air contaminated with ozone (O_3), nitrogen oxides (NO_x) and some selected volatile organic compounds (VOCs). A special construction was set up to investigate the efficiency of such type of material in the **LEAK** chamber. The photocatalytically active material was compared with an inactive one, which had the same composition as the active, but without the photocatalyst titanium dioxide (TiO_2). By comparing both materials, it was hence possible to identify unambiguously the photocatalytically-driven effects. The active material showed a clear photocatalytic effect on O_3 and NO_x under irradiation that indicated the applicability of such materials to improve urban air quality. However, no photocatalytic influence was observed on the selected VOCs toluene and isoprene, emphasizing the importance of testing each individual class of compounds. The obtained kinetic parameters can be used for modelling to improve the understanding of the ongoing surface reactions. Besides these results, the product studies during the chamber experiments with NO_x , revealed a clear formation of O_3 at a relative humidity of $\geq 50\%$, possibly via the photocatalytic decomposition of adsorbed nitrate followed by the photolysis of the nitrate radical. This was the first time that such an undesired O_3 formation was observed on a cement based photocatalytically active material. Furthermore, a clear photocatalytically-driven formation of small (C1–C5) carbonyl compounds was observed even during clean air experiments. This observation indicated a photocatalytic degradation of the organic binder or additives of the substrate material, emphasizing the importance to test also each individual material composition. In conclusion, chamber studies are well suitable to test the reactivity/impact of active surfaces on air pollutants, with its main advantage to study in detail secondary chemistry ongoing, like the observed formation of harmful reaction products that have to be clearly characterized prior any application of such materials in a urban environment.

Enabling the study of more realistic source mixtures (sub-task 10.3.2)

FORTH has continued the development of its mobile dual chamber system. This system consists of two identical pillow-shaped smog chambers (1.5 m^3 each) mounted on metal frames. The two chambers are surrounded by UV lamps in a hexagonal arrangement yielding a J_{NO_2} of



Figure 1.2.10-17: Picture of the uncovered dual chamber system with the UV lights on during a test field deployment in Patras. The corresponding instrumentation is housed in the mobile lab in the left.

0.1 min^{-1} (Figure 1.2.10-20). Moreover, it can be used either with natural sunlight or the UV lamps. The system can be easily disassembled and transported enabling the study of various atmospheric environments. The system has been evaluated in a series of field deployments in Patras and Finokalia, Greece. Minimum levels of contamination were seen, signifying that it is possible to obtain clean particulate free conditions in the chambers during field deployments. The two chambers yielded similar results for aerosol composition and particulate loading when filled with ambient air. Size

dependent wall loss profiles were estimated for both chambers, showing that higher wall loss rates occur in the field and that they should be measured before each experiment.

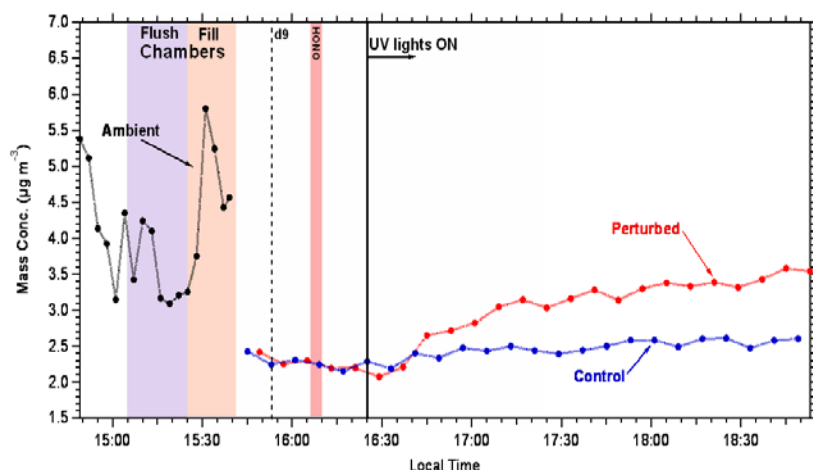


Figure 1.2.10-18: Evolution of the organic aerosol concentration in the two chambers. Formation of SOA was observed in the perturbation chamber which had higher OH levels. The experiment shows that approximately $1 \mu\text{g m}^{-3}$ can be formed in one hour or so at OH levels equal to 10^7 molecules cm^{-3} .

This SOA could not be explained by the measured volatile organic compounds (VOCs). Measurements of intermediate volatile organic compounds (IVOCs) are planned for future experiments. There was only $0.1 \mu\text{g m}^{-3}$ of sulfate also formed in the same experiment. One of the interesting results is that there was also new particle formation in the perturbation chamber. The particles reached 20 nm after approximately one hour of exposure to OH. This shows the potential of the system to be used for nucleation and growth experiments under ambient conditions.

During the next period, the system will be extended with the addition of an aethalometer for measurements of absorption at different wavelengths. A MAAP (multi-angle absorption photometer) is currently used for equivalent black carbon (eBC) measurements.

Experiments examining both fresh SOA formation and chemical aging of the existing organic aerosol (OA) will be performed with emphasis on both the absorption properties of the particles and new particle formation/growth. A paper describing the design, operation, and testing of the system by Kaltsonoudis et al. (2018) will be submitted for publication during the summer.

UEF has started investigations on the effect of the injection order and dilution of combustion emissions and reactant gases on chamber measurements and results. In *ILMARI chamber* the sample is diluted using a 3 stage dilution system (Figure 1.2.10-22) and the total dilution ratio is defined by CO_2 measurements. The current injection order in the experiments using the combination of exhaust emissions and single precursors is:

- 1) Combustion exhaust;
- 2) O_3 to convert NO to NO_2 to enable faster start for photochemistry;
- 3) Precursor VOC and marker (e.g., butanol-d9) injection;
- 4) HONO (or H_2O_2), or O_3 injection, whichever applicable;
- 5) VOC-to- NO_x ratio adjustment by adding propene (or NO_2) if needed
- 6) Lights on.

In the first tests both chambers were filled with ambient background urban air and HONO was injected in the perturbation chamber. Both chambers were exposed to the UV light of the chamber. In a typical experiment approximately $1 \mu\text{g m}^{-3}$ of secondary organic aerosol (SOA) was formed in the perturbation chamber (Figure 1.2.10-21) with an average OH of 10^7 molecules cm^{-3} .

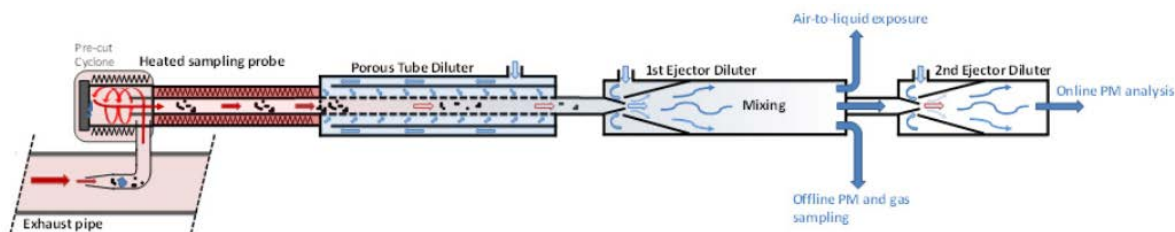


Figure 1.2.10-19: 3-stage dilution system used in ILMARI: after the heated sample line the emission is diluted by porous tube diluter and 1-2 ejector dilution depending on the emission concentration. Room temperature dilution air is used in all three diluters.

These protocols can be combined to study the simultaneous injection of the emissions from different combustion sources. In a recent measurement campaign (EUROCHAMP TNA, ILMARI-003-2017, 2018), simultaneous injection of wood combustion aerosol and diesel engine emission was applied successfully.

The NCAS-UMAN chamber has been coupled to a light duty diesel engine (VW 1.9L SDI, EURO-4 car equivalent), mounted on a test rig (CM12; Armfield Ltd., Hampshire, UK) and coupled to an eddy current dynamometer allowing control of engine speed and load conditions.

The collapsible 18 m³ chamber design enabled efficient cleaning and rapid filling at a high flow rate (3 m³ hr⁻¹) by a clean air source. A three-way valve enabled controlled amounts of the exhaust to be injected in the chamber allowing for a wide range of dilution ratios to be achieved. Using this setup, a comprehensive set of experiments has been conducted at realistic engine speed and load conditions and under a range of dilution ratios. The use of the chamber proved effective at enabling measurements of diesel exhaust using long sample times, even during unstable engine conditions. This approach has the advantage over direct sampling with diluters, in that even transient conditions can be sampled without requiring fast analysers. A further advantage is the wide range of exhaust dilution that can be studied, in

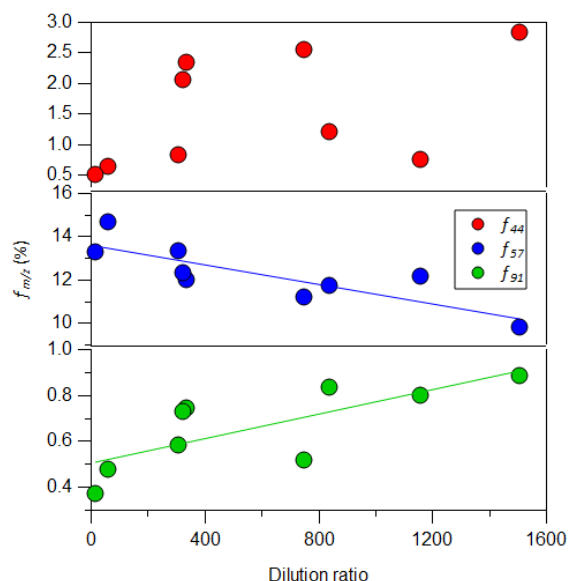


Figure 1.2.10-60: Fractions of the AMS organic signals at $m/z = 44$ (polyacids), 57 (alkanes), and 91 (aromatics) as a function of exhaust dilution ratio in the Manchester chamber.

terms of its effect on the particles. Based on CO₂ measurements in the raw (undiluted) exhaust and in the chamber, dilution factors of between 15 and 1500 have been achieved without the use of ejector diluters. Experiments using the same engine conditions were used to investigate the effect of dilution on particle properties. Single particle measurements showed that the initial coating thickness of particles was higher at the lowest dilution ratios, particularly during the cold start engine experiments. Furthermore, measurements using an aerosol mass spectrometer showed trends for the fractional contributions of key m/z fragments to the total organic mass signal (Figure 1.2.10-23). The slopes for f_{57} (alkanes) and f_{91} (aromatics) are statistically significant ($p < 0.05$; $R^2=0.69$ and 0.58 , respectively), indicating that increasing dilution reduces f_{57} and increases f_{91} , in turn implying that f_{57} represents semi-volatile alkanes and f_{91} less volatile aromatics. As for f_{44} , which represents multifunctional oxygenated species, one might

expect these to be involatile and give a positive trend with dilution factor. While this may be the case, the data are too variable for a trend to be deemed statistically significant. A publication outlining the influence of varying engine conditions on unregulated VOC and IVOC emissions (Pereira et al., 2018) has just been accepted.

PSI performed experiments of residential wood burning smog chamber experiments, in preparation for box model simulations, based on the volatility basis set (VBS) approach, performed within WP11. The experiments were conducted at different temperatures (-10, 2, 15°C), under different burning conditions (smouldering phase and flaming phase) and with three different residential logwood stoves (Bruns et al. 2016, Bertrand et al. 2017). SOA precursor compounds (VOCs) and total OA were simultaneously monitored by PTR-ToF-MS and HR-ToF-AMS respectively. Smog chamber data were complemented by real-time measurements of primary emissions which enabled the identification of the nature of SOA precursors lumped in different classes according to their chemical composition. The knowledge of the SOA precursor's nature was used to better constrain model parameters, in particular SOA production rates and molecular characteristics of the condensable gases formed. The consumption of VOCs from emissions over time was monitored and 95% of the total mass measured was selected as SOA precursors (86 compounds) and grouped into 6 classes according to their chemical composition. These classes include furans, single-ring aromatics, PAHs, oxygenated aromatics, and organic compounds containing more or less than 6 carbon atoms. The amounts of VOCs oxidized in the chamber were calculated and the resulting amount of condensable gases was used as input in the model to parametrise SOA formation. Furan and oxygenated aromatics generally contributed most to SOA formation, while the contribution of PAHs is the highest at low temperature (-10 °C).

These results were then used as input to the VBS box modelling described in Section 11.2.1, and the results will contribute to Deliverable D11.4 (due in Month 36).

TROPOS performed studies on atmospheric product formation using real emissions from biomass burning. Therefore, **the Leipzig Biomass Burning Facility (LBBF)** was connected to **LEAK** to study the combustion of biomass (e.g. straw) under defined conditions. In these experiments 400g straw were burned and the exhaust was sucked into an insulated chimney. In the centre of the chimney a fraction of the exhaust was transferred in a heated diluter (injection diluter, Dekati) and then injected into LEAK *via* a heated transfer line. The dilution ratio was calculated by measuring the CO mixing ratio in the chimney (emission gas analyser, MGA12) and after the diluter (CRDS, Picarro) and the ratio was approx. 1:600 in the experiments. Initial particle mass concentration was 60-105 $\mu\text{g}/\text{m}^3$ assuming a particle density of 1 that means at atmospherically relevant conditions. The atmospheric aging of the exhaust was executed by the photolysis of H_2O_2 as source for OH-radicals. The

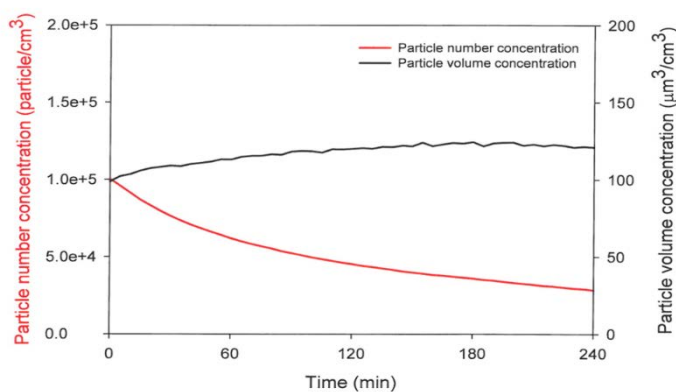


Figure 1.2.10-21: Evolution of particulate mass expressed as particle volume and particle number concentration during the oxidation of wheat straw exhaust.

formation of secondary particulate mass was monitored by use of a scanning mobility particle sizer (Figure 1.2.10-24). **These experiments are part of Milestone 55.**

FORTH has been investigating the process that take place during the chemical aging of the first generation products of the oxidation of anthropogenic and biogenic VOCs. The first set of experiments focused on the aging of the products of α -pinene ozonolysis at low and high NO_x conditions. For the low NO_x conditions, with an OH exposure equivalent to 2-4 days of typical atmospheric oxidation conditions, the OH aging of the α -pinene ozonolysis products formed 20-40% additional SOA mass for the experimental conditions used in this work. Elevated RH

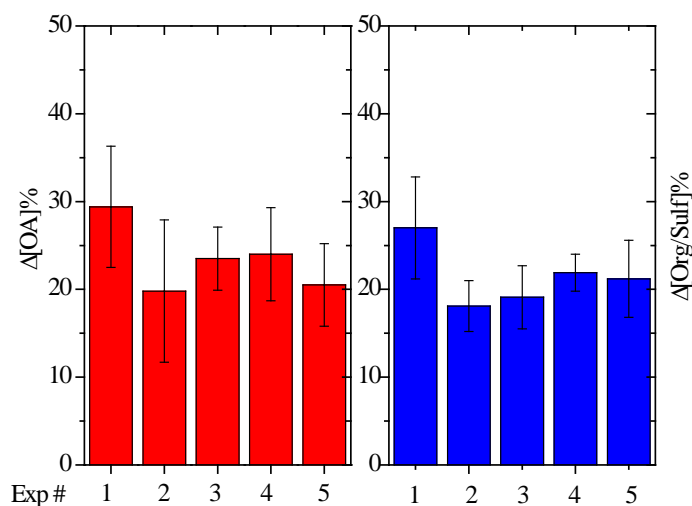


Figure 1.2.10-22: SMPS-derived percent change in the particle wall-loss corrected SOA (red columns) mass concentration after aging and AMS-derived percent change in organic to sulfate ratio (blue columns) after aging for five experiments under different conditions.

up to 50% has minimum effect on SOA production due to aging. The aging effects on additional SOA formation were constrained quantitatively using both SMPS and AMS measurements (Figure 1.2.10-25).

A more oxygenated product distribution was observed after aging. A stepwise increase of 0.02-0.04 in O:C was observed within half an hour after the first introduction of OH. After the second-generation products were exposed to additional OH, the O:C grew continuously until the end of the experiments with an absolute increase of up to 0.04. During this

period, minimum SOA production was observed. Details about this work can be found in Wang et al. (2018a). For the α -pinene ozonolysis experiments performed with high initial NO_x conditions, FORTH observed up to 25% additional SOA formation after aging, and an absolute increase of 0.03-0.05 in O:C with OH exposure equivalent to 2-6 h of ambient daytime conditions. The first-generation yields of these high NO_x experiments ranged from 14-16 % for SOA of 24-50 $\mu\text{g m}^{-3}$, about half of those from low-NO_x α -pinene ozonolysis experiments. This work is described in Wang et al. (2018b).

The **FZJ SAPHIR chamber** will be equipped with a new inlet system for the sampling of ambient air that is representative for mid-latitude European air influenced by biogenic and anthropogenic emissions. In order to avoid the influence of local sources like passing-by vehicles, the air will be sampled from 50 m above the ground. A 50 m-high tower was erected next to the SAPHIR chamber, but will be shortened to 10 m after an experiment period of 1 to 2 years (Fig. 10.3.8). The inlet line that will be mounted at the tower is made of stainless steel coated with SilcoNert[®] 2000 which makes the surface chemically inert. Inlet lines with SilcoNert[®] 2000 coating give a quantitative transmission of gaseous trace gases as shown in a comparison of OH reactivity instruments (Fuchs et al., 2017).

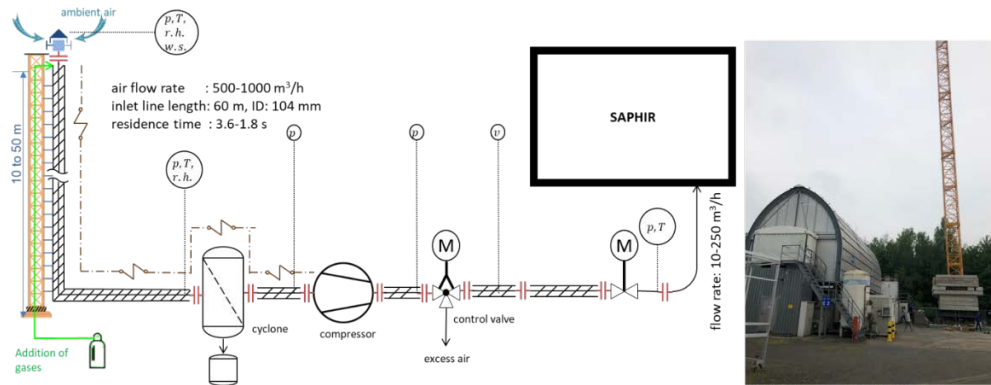


Figure 1.2.10-23: Installation of an inlet line for the SAPHIR chamber that allows sampling ambient air away from the surface layer so that local sources are not affecting the representativeness of the air mixture.

For the sampling of ambient air mixtures into SAPHIR best practice sampling was taken into account:

- Sampling from aloft (>10 m) to avoid the influence from local sources.
- Use of stainless steel coated with SilcoNert[®] 2000 to minimize wall loss of trace gases.
- Temperature control of the inlet lines by heating (~2°C above ambient) to avoid condensation of water vapour.
- Monitoring of temperature and flow rate at various locations of the inlet system.
- Use of a cyclone to remove large particles (>10 µm).
- Use of a high volume flow (>500 m³/h) that is only partly needed to flush the chamber with ambient air to minimize the residence time (<4 s) of air in the inlet system.

Enabling the study of the atmospheric processing of bioaerosols (sub-task 10.3.3)

The performance of the INFN chamber (*ChAMBRe*) to perform experimental studies on primary biological aerosol particles and bacteria in particular, has been quantitatively assessed. A protocol to handle the injection and extraction phases has been thoroughly tested both with Gram positive and Gram negative bacterial strains. With a clean atmosphere maintained inside ChAMBRe, the ratio between injected and extracted viable bacteria turned out to be reproducible at a 10 % level (Massabò et al., 2018), assessing this way the chamber sensitivity for systematic studies on bacterial viability versus environmental conditions. Such result is the first methodological step in view of a forthcoming systematic study of the correlation between bacterial viability and pollution levels.

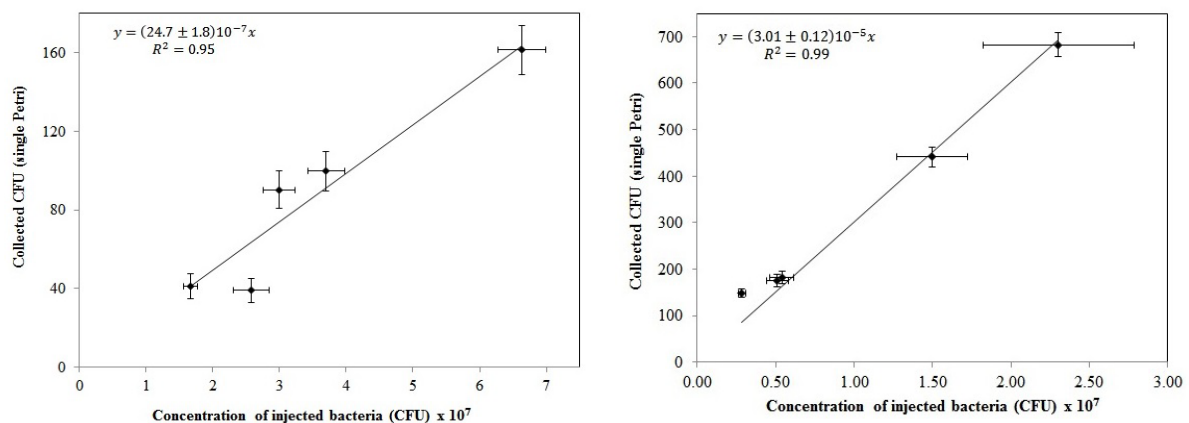


Figure 1.2.10-74: Average count on four Petri dishes exposed in each experiment vs. the number of B. Subtilis (left panel) and E. coli (right panel) bacteria injected in ChAMBRe (in units of 10⁷ CFU).

Strengthening of the instrumental capability of atmospheric simulation chambers to investigate atmospheric oxidation processes (Task 10.4)

New measurement technology for radical detection (sub-task 10.4.1)

Concerning RO₂ and HO₂ measurements, NCAS-Leeds has developed a new method for CH₃O₂ detection via the FAGE (Fluorescence Assay by Gas Expansion) technique converting CH₃O₂ to CH₃O via reaction with NO and detecting the CH₃O by laser induced fluorescence at ~298 nm (Onel et al., 2017a). Detection limits are ~10⁹ cm⁻³ for 5 minute averaging (so applicable to chamber measurements lasting ~ 1 hr in total) and ~10⁸ for 1 hr averaging giving the method potential for ambient CH₃O₂ detection in the remote atmosphere. Further work is currently underway to extend the methodology to look at higher RO₂ species; C₂H₅O₂ has been detected, but the reduced fluorescence quantum yield from higher alkoxy species will tend to reduce sensitivity. Nevertheless, the method should still be applicable to the higher radical concentrations of chamber measurements.

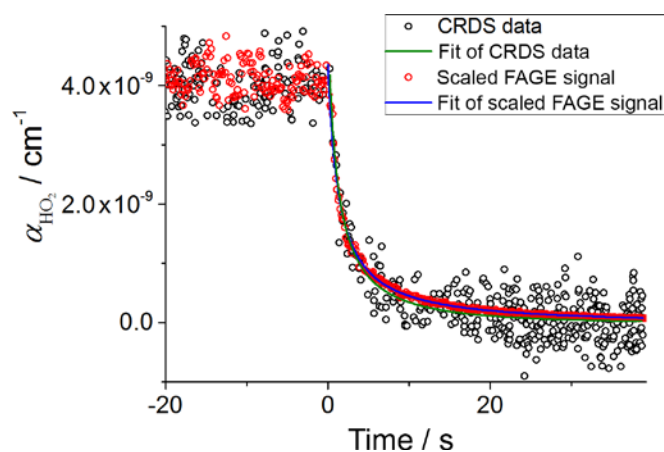


Figure 1.2.10-25: Inter-comparison of HO₂ decays recorded by CRDS and FAGE methods.

Additionally, NCAS-Leeds have performed the first direct inter-comparison of HO₂ measurements comparing FAGE and CRDS (cavity ring-down spectroscopy) measurements in the *HIRAC chamber*. A figure comparing the FAGE and CRDS HO₂ decays is shown below. This work is important in validating the FAGE technique, which, whilst being more sensitive, does rely on calibration to provide accurate values. The work has been published in AMT (Onel et al., 2017b) and a further

publication on an inter-comparison between CH₃O₂ FAGE and CRDS measurements is in preparation. Application of our CH₃O₂ instrument to studies of the CH₃O₂ self-reaction and the CH₃O₂ + HO₂ cross reaction are currently taking place.

CNRS-ICARE installed a chemical ionization mass spectrometry (CIMS) dedicated to OH and

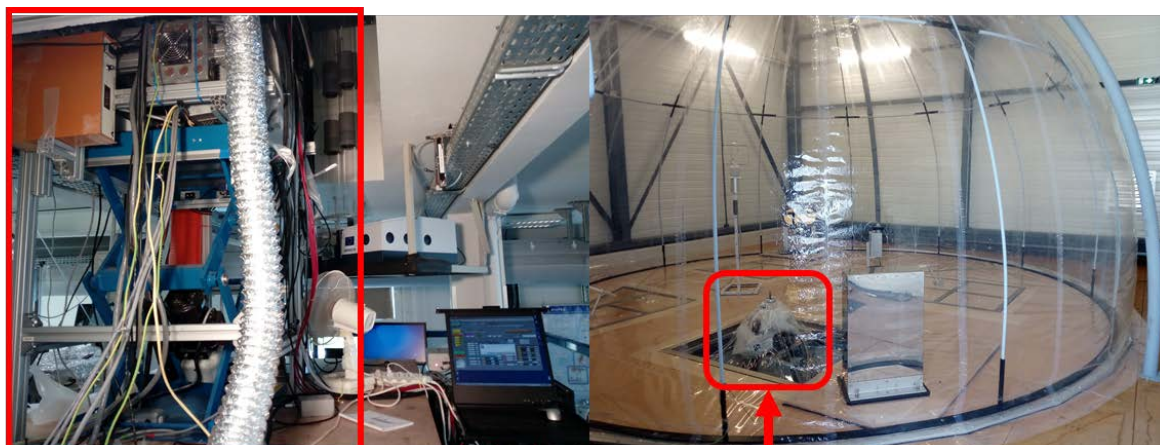


Figure 1.2.10-86: The chemical ionization mass spectrometry (CIMS) instrument for OH/RO₂ and H₂SO₄ measurements at HELIOS.

RO₂ radicals, as well as sulfuric acid concentration measurements at **HELIOS** (CNRS-ICARE) which is currently tested (Figure 1.2.10-29). Eventually CNRS-ICARE has not been able to commission a new LIF instrument for OH/HO₂ radical measurements which led to dropping down this specific project. On the other hand, to increase the capacities of HELIOS to investigate the atmospheric chemistry of NO₃/N₂O₅, a dedicated system for their measurements based on the cavity ring down spectroscopy is being built and should be available for the chamber studies within next few months.

UCC is designing two spectroscopy-based systems for the sensitive and selective detection of radical species in the new **IASC facility**. The first is an Incoherent Broadband Cavity Enhanced Absorption Spectroscopy (IBBCEAS) instrument for the *in situ* measurement of NO₃ radicals. This instrument is based on the original design of Venables et al. (2006), but will utilize a supercontinuum light source instead of a xenon arc lamp. This will improve the sensitivity of the technique to better than 2 pptv for a 1 min. acquisition time. The second system is a cavity ring-down spectroscopy instrument for the optical detection of OH radicals during atmospheric oxidation reactions. The ring-down setup will utilize a frequency doubled Nd:YAG pumped dye laser to address the detection of OH in an open path cavity. The strong rotational lines $Q_1(2)$, $Q_1(3)$, and $P_1(1)$ of the $A^2\Sigma^+(v'=0) \leftarrow X^2\Pi(v''=0)$ vibronic transition between 307.95 and 308.2 nm will be used for that purpose. In the first experiments a detection limit of 0.4 pptv in a 5 min. integration time is anticipated under ideal conditions. This is very close to, but not quite reaching typical ambient OH concentrations (ca. 0.1 pptv)

CNRS-LISA developed an Incoherent Broad Band Cavity Enhanced Absorption Spectroscopy (IBBCEAS) instrument and interfaced it to the CSA simulation chamber for *in situ* measurements of very low NO₃ radical concentrations. It involves irradiation of a high finesse

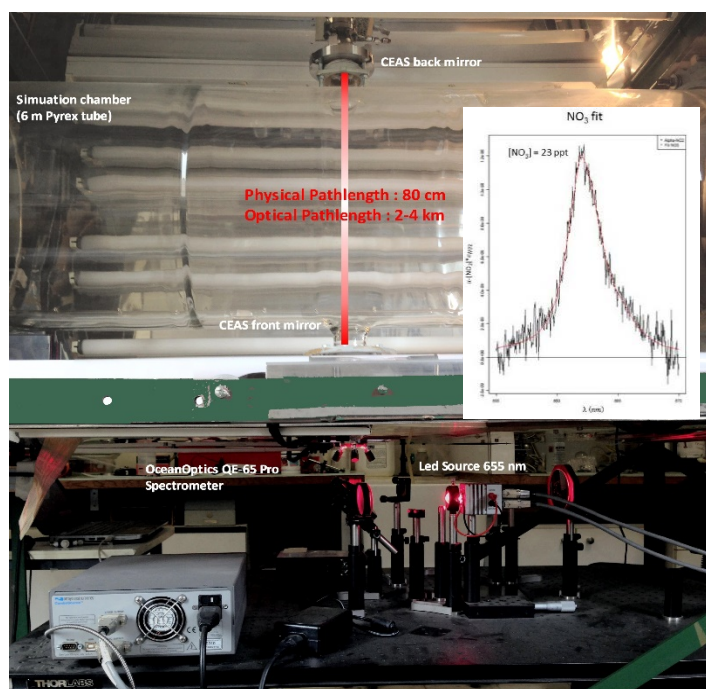


Figure 1.2.10-27: Recorded spectrum for 23 ppt of NO₃ and fit obtained by the software developed at CNRS-LISA.

optical cavity by an incoherent broadband light source centred on the 662 nm absorption band of the NO₃ radical. The optical cavity (82 cm of effective length) allows for several kilometres of effective absorption (up to 3 km, depending on the property of the mirrors) and high detection limits (up to 4 ppt for an integration time of 10 seconds). The technique is fully operational since March 2017 and has already been used to study fast reactions involving complex biogenic volatile organic compounds (with rate constants up to $1 \times 10^{-10} \text{ cm}^3 \text{ molecule}^{-1} \text{ s}^{-1}$). An example of a spectrum measured in the CSA for a mixture NO₂/NO₃ in air is given in Figure 1.2.10-30.

TROPOS used an NO₃⁻-CI-Api-TOF mass spectrometer for measuring the OH-radical

concentration using the method of Eisele and Tanner (1993). Here, SO_2 was introduced into the inlet of the mass spectrometer which reacts with OH-radicals and the formation of H_2SO_4 . The H_2SO_4 concentration is then measured by the mass spectrometer and serves as measure for OH-radicals. These experiments have been performed at the flow tube at TROPOS. Photolysis of ozone and H_2O_2 as well as the ozonolysis of tetramethylethene (TME) was used as OH-radical source. In the experiments with H_2O_2 , a dark formation of H_2SO_4 was observed, which means that this method was not useful. The photolysis of ozone and the ozonolysis of TME worked and in the ozonolysis the influence of Criegee-intermediates seems to be negligible. Preliminary experiments using this method on the simulation chamber LEAK were also performed.

New measurement technology towards a carbon balance (sub-task 10.4.2)

CEAM is constructing a CEAS (cavity enhanced absorption spectroscopy) to follow up several carbonyl secondary species like glyoxal or methylglyoxal. In fact, glyoxal is one important small compound that has been shown to be detectable by this technique. Accordingly, and after a thorough review of the extensive literature present (Thalman et al., 2015), a CEAS with two different kind of interchangeable cells (stainless-steel and quartz) with different diameters ($D = 15$ cm and 2.54 cm, respectively) and lengths ($L = 90$ cm and 64 cm, respectively) has been designed.

NCAS-UMAN conducted a set of experiments using Chemical Ionization mass spectrometry combined with a time-of-flight detector (TOF-CIMS) with the aim of identify and quantify OVOCs including organic acids and organic nitrates. The experiments focused on alpha-pinene SOA and utilised an iodide chemical ionisation scheme with the aim of looking at the detailed composition of gas phase oxidation products as well as condensed phase composition using a Filter Inlet for Gases and AEROSols (FIGAERO).

A second set of experiments investigating the formation of highly oxidised multifunctional organic compounds (HOMs) have been conducted using a nitrate ionization scheme and focused on a-pinene, isoprene and mixtures of both as SOA precursors. A third set of experiments investigated the formation of organic nitrates during the oxidation of benzene using hydroxyl radical in the presence of nitrogen oxides. Figure 1.2.10-31 illustrates the formation of organic nitrate in this oxidation system through the growth of a peak corresponding to $\text{C}_6\text{H}_5\text{NO}_3$ identified as nitrophenol. Similarly, the growth of $\text{C}_6\text{H}_4\text{N}_2\text{O}_5$ and $\text{C}_6\text{H}_3\text{NO}_4$ identified as dinitrophenol and nitro-benzoquinone, respectively followed the same trend as nitrophenol.

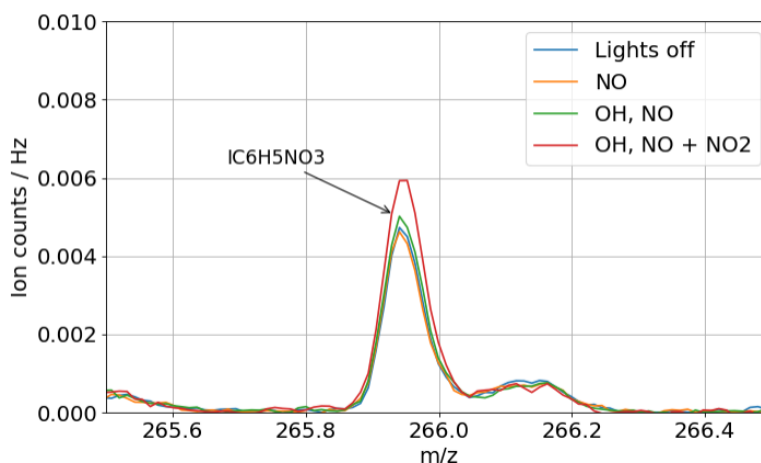


Figure 1.2.10-28: Growth of $\text{C}_6\text{H}_5\text{NO}_3$ identified as nitrophenol during benzene + OH experiment in the presence of NO_x . Benzene, NO_x and O_3 are introduced into the chamber under dark conditions until steady state is reached (blue curve). A UVA lamp is switched on and photolyses NO_2 leaving only NO (orange curve). The TUV lamp is switched on generating OH from O_3 photolysis (green curve). The UVA lamp is then switched off (red curve). Signal is greatest when NO_2 is present which is consistent with the production mechanism of this compound.

CNRS-ICARE has installed at *HELIOS* an Aerodyne High-Resolution Time-of-Flight Chemical Ionization Mass Spectrometer (HR-ToF-CIMS). The system has been tested for the characterization of the reaction products from the ozonolysis of biogenic volatile organic compounds in the presence

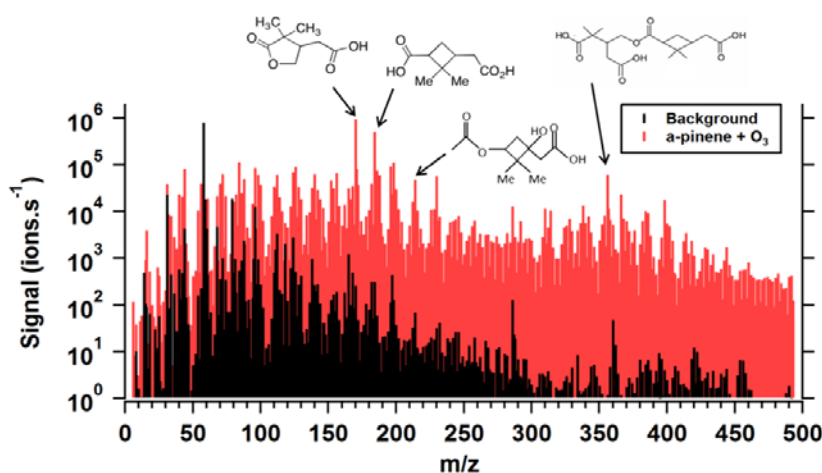


Figure 1.2.10-29: Comparison of aerosol phase mass spectra before (black) and after (red) a-pinene ozonolysis reaction.

of SO_2 , and their role in SOA production and growth. In order to monitor both the gas and particle phase, a Figaero (Filter Inlet for Gases and Aerosols) inlet was coupled with the HR-ToF-CIMS. Particulate matter is collected on a Teflon filter during gas-phase monitoring, and then thermally desorbed following a programmed temperature profile. Acetate primary ions are firstly generated using a ^{210}Po radioactive source which then ionizes analyte compounds in an ion-molecule reactor. This reagent allows us to be complementary with a PTR-ToF-MS by the detection of more oxygenated compounds such as organic acids, and also including organosulfate compounds which can have a significant influence on SOA production. α -pinene, isoprene and limonene ozonolysis are being studied in various but atmospherically realistic concentrations under dry conditions, in the absence and presence of SO_2 . The observed products in the gas and particle phases are in good agreement with the literature, and organosulfate compounds are still under analysis but seem to correspond to the ones identified by Orbitrap-HPLC-ESI-MS measurements so far. More than 600 different potential compounds have been detected up to $m/z = 473$ (Figure 1.2.10-32). NO_3 and iodide ion sources are also expected to be used in further experiments to be more selective towards highly oxygenated and organosulfate compounds.

CEAM carried out an optimization and adaptation of off-line with passive sampling, to on-line methods with active sampling, based on SPME double derivatiation for the analysis of highly oxygenated compounds in gas-phase. CEAM found that the optimal conditions compatible with the previous derivatization of carbonyl for a quantitative and reproducible process were: load the fibre with PFBHA, sample, load the fibre with MSTFA + TMCs, inject into the GC-MS (see Figure 1.2.10-33).

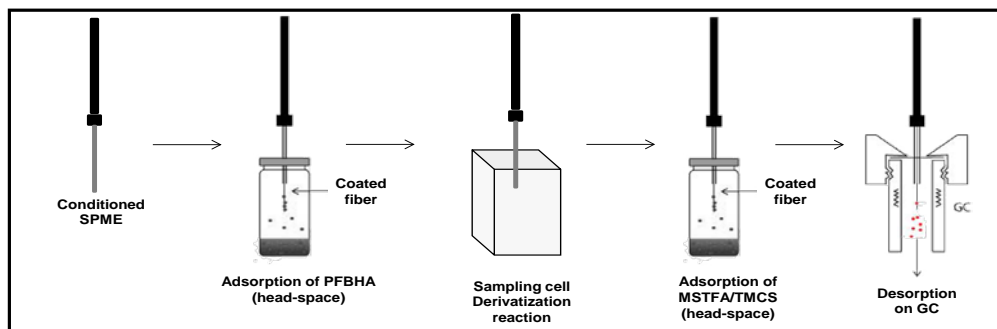


Figure 1.2.10-30: Derivatization protocol for hydroxy-carbonyl compounds.

This methodology is still in the process of validation since only 3-hydroxy-4-butanone are used as a model compound. Experiments with different mixtures of compounds and conditions (study of the competitiveness RH, interferences) were carried out during the small oxygenated inter-comparison that took place in *EUPHORE* from 21 to 31 May within WP3 and the results are still being analysed. This inter-comparison campaign will allow the comparison and validation of this methodology with a high number of on-line and off-line analytical techniques.

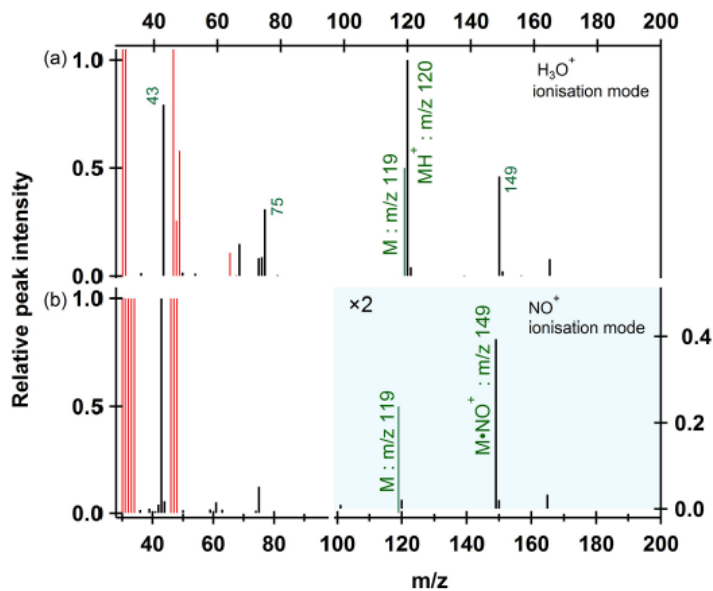


Figure 1.2.10-31: Recorded mass spectra of nitroxyacetone (black bars) with (a) H_3O^+ ionization mode ($E/N = 75$ Td) and (b) NO^+ ionization mode (with Radio Frequency mode and E/N estimated to 40 Td) (b). The thin green lines refer to the expected molecular ion of the analyte.

instrument has been operated in NO^+ mode by using dry air as reagent ion source gas. Different experimental conditions have been tested and optimized for synthesized standards of pure organic nitrates: alkyl nitrates, hydroxy-nitrates, carbonyl-nitrates and peroxyacyl nitrates. This study has shown that hydroxy- and carbonyl-nitrates have a high affinity towards NO^+ , leading to the formation of an adduct that allows the easy identification of the organic nitrate (R) from the R-NO^+ ion signal. Examples of spectra for nitroxyacetone are shown in Figure 1.2.10-34 for both ionization modes. Good detection limits, of few tens ppt per min have been obtained for these compounds. Alkyl nitrates have been shown to exhibit a moderate affinity towards NO^+ ionization leading to detection units of few hundreds of ppt. Finally, this method exhibits lower but nevertheless satisfying capabilities for the detection of peroxyacyl nitrates with detection limits in the ppb range. This method is fully operational on CSA and CESAM chambers and has recently been used for the study of $\text{VOC}+\text{NO}_3$ reactions. This work has been published in Duncianu et al. (2017).

BUW performed preliminary trials at *QUAREC* toward using mass spectrometry coupled with FT-IR data to achieve information on short lived/ reactive compounds formed in photochemical smog systems, relevant for urban air quality. Changes of personnel and the movement of the *QUAREC* chamber to a new laboratory did delay the work within this task. *QUAREC* is being moved during May – June 2018 to a new laboratory on the main campus. Following the

CNRS-LISA developed an innovative method for the measurement of organic nitrates by PTR-ToF-MS. Organic nitrates are key species which are formed by the degradation of VOCs under high NO_x and/or night-time conditions. However, few techniques are available for the measurement of individual organic nitrates in simulation chambers thus limiting the understanding of these chemical processes. Here, the operational protocol has been optimized in order to limit the fragmentation of organic nitrates in the PTR. In addition to the “classical” H_3O^+ ionization mode, the

relocation of the chamber, some maintenance work will be performed to upgrade it. Among other issues, the work comprises renewing the irradiation system (UV- and VIS-lamps) and reconditioning the mirrors of the White system.

Some efforts were spent in the design of sampling inlets for coupling of QUAREC with a GC-MS-MS instrument (Bruker, Model EVOQ GC-TQ) and, besides the existing FT-IR system, with an UV-VIS spectrometer (Horiba, Model iHR320). This allows for the possibility to study the evolution of complex systems such as those represented by real emission sources. Concurrently, it will allow achieving spectral information on various atmospheric species hence contributing to the evaluation of their atmospheric lifetime. This will target especially the range of volatile organics with known carcinogenic and mutagenic effects on living organisms and human health.

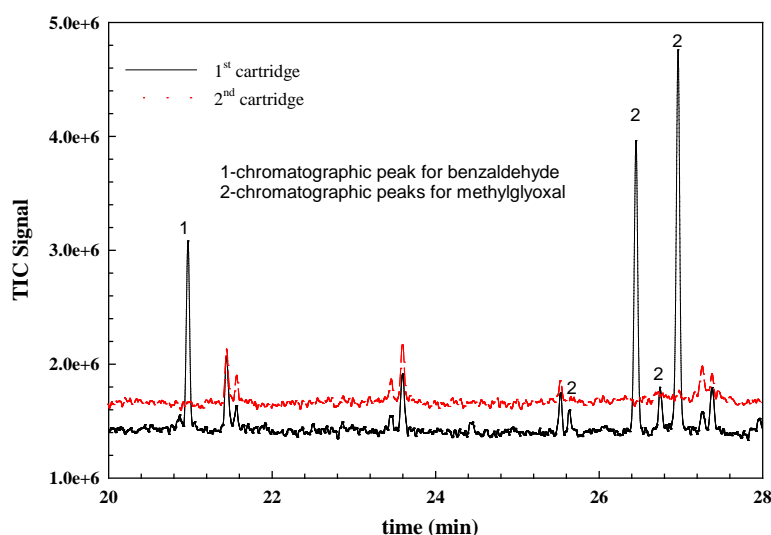


Figure 1.2.10-32: Typical chromatogram obtained (black line) after hexane extraction of the corresponding pentafluorobenzyl oximes of benzaldehyde (peak no. 1) and methyl glyoxal (peaks no. 2) collected from a 40 ppb mixture of these compounds in the ESC-Q-UAIC chamber at a flow rate of 1.01 l/min for 60 minutes. (Two chromatographic peaks will be observed for some of the interest carbonyls because of (E) and (Z) isomers).

The determination of selected carbonyl compounds in air. The analytes applicable to this method are derivatised to their corresponding pentafluorobenzyl oximes. The oxime derivatives are then extracted from the C18 solid phase with hexane. The hexane extracts are analysed by gas chromatography with ion-trap mass spectrometer detection (GC-MS). The GC uses a capillary column, helium as carrier gas and a fast oven ramp rate to dramatically decrease analysis time.

One important goal of this study is to generate accuracy, precision and method detection limit (MDL) data for at least the following compounds: formaldehyde, acetaldehyde, benzaldehyde, glyoxal and methyl glyoxal. It is expected that this method will be applied to the determination of target analytes over the concentration ranges typically found in simulation chamber (e.g. ppb level). Until now, the UAIC-CERNESIM group has obtained some preliminary results that encourages us for the next studies steps. As a first step, a mixture of methylglyoxal and benzaldehyde has been analysed. Thus, the preliminary experiments have shown that at least two of the target compound could be specified and quantified quite well. A typical GC-MS chromatogram is presented in Figure 1.2.10-35. This figure also highlights the fact that for such

The UAIC-CERNESIM unit performed experiments for the development of the off-line techniques to specify and quantify carbonyl compounds by a gas chromatography technique. The main objective of this study was to determine the optimal condition with respect to the ESC-Q-UAIC chamber characteristics for measurement of small carbonyls by using GC-MS system. The proposed method involves a gas chromatographic method optimized for the

studies, it is sufficient to use a single derivatised cartridge (red dash line from the figure does not show any information about the benzaldehyde and methyl glyoxal, is only background signal). However, more experiments are being undertaken in order to achieve all the proposed goals.

Organic hydroperoxides and peroxy acids have gained a lot of attention in recent years. Aerosol components with multiple peroxy functional groups (often defined as HOMs, highly oxygenated molecules) might play a crucial role in atmospheric particle formation. In addition, peroxides in general might also be relevant to explain the toxicity of particles in polluted air due to their oxidising properties. Despite their importance, there is an almost complete lack of appropriate standards to identify and quantify peroxides (and HOMs) in the atmosphere. NCAS-UCAM developed a synthesis method for several atmospherically relevant peroxydic acids, and characterised them in detail using HPLC-MS, MSMS fragmentation pattern and NMR. These detailed MSMS studies identified specific and diagnostic mass spectrometry signals, unique for peroxy acids, which will allow to identify unknown peroxy acids in aerosols in future studies to better understand organic aerosol formation processes and their toxicity. (Steimer et al., 2017).

NCAS-UCAM developed a novel online extractive electrospray ionisation mass spectrometry (EESI-MS) instrument to characterise organic aerosol components at a molecular level. Compared to many other online aerosol mass spectrometry techniques, EESI offers a very soft ionisation process, which leads to minimal fragmentation of organic aerosol components, facilitating their identification. SOA composition of particles generated in *CASC chamber* from alpha-pinene ozonolysis were analysed with online EESI and EESI-MS spectra were compared to conventional offline ESI-MS spectra. Good agreement between the online and offline technique was found in terms of the compounds identified. Major SOA components were detected at SOA loadings down to ca. $5 \mu\text{g m}^{-3}$. Experimental results were compared with a detailed chemical oxidation mechanism for alpha-pinene, the near-explicit Master Chemical Mechanism (MCM v3.3.1), and NCAS-UCAM showed that MS peak abundances scale with modelled concentrations for condensable products (e.g., pinonic acid, pinic acid, OH-pinonic acid) demonstrating the potential of this new online aerosol mass spectrometry technique.

References for WP10:

- Cain, K. P. and Pandis, S. N. (2017). A technique for the measurement of organic aerosol hygroscopicity, oxidation level, and volatility distributions. *Atmos. Meas. Tech.*, 10, 4865-4876.
- Coll, P., Lanone, S., Zysman, M., Cazaunau, M., Doussin, J.F., Derumeaux, G., Pini, M., Gratien, A., Pangu, E., Hüe, S., Relaix, F., Der Vatanian, A., Coll, I., Foret, G., Thavaratnasingam, L., Amar A., Mäder, M. and Boczkowski, G., Pollu-Risk: an innovative experimental platform to investigate Health impacts of Air Quality, AIR POLLUTION 2018 Conference, 19-21 June 2018, Napoli, Italia, Air Pollution XXIV, Wessex Institute of Technology Press, J.W.S. Longhurst, C. Capilla, C.A. Brebbia and J. Barnes (eds), 2018
- Di Biagio C., P. Formenti, Y. Balkanski, L. Caponi, M. Cazaunau, E. Pangu, E. Journet, S. Nowak, S. C., M. O. Andreae, K. Kandler, T. Saeed, S. Piketh, D. Seibert, E. Williams, and J.-F. Doussin. Global scale variability of the mineral dust longwave refractive index: a new dataset of in situ measurements for climate modelling and remote sensing, *Atmospheric Chemistry and Physics*, 17, 3, pp:1901-1929; 2017a.
- “Di Biagio, C., Formenti, P., Cazaunau, M., Pangu, E., Marchand, N., and Doussin, J. F.: Aethalometer multiple scattering correction Cref for mineral dust aerosols, *Atmos. Meas. Tech.*, 10, 2923-2939, 2017b

- Duncanu, M., David, M., Kartigeyane, S., Cirtog, M., Doussin, J.-F. and Picquet-Varrault, B., Measurement of alkyl and multifunctional organic nitrates by Proton Transfer Reaction Mass Spectrometry, *Atmospheric Measurement and Techniques*, 10, 1445-1463 (2017).
- Eisele F. L., and Tanner D. J.: Measurement of the gas phase concentration of H₂SO₄ and methane sulfonic acid and estimates of production and loss in the atmosphere, *J. Geophys. Res.*, 98, 9001-9010, 1993.
- France, J. L., King, M. D., Frey, M. M., Erbland, J., Picard, G., Preunkert, S., MacArthur, A., and Savarino, J.: Snow optical properties at Dome C (Concordia), Antarctica; implications for snow emissions and snow chemistry of reactive nitrogen, *Atmos. Chem. Phys.*, 11, 9787-9801, 10.5194/acp-11-9787-2011, 2011.
- Frey, W., Hu, D., Dorsey, J., Alfarra, M. R., Pajunaja, A., Virtanen, A., Connolly, P., and McFiggans, G.: The efficiency of secondary organic aerosol particles to act as ice nucleating particles at mixed-phase cloud conditions, *Atmos. Chem. Phys. Discuss*, in review, 2018.
- Fuchs, H., Novelli, A., Rolletter, M., Hofzumahaus, A., Pfannerstill, E. Y., Kessel, S., Edtbauer, A., Williams, J., Michoud, V., Dusanter, S., Locoge, N., Zannoni, N., Gros, V., Truong, F., Sarda-Esteve, R., Cryer, D. R., Brumby, C. A., Whalley, L. K., Stone, D., Seakins, P. W., Heard, D. E., Schoemaeker, C., Blocquet, M., Coudert, S., Batut, S., Fittschen, C., Thames, A. B., Brune, W. H., Ernest, C., Harder, H., Müller, J. B. A., Elste, T., Kubistin, D., Andres, S., Bohn, B., Hohaus, T., Holland, F., Li, X., Rohrer, F., Kiendler-Scharr, A., Tillmann, R., Wegener, R., Yu, Z., Zou, Q., and Wahner, A.: Comparison of OH reactivity measurements in the atmospheric simulation chamber SAPHIR, *Atmos. Meas. Tech.*, 10, 4023-4053, 2017.
- Fuller, S. J., Wragg, F.P.H., Nutter, J., and Kalberer, M.: Comparison of on-line and off-line methods to quantify reactive oxygen species (ROS) in atmospheric aerosols, *Atmos. Environ.*, 92, 97-103, 2014.
- Gallimore, P. J., Mahon, B. M., Wragg, F. P. H., Fuller, S. J., Giorio, C., Kourchev, I., and Kalberer, M.: Multiphase composition changes and reactive oxygen species formation during limonene oxidation in the new Cambridge Atmospheric Simulation Chamber (CASC), *Atmos. Chem. Phys.*, 17, 9853-9868, 2017.
- Gallimore, P. J., Giorio, C., Mahon, B. M., and Kalberer, M.: Online molecular characterisation of organic aerosols in an atmospheric chamber using extractive electrospray ionisation mass spectrometry, *Atmos. Chem. Phys.*, 17, 14485-14500, 2017.
- Kaltsonoudis C., E. Louvaris, K. Florou, N. Wang, A. Liangou, S. Jorga, and S. N. Pandis (2018) A new portable smog chamber facility for field studies, *Atmos. Meas. Tech.*, to be submitted.
- Kumar, N. K., Corbin, J. C., Bruns, E. A., Massabó, D., Slowik, J. G., Drinovec, L., Močnik, G., Prati, P., Vlachou, A., Baltensperger, U., Gysel, M., El-Haddad, I., and Prévôt, A. S. H.: Production of particulate brown carbon during atmospheric aging of wood-burning emissions, *Atmos. Chem. Phys. Discuss.*, in review, 2018.
- Liu, D., J. Whitehead, M. R. Alfarra, E. Reyes-Villegas, Dominick V. Spracklen, Carly L. Reddington, S. Kong, Paul I. Williams, Y.-C. Ting, S. Haslett, Jonathan W. Taylor, Michael J. Flynn, William T. Morgan, G. McFiggans, H. Coe and James D. Allan: Black-carbon absorption enhancement in the atmosphere determined by particle mixing state, *Nature Geoscience*, 10: 184, DOI: 10.1038/NGEO2901, 2017.
- Massabò D., Danelli S.G., Brotto P., Comite A., Costa C., Di Cesare A., Doussin J.F., Ferraro F., Formenti P., Gatta E., Negretti L., Oliva M., Parodi F., Vezzulli L., Prati P., ChAMBR: a new atmospheric simulation Chamber for Aerosol Modelling and Bio-aerosol Research, *Atmos. Meas. Tech. Discuss*, in review, 2018.
- Pereira, K. L., R. Dunmore, J. Whitehead, M. Rami Alfarra, J. D. Allan, M. S. Alam, R. M. Harrison, G. McFiggans, J. F. Hamilton, The Effect of Varying Engine Conditions on Unregulated VOC Diesel Exhaust Emissions, *Atmos. Chem. Phys.* accepted 2018.
- Steimer, S. S., Kourchev, I., and Kalberer, M.: Mass spectrometry characterization of peroxydicarboxylic acids as proxies for reactive oxygen species and highly oxygenated molecules in atmospheric aerosols, *Anal. Chem.*, 2017.
- Thalman, R., et al. Instrument inter-comparison of glyoxal, methyl glyoxal and NO₂ under simulated atmospheric conditions, *Atmos. Meas. Tech.*, 8, 1835-1862, 2015.
- Venables D.S., Gherman T., Orphal J., Wenger J.C., Ruth A.A., High sensitivity in situ monitoring of NO₃ in an atmospheric simulation chamber using incoherent broadband cavity-enhanced absorption spectroscopy. *Environ. Sci. Technol.* 2006, 40(21):6758-63.
- Wang N., E. Kostenidou, N. M. Donahue and S. N. Pandis (2018a) Multi-generation chemical aging of α -pinene ozonolysis products by reactions with OH, *Atmos. Chem. Phys.*, 18, 3589-3601, 2018.
- Wang N., M. Schervish, N. M. Donahue and S. N. Pandis (2018b) Multi-generation chemical aging of α -pinene ozonolysis products formed under high NO_x conditions, to be submitted.
- Zhou, J., et al. Particle-bound reactive oxygen species (PB-ROS) emissions and formation pathways in residential wood smoke under different combustion and aging conditions, *Atmos. Chem. Phys.* 18, 6985-7000, 2018

Work Package 11: Model development and evaluation to enhance and optimally exploit the chamber infrastructure (JRA2)

Development and evaluation of models to support infrastructure and aid interpretation of chamber experiments (Task 11.1)

Development and evaluation of chemical schemes in the gas and condensed phases (*sub-task 11.1.1*)

CNRS-LISA and NCAS-York have been working with Atmospheric Chemistry Services on the update and extension of structure-activity relationships (SARs) for the estimation of rate coefficients and branching ratios for gas-phase reactions of OH with aliphatic and aromatic organic compounds, for use in automated mechanism construction. This work has been summarised in Jenkin et al., (2018a) and Jenkin et al., (2018b), respectively. The group contribution methods were optimized using databases including sets of preferred rate coefficients for 489 aliphatic species and 67 mono-aromatic species. The overall performance of the SARs in determining $\log k_{298K}$ are summarized in Figure 1.2.11-1

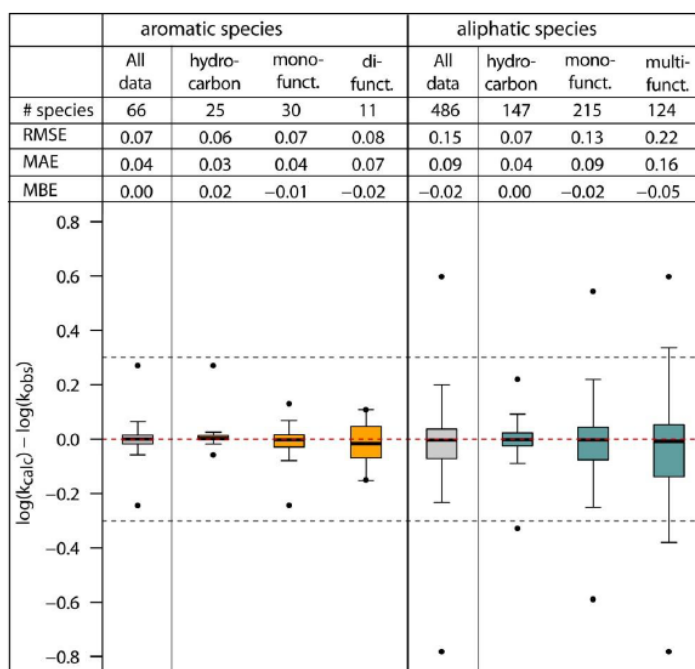
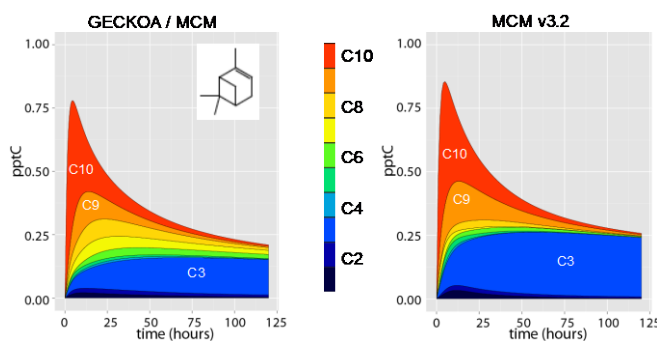


Figure 1.2.11-1: Root mean square error, mean absolute error, mean bias error and box plots for the error distribution in the estimation of k_{298K} values for full set and subsets of the aliphatic (Jenkin et al., (2018a)) and aromatic (Jenkin et al., (2018b)) species in the respective databases.

The above OH abstraction and addition SARs have now been coded into the **GECKO-A mechanism** generator for testing and evaluation under a range of different atmospheric and chamber relevant chemical scenarios. Figure 1.2.11-3 shows an example comparison between the new **MCM/GECKO-A** derived mechanism for α -pinene and the **MCM**.



NCAS-York has been working on a protocol for the self-generation of photolysis processes in chemical mechanisms. The protocol is based on a comprehensive literature review, which led to an extended database of 378 photolysis processes. Updates to the photolysis protocol have led to a refined description of photolysis in the Master Chemical Mechanism, where more compound classes are considered for photolysis, with more differentiation of structural and substituent effects. One focus was on the treatment of polyfunctional species. Figure 1.2.11-2 demonstrates that overall absorption cross sections, needed to describe the photolysis process in polyfunctional compounds containing both a ketone and a nitrate group, are the sum of the cross sections of the individual constituent chromophores. Any significant deviations in the synthesised spectrum (orange curve) from the experimental data (blue line) is in a wavelength range not relevant for tropospheric photochemistry (< 290 nm). Based on the analysis of the available

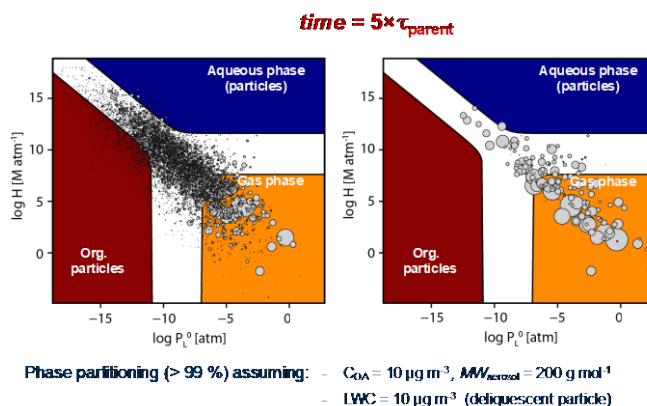


Figure 1.2.11-2: Comparison of the MCM and MCM/GECKO-A oxidation mechanisms of α -pinene under “continental scenario” conditions. Top panel – organic carbon budget, carbon chain length (gas-phase only). Bottom panel – Species oxidation trajectory phase diagrams.

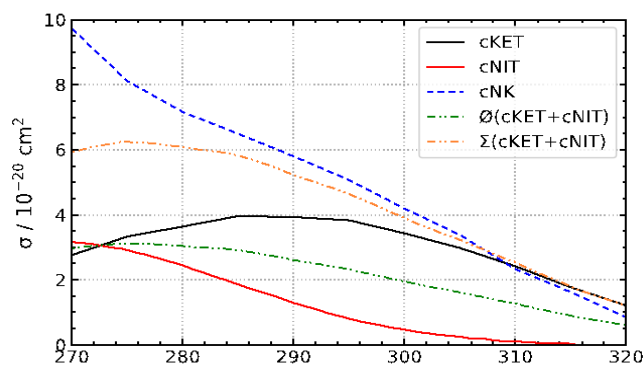


Figure 1.2.11-3: Example for the synthesis of absorption cross sections in polyfunctional compounds. cKET - cyclohexanone, cNIT - cyclopentyl nitrate (due to missing cyclohexyl nitrate data), cNK - 1-nitrooxy-2-oxo-cyclohexane. \emptyset denotes the average of the data, Σ the sum.

These are key intermediate species in the oxidation of aromatic compounds and furans. Modelling has been performed with an NCAS-York DSMACC chamber optimized box model in conjunction with the Master Chemical Mechanism v3.3.1 (MCMv3.3.1; <http://mcm.leeds.ac.uk/MCM>). This work recommends significant changes to the current MCMv3.3.1 chemical mechanism. The updated chemistry will be incorporated into upcoming versions of the MCM/GECKO-A chemical mechanism. These improvements will also feed into further analysis of aromatic photochemistry in chambers.

FZJ, BUW, CNRS-LISA and NCAS-York all contribute to the recently formed International Expert Panel for the “Development and Evaluation of Databases and Estimation Methods for

experimental data, this is one of the key rules in the new protocol, which is currently being coded into the **GECKO-A** mechanism generator by **CNRS-LISA**, based on rules and code provided by **NCAS-York**.

NCAS-York, UCC and BUW have worked on the analysis and interpretation of measurements of unsaturated 1,4 dicarbonyl photolysis experiments performed in the **EUPHORE** chamber.

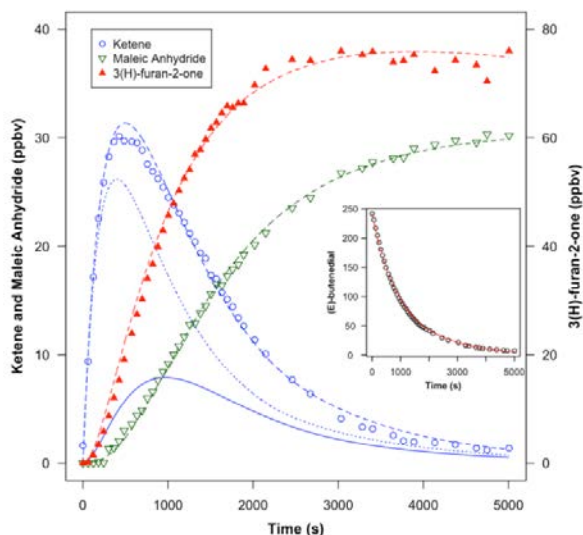


Figure 1.2.11-2: Measurements (points) and model simulation (lines) of major products of (E)-butenedial photolysis. The model uses an updated/optimised version of the MCMv3.3.1 chemical mechanism to give a good fit to the measurements.

Predicting Air Quality Impacts of Emitted Organic Compounds”, assembled on the behalf of the Coordination Research Council Atmospheric Impacts Committee. As part of this work, a perspective article on mechanism development and structure-activity relationships for gas-phase atmospheric chemistry mechanisms was put together by the panel and published in the International Journal of Chemical Kinetics (Vereecken et al., 2018). The idea of this paper was to provide a general overview and future directions of what could be improved in

atmospheric modelling, with emphasis specifically on the areas covered by the SAR panel working groups. Major sections included:

Discussion of gas-phase atmospheric

mechanism development and needs and approaches for improving mechanisms

The need for (evaluated) compilations of experimental and theoretical data

An overview of SARs and the methods employed

Discussion of the current status and problems with SARs and estimates for various reaction types – including multi-functionalisation

Discussion of SARs for thermochemistry as related to atmospheric mechanisms

A summary and outlook section that mentions the formation and planned work for the panel going forward

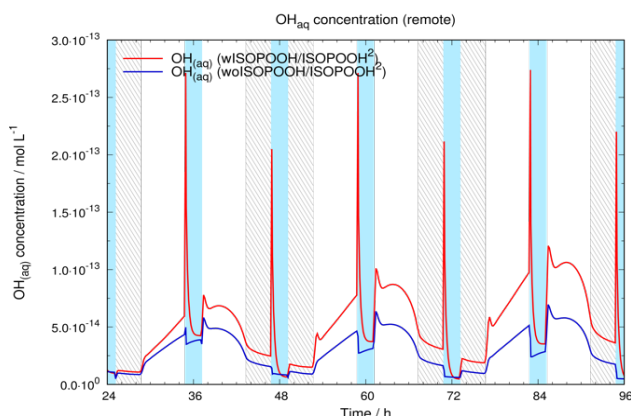
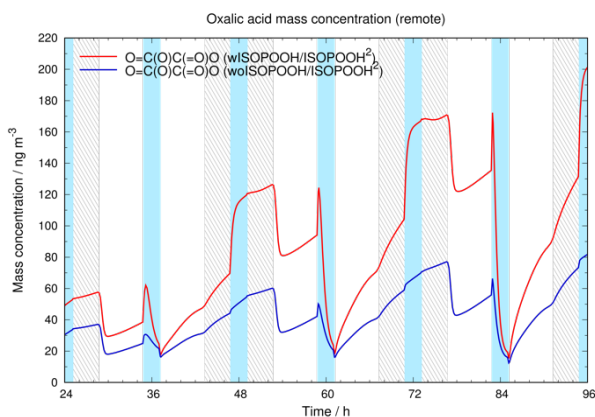


Figure 1.2.11-3: Modelled aqueous-phase OH (top) and oxalic acid (bottom) concentration with (red line) and without (blue) implemented chemistry of ISOPOOH/ISOPOOH₂ under remote environmental conditions. Blue solid and striped bars mark cloud and night-time conditions, respectively.

Recent **TROPOS-ACD** multiphase chemistry investigations into oxygenated organic hydroperoxides, ISOPOOHs and ISOPOOH₂ (dihydroxy dihydroperoxide)

have focused on their potential to act as OH sources and aqSOA precursors. The tropospheric gas-phase oxidation of isoprene under low NO_x conditions has attracted considerable attention in recent years. It leads to the formation of ISOPOOHs and ISOPOOH₂ that can chemically interact with deliquesced particles and clouds. For these studies, a first advanced multiphase chemistry module for ISOPOOHs/ISOPOOH₂ was developed. The module considers gaseous ISOPOOH₂ formation and, the phase transfer, aqueous photolysis, thermal decomposition and subsequent chemistry of ISOPOOHs/ISOPOOH₂ and its products. The developed module was

coupled to the existing multiphase mechanism **MCMv3.2/CAPRAM4.0**. Detailed studies with the air parcel model SPACCIM were performed for a remote environmental scenario. Simulations have shown that multiphase ISOPOOHs/ISOPOOH₂ chemistry can act as an important source for aqueous OH and aqSOA in both aerosols and clouds and affect the OVOC gas-phase compositions. In detail, the model runs have demonstrated that the gas-phase concentrations of ISOPOOH compounds are substantially lowered considering the new reaction module and that cloud chemistry may act as a potential sink for ISOPOOHs. Furthermore,



modelled aqueous concentrations of OH and important aqSOA compounds, such as oxalic acid, are substantially increased under both aerosol and cloud conditions (see Figure 1.2.11-5). For example, the modelled aqueous OH concentration is, on average, a factor of 1.8 higher in the simulation including ISOPOOHs/ISOPOOH₂ chemistry. These results constitute Deliverable D11.1 and further mechanism developments are still ongoing.

The **FORTH** team has used the **MCM mechanism** both as an evaluation exercise but also to find new ways of using such chemical schemes for the interpretation of their chamber measurements. The model was used for the simulation of the α -pinene ozonolysis system under high NO_x conditions. The experiments had two phases: the first generation of reactions and then a chemical aging stage in which HONO or HOOH was added to the chamber to produce OH. Because of the second stage, a radical scavenger could not be used in the first stage. As a result, the existing α -pinene could react with ozone, OH or the NO₃ radical. The MCM-based model performed well for both the high-NO_x and low-NO_x initial stage of the reactions.

In the ozonolysis experiments with high initial NO_x, the model results show that a significant fraction of α -pinene reacted with NO₃ despite the UV illumination (Figure 1.2.11-6). This is mostly due to the rapid and sustained production of NO₃ from the reactions between NO_x and excess O₃, and the lack of NO to efficiently scavenge the NO₃ and the rapid reaction rate of NO₃ with α -pinene.

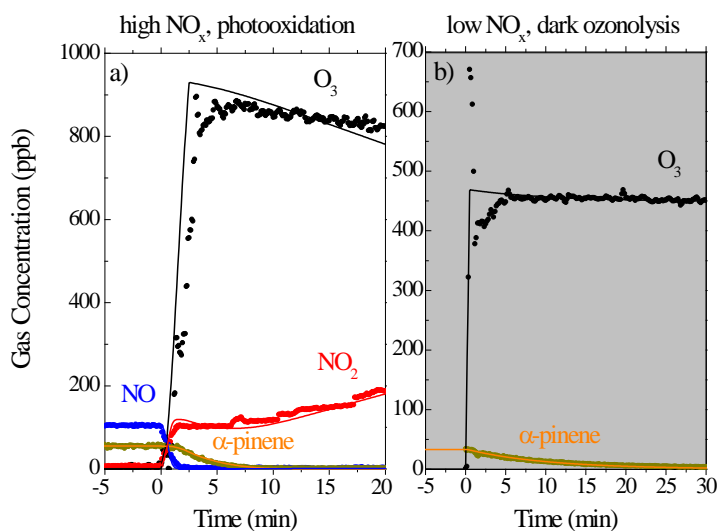


Figure 1.2.11-4: Model results of the gas and VOC concentrations (lines) together with the measurements (symbols) for a high and a low-NO_x dark ozonolysis experiment. The shaded area corresponds to periods when the lights were off in the chamber.

The α -pinene reacting with the three oxidants for a typical experiment are shown in Figure 1.2.11-6. The ozonolysis of α -pinene produced OH, which in turn reacted with α -pinene. The NO_3 pathway kicked in at $t=1$ min due to the fact that the NO_3 has to be generated first through $\text{NO} + \text{O}_3 \rightarrow \text{NO}_2$ and $\text{NO}_2 + \text{O}_3 \rightarrow \text{NO}_3$. The MCM captured well the precursor consumption and was capable of revealing the relative reaction channels and associated radical production under various NO_x regimes. For all aging experiments in this work, the first-generation chemistry was in the high NO_x regime even if half of the precursor reacted with NO_3 . This work illustrates the utility of chemical scheme for the interpretation of the results. This work is described in detail in Wang et al. (2018) that will be submitted for publication during the summer.

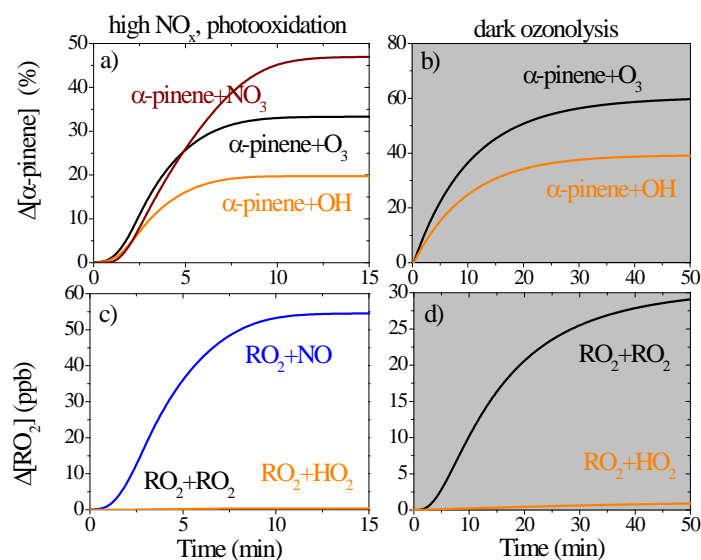


Figure 1.2.11-5: Model results of the fractions of α -pinene reacted with O_3 , NO_3 and OH and fate of RO_2 for a high and a low- NO_x dark ozonolysis experiment.

NCAS-UEA have overseen the release of **MISTRA** into the public domain. The microphysical marine boundary layer **model MISTRA** was originally developed as a microphysical model only and later extended to include gas, aerosol and cloud droplet chemistry. Apart from a description of the dynamics and thermodynamics, **MISTRA** includes a detailed microphysical module that calculates particle growth explicitly and treats feedbacks between radiation and particles. **MISTRA** has since been expanded on by several researchers to include a snow module, foremost and most recently Josué Bock (formerly **NCAS-UEA**; now at Météo France, Toulouse). A public release version of the model (version 9.0) with detailed installation instructions is now available at: <https://github.com/JosueBock/Mistra>. This public release version includes microphysics and chemistry, but not yet the snow module which is under continued development. Prior to the public release, important parts of the code were updated to Fortran90. Many bugs (e.g. related to the treatment of solar radiation) were eliminated. The portability of the code has been improved, and the model can now be run on multiple platforms. **MISTRA** v9.0 is distributed under the European Public Licence EUPL-v1.1.

Development and evaluation of codes for aerosol microphysics, mixing and wall effects in chambers (sub-task 1.1.2)

NCAS-UMAN have built on the previous chamber model developments to develop a user-friendly and portable coupled model of

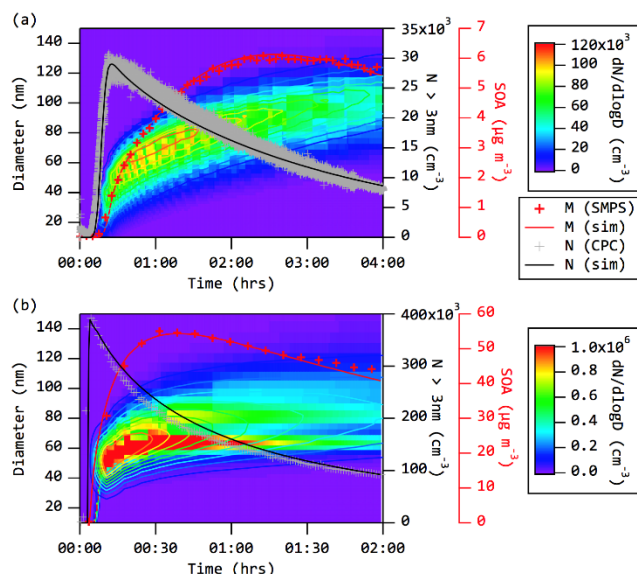


Figure 1.2.11-6: a-pinene ozonolysis in MICC and AIDA simulated using MCM in KPP coupled to MANIC using Perl mechanism generator (ASIT), with only wall loss (with effective absorptive wall mass for vapours) tuned.

gas-phase photochemistry and aerosol microphysics including wall treatments. The original chamber model was based on the ASIT Perl mechanism generator which, combined with the Kinetic PreProcessor (KPP), produced the Fortran coded **Model of Aerosol Numerics Including Chemistry (MANIC)**. Figure 1.2.11-8 shows a comparison between the chamber model simulations and the aerosol size distributions generated in nucleation experiments in a-pinene ozonolysis in the *MAC* and *AIDA* chambers with the *MCM* plus additional simplified ELVOC generation from the early rapid auto-oxidation.

The current work has recoded the model into a single user-friendly Python framework in order to maximize usage across EUROCHAMP partners. This was initiated in a number of parallel work streams. A flexible model for gas-phase chemistry was successfully built enabling the parsing of mechanisms from a variety of sources. It has been validated by comparisons using the MCM, using test cases from the MCM website. A module for the gas-particle partitioning of semi-volatile species was built that also simulates partitioning to chamber walls. Both chemical and physical models are based upon ordinary differential equations which are solved numerically using the CCode function of the *assimulo* package of ode solvers (<https://anaconda.org/chria/assimulo>).

These two models have been coupled with microphysics represented by a moving-centre sectional scheme, allowing evolution of particle sizes and compositions. Figure 1.2.11-9 shows simulation results of α -pinene ozonolysis into an ammonium sulphate aerosol seed distribution using the unmodified MCM 3.3.1. Contrary to the case in Figure 1.2.11-8, no ELVOC species are added to the mechanism, resulting in negligible particle growth.

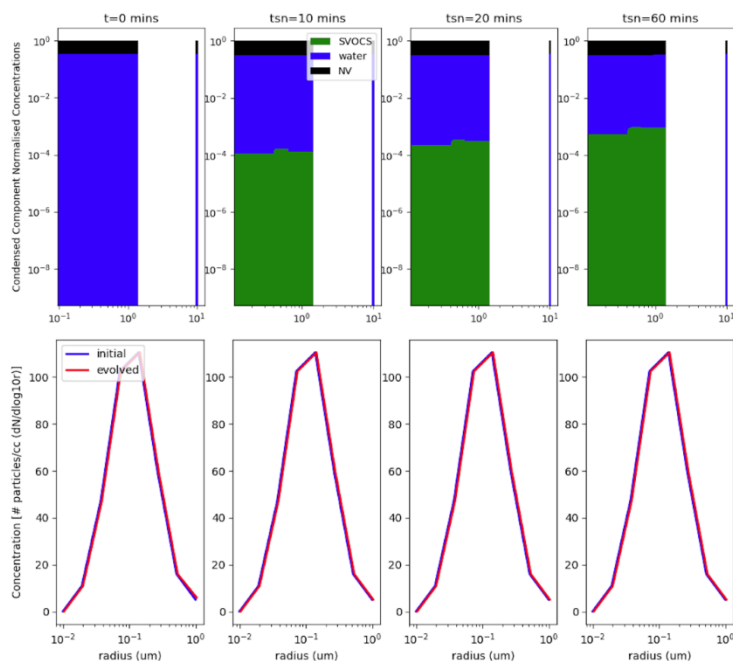


Figure 1.2.11-7: Coupled gas-aerosol simulation of ammonium sulphate seeded ozonolysis of α -pinene. The top panels show the particle composition distribution represented by 16 discrete size bins as it evolves over the first hour of the simulated experiment. As vapour-phase oxidation products are produced, they increasingly condense onto the particles. However, they are insufficiently low in volatility to lead to substantial additional mass in the particles. This is seen in the lower panels, where there is negligible growth of the particles. Contrasting this to the good agreement between model and measurement shown in Fig. 11.8 indicates the requirement to include ELVOC compound generation in α -pinene ozonolysis

for a variety of gas-phase chemistry scenarios studied in EUROCHAMP aerosol chambers (so far, α -pinene ozonolysis, α -pinene photo-oxidation moving onto photo-oxidation in α -pinene / isoprene mixtures). The large number of species in these systems requires good computation efficiency for reasonable model performance. NCAS-UMAN currently runs at 1/3 wall-clock time, aiming to improve for future Monte Carlo type simulations. Ongoing developments include the production of an installation package and model manual.

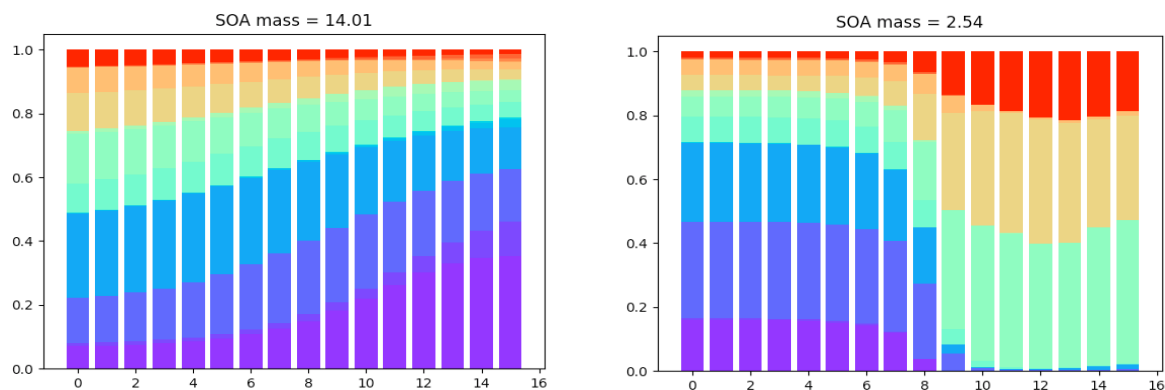


Figure 1.2.11-8: Composition distribution snapshots 1 hour into the simulated partitioning to an initially lognormal size distribution of moist ammonium sulphate particles – left hand panel assuming ideality, right hand panel with explicit non-ideality using AIOMFAC.

Component non-ideality can be explicitly considered using a variety of treatments. These may be particularly important when considering the formation of secondary organic aerosol on inorganic seed particles, where significant interactions may be experienced, leading to such effects as salting in or out and liquid-liquid phase separation. Figure 1.2.11-10 shows the results of idealized simulations partitioning 21 components to an evolving distribution, initially comprising ammonium sulphate seed particles at 60% RH. It can be seen that explicit consideration of non-ideality leads to an almost six-fold decrease in organic particle mass formed. Such effects will have a substantial impact on interpreting yield data.

The combined gas- and particle-phase model is undergoing testing

The **FORTH** team has continued the development of their **Aerosol Parameter Estimation (APE) model** (Pierce et al., 2008) that simulates the processes of condensation/evaporation, coagulation and particle wall loss during a chamber experiment (Wang et al., 2018). By

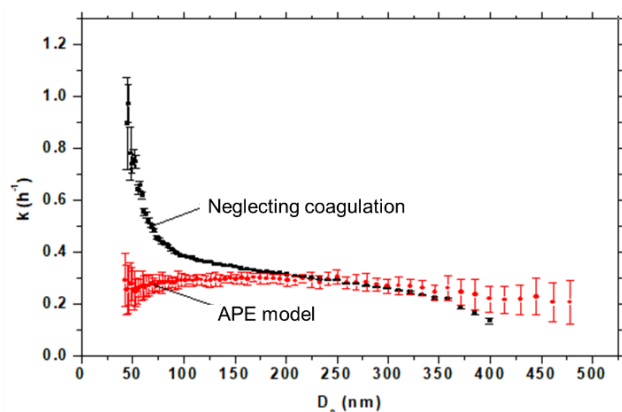


Figure 1.2.11-9: Estimated particle wall-loss rate constant, k , for a typical loss characterization experiment in the FORTH chamber neglecting coagulation (black symbols) and using the APE model that corrects for coagulation.

assuming Brownian coagulation is the only other particle process occurring in the chamber (i.e. no condensation/ evaporation occurred during the analysed portion of the experiment). The size-dependent, instantaneous particle loss rates are calculated directly from the SMPS-measured seed number size distribution at each time step. These instantaneous $k(D_p)$ values are then averaged over the initial seed loss period of the experiment (or a separate experiment where $k(D_p)$ was characterized). This determined $k(D_p)$ can then be applied to the SOA formation period of experiments to correct for the size-dependent wall loss. This approach, focusing on specific wall-loss characterization experiments, has the advantage that the functional dependence of the wall-loss rate constant is directly calculated from the measurements by simply removing the effect of coagulation.

The results of the application of the simplified **APE model** can be seen in Fig. 1.2.11-11. Ammonium sulfate seeds were injected in the **FORTH chamber** and the evolution of their concentration was monitored with an SMPS. The size-dependent wall loss rate constant $k(D_p)$ was first estimated using the traditional approach; as the negative of the slope of the $\ln [N(D_p)]$ versus time line. This approach assumes that coagulation is negligible and predicts a steep increase in the losses for smaller particles. The predictions of the APE model suggest that most of the losses of the smaller particles in this characterization experiment were due to coagulation and not to losses to the walls. Tens of such experiments have been performed in the FORTH indoor and mobile outdoor chambers. Particle number losses due to coagulation can be significant for small particles (< 150 nm under conditions in this work). It is thus important to correct for this coagulation effect when calculating the particle wall-loss rate constants especially for experiments in which the behaviour of the nanoparticles is important (e.g., when they carry a significant fraction of the total particle mass). **The modified APE model will be made available to the EUROCHAMP community.**

constraining the unknown parameters with the SMPS-measured particle size distribution, the model can predict SOA formation for each experiment accounting for wall losses. The predicted particle wall-loss rates are both size- and time-dependent. A version of the APE model that can be directly applied to wall-loss characterization experiments (e.g., loss of ammonium sulphate particles to the walls) has been developed. The modified version of the **APE model** calculates the size-dependent wall-loss rate necessary to reproduce the observed size distribution

The **FORTH team** has used a Molecular Dynamics (MD)-based simulator to gain insights about the morphology of particles formed in atmospheric simulation chambers but also in the atmosphere. Simulations are performed in the isothermal-isobaric statistical ensemble at atmospheric conditions with a pre-specified number of molecules of the above compounds leading to the formation of a particle (Karadima et al., 2017).

Results of simulations of nanoparticles containing pure components or mixtures as proxies for chamber and atmospheric organics are shown in Figure 1.2.11-12 showing that organic molecules reside mostly on their own phase without dissolving in the ammonium sulphate solution in the particles and that they also reside close to the surface. The effect of the relative humidity (RH), organic content of the particles, and presence of multiple organic molecules in the same particle has been investigated (Karadima et al., 2018).

The behaviour was highly dependent on the molecular components. For example, cis-pinonic acid, which is a surfactant, was located mainly in the outer region of the particles, irrespective of its concentration. At higher organic mass fractions, the presence of cis-pinonic acid molecules in the interior regions increases; the majority of the molecules, however, accumulates near the surface. According to our simulations, MBTCA is more likely to be detected inside a particle's core than the less oxygenated cis-pinonic acid molecule. When both molecules are present in the same particle cis-pinonic acid creates a thin coating at the surface, which shields MBTCA molecules that reside further inside the particle. This work will be submitted for publication during the summer.

UEF has contributed to task 11.1.2 by developing a method for deriving organic aerosol properties from chamber experiments. The method is based on combination of numerical models that describe the aerosol evolution and the Monte Carlo Genetic Algorithm for optimizing the properties of interest. So far, the optimization algorithm has been coupled with a dynamical model for liquid particle evaporation/growth and with the Kinetic multi-layer model of gas-particle interactions in aerosols and clouds (KM-GAP) in order to derive volatility distribution (volatility basis set, VBS) and particle viscosity. Similarly, by implementing

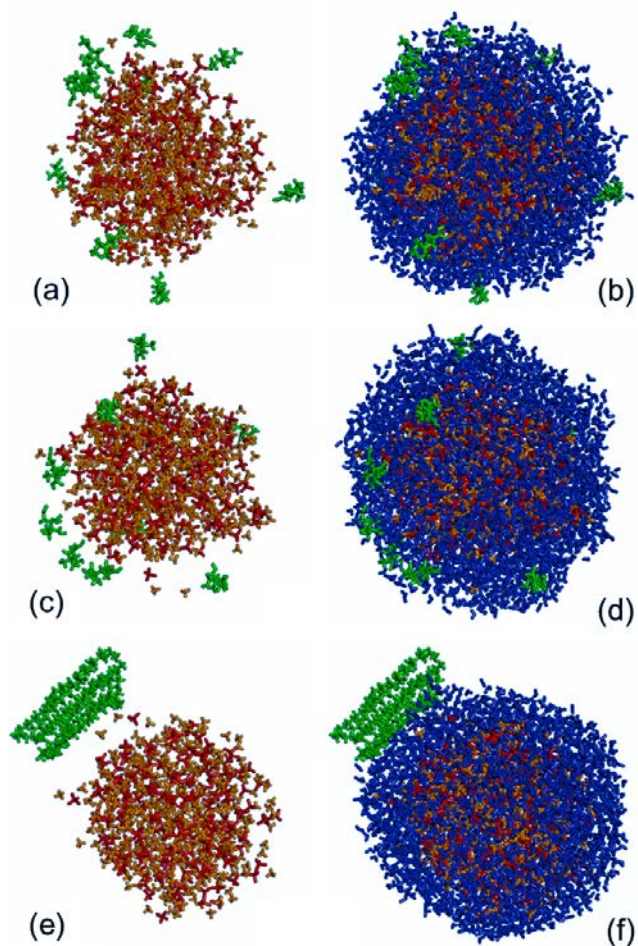


Figure 1.2.11-10: Snapshots of nanoparticles containing Cis-pinonic acid (a–b), MBTCA (c–d), and n-eicosane (e–f) for low organic mass fraction (7–10 %) and 50% RH omitting (a, c, e), and including (b, d, f) water molecules. Color notation: green for the organics: CPA, MBTCA, and n-eicosane, red for sulfate, orange for ammonium, and blue for water.

different numerical models, the method can be used for deriving other properties that can not be calculated analytically from the experimental data.

The **KIT team** has conducted CFD simulations of flow fields in the *AIDA* simulation chamber. For a better interpretation of dynamic chamber experiments such as cloud formation in adiabatic expansions KIT improves, constrains and evaluates Computational Fluid Dynamic (CFD) models. CFD simulations describing the flow fields, temperature, and humidity distributions within the AIDA chamber of KIT had been done using the ANSYS-CFX software. For future studies KIT uses the **COMSOL Multiphysics software** and has consequently developed a new CFD model for this software based on the AIDA 3D-CAD model (Inventor). The correct coupling of the physics modules was tested with a 2D representation of the AIDA chamber using rotational symmetry which reduces the computational effort substantially. The turbulent flows are represented with a $k-\epsilon$ model. Heat transfer and transport of trace species like water vapour are also included. Most challenging is still the parameterization of a realistic representation of the mixing fan.

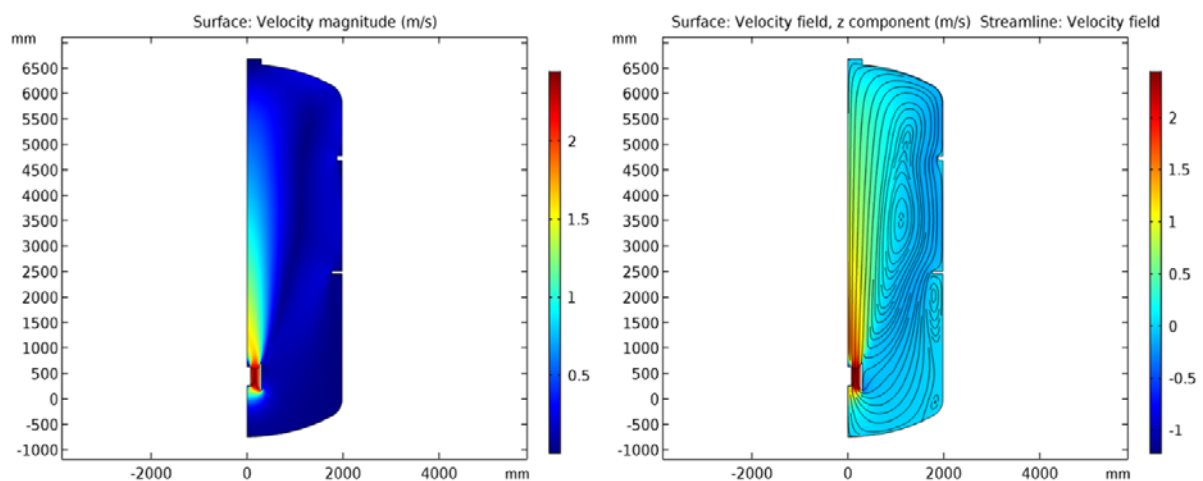


Figure 1.2.11-11: Stationary flow fields inside the AIDA simulation chamber as calculated using COMSOL Multiphysics.

Comparison of the average temperature and relative humidity with measured values showed a good agreement with the CFD model for an adiabatic expansion experiment with reducing the chamber pressure from 1010 to 870 hPa within 240 seconds. Further validation of the new CFD model will be done by comparison with experiments including dedicated flow measurements.

The **TROPOS** team has conducted development work on the modelling of turbulence driven fluctuations in temperature, humidity, aerosol concentration and cloud processes that may affect cloud dynamical processes on various scales and thereby feed-back on the turbulent flow itself. These complex interactions make necessary the use of numerical models for the determination of suitable experimental conditions and the interpretation of experimental data. Within this task TROPOS has been adapting an existing combined computational fluid and aerosol dynamics model (Fluent/FPM) for modelling fluid flow and microphysical processes inside *LACIS-T*. Due to limitations in both, the performance of the used microphysics model (population balance approach), and the high costs of the utilized CFD-code FLUENT, it was decided to additionally use and adapt the open source CFD toolbox OpenFOAM and the discrete phase model therein. Where feasible and meaningful, comparative investigations with both models have been carried

out. The related works are still ongoing. To document the general applicability and feasibility of the new OpenFOAM based model, Figure 1.2.11-143 depicts size distributions of hygroscopically grown and/or activated droplets for a sample experiment with LACIS-T.

NCAS-UMAN have developed an accessible cloud microphysics model to aid the interpretation of experiments carried in cloud chambers such as *MICC* and *AIDA*. The model is based on the underlying science of the **ACPIM model** (Connolly et al., 2012) and includes detailed cloud microphysical processes. The model is written in python 3 and development is ongoing to provide an interactive, easy to use, graphical interface.

Aerosol and cloud particles are represented by a series of size bins. Water condenses onto aerosol particles to form droplets. When ice is nucleated the aerosol particles within the ice are moved into the ice particle size distribution. The model follows two moments of aerosol, drops and ice crystals (i.e. both the number and mass are carried). Aerosol particles are represented by lognormal size distributions with any arbitrary composition. Droplet formation is calculated following the kappa-Köhler equation (Petters & Kreidenweis, 2007) and homogeneous ice nucleation follows Koop et al. (2000) and is based on water activity. Heterogeneous freezing is calculated according to the $n_s(T)$ parameterisation (Connolly et al., 2009 and Niemand et al., 2012) and is based on the number of ‘ice active sites’ present on the surface of an INP. Values for a and b in $n_s(T) = 10^{(aT+b)}$ are required for each INP type. Pressure and temperature drop rates are prescribed based on observations from chamber experiments. Values for a and b in $dy/dt = a e^{bt}$ for both temperature and pressure are required as input to the model. Currently, no collisions between particles occur in the model.

Example simulation – model output from a typical simulation of a chamber experiment is shown in Figure 1.2.11-15. In this example the model was initialized with two lognormal models of aerosol, one representing ammonium sulphate and the other k-feldspar. The values for the model parameters used are given in Table 1. Values in the square brackets are for each of the two modes of aerosol.

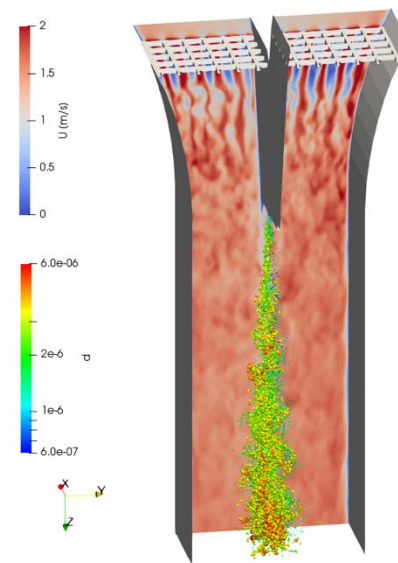


Figure 1.2.11-12: Spatial velocity and droplet (droplets coloured according to size) distributions inside LACIS-T. The turbulence induced inhomogeneities in the velocity and droplet (both spatial and size) distributions are clearly visible.

Aerosol number concentration (cm ⁻³)	[688, 200]
Aerosol median diameter (nm)	[100, 200]
Geometric standard deviation	[0.51, 0.5]
κ	[0.61, 0.0061]
Molecular weight (g mol ⁻¹)	[132, 556]
Density (kg m ⁻³)	[1770, 2560]
n ^s a	[0, -0.1963]
n ^s b	[0, 60.2118]
RH	0.9
T (K)	250

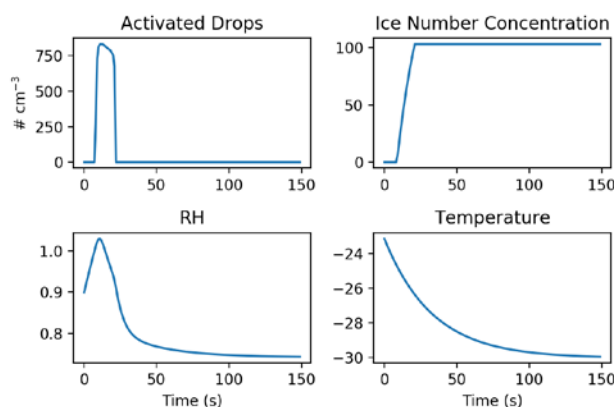


Figure 1.2.11-13: Simulation results with initial conditions indicated

The model has been tested against the **ACPIM model** using the Monte-Carlo sampling technique to randomise simulation initial conditions showing very good agreement. Further model evaluation will take place as an ongoing activity as more features are added to the model. Development of the model core and all standard functionality is now complete. Design and development of a user interface suitable for non-modellers is in progress, along with a protocol and model user manual, describing best standard practice for modelling cloud chamber experiments.

The model is available for all EUROCHAMP activities to all partners. It is currently on a private github repository whilst planning the method for web availability and source code distribution in the LADP pillar of the EUROCHAMP DC.

Development of modelling tools for optimal exploitation of chamber results through parameterizations for, and implementation in, 3-D atmospheric models (Task 11.2)

Development of modelling tools for the translation of EUROCHAMP results to VBS parameterizations (sub-task 11.2.1)

The **FORTH** team is continuing the development of the algorithm originally proposed by Stanier et al. (2008) for the fitting of smog chamber and other accompanying data to the Volatility Basis Set (VBS). Important aspects of the algorithm include: selection of minimum and maximum saturation concentration (C^*) values, selection of the number of basis set compounds, and estimation of uncertainty bounds for the regression prediction. Conceptually, the algorithm is trying to fit the available chamber measurements at different organic aerosol concentrations and temperatures using the VBS (Figure 1.2.11-16).

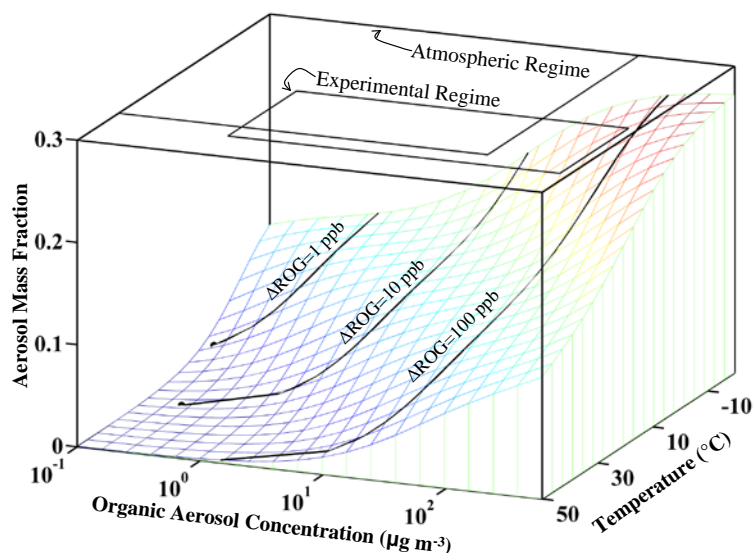


Figure 1.2.11-14: Conceptual diagram showing the yield (aerosol mass fraction, AMF) surface for a hypothetical set of semi-volatile oxidation products. Low temperatures and high existing aerosol loadings favor condensed phase partitioning (high AMF). Lines labelled Δ ROG show the expected temperature dependent AMF and aerosol concentrations for oxidation of fixed amounts of precursors under conditions of no pre-existing aerosol. Rectangles drawn over the surface show that experiments and the atmosphere can be considered with respect to their ranges of aerosol concentrations and temperatures.

An application of the algorithm is illustrated in Figure 1.2.11-17 for m-xylene SOA formation experiments at high NO_x. Results from three different studies under different conditions are integrated to obtain the optimum VBS parameters. One of the major advantages of this algorithm is that it shows the uncertainty of the obtained parameterization for different temperatures and organic aerosol levels. In this way it can guide the performance of future experiments.

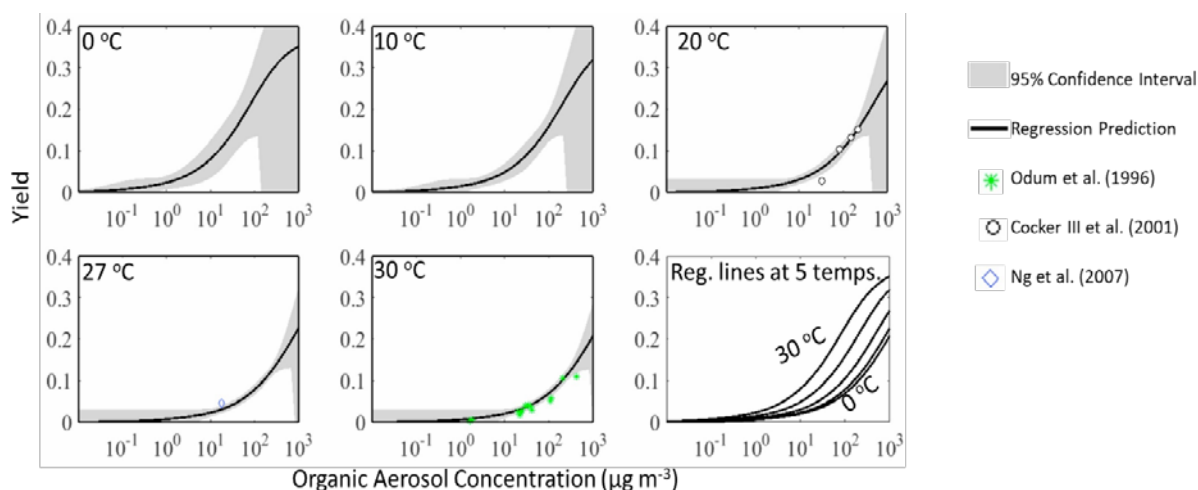


Figure 1.2.11-15: Fit of m-xylene photolysis SOA data at high NO_x using the Stanier et al (2008) algorithm. Regression lines (solid black lines) are shown for 5 different temperatures and have been calculated by fitting data (symbols) using the VBS Confidence intervals on regression are shown by grey shading.

This algorithm will be extended to include thermodenuder measurements to better constrain the enthalpy of vaporization and isothermal dilution measurements.

The **FORTH** team has also developed an algorithm for the derivation of VBS parameters combining thermodenuder measurements and isothermal dilution measurements. This approach can be applied to both primary and secondary organic aerosol and is based on the algorithm of Karnezis et al. (2014). This approach is illustrated in Fig. 1.2.11-17 for primary OA from cooking (COA). The COA from meat cooking was passed through a thermos-denuder and the mass fraction remaining was measured. At the same time, it was injected in a dilution chamber

where it was diluted isothermally by a factor of 10.

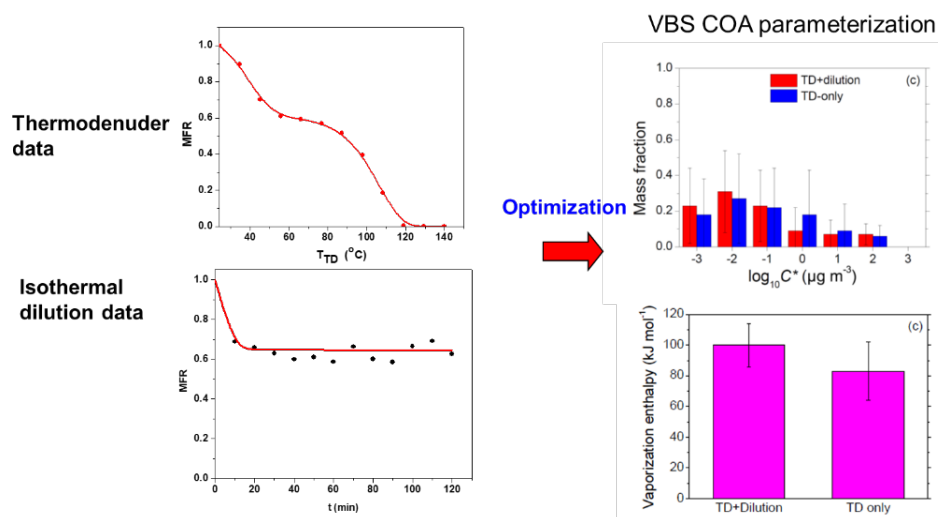


Figure 1.2.11-16: Illustration of the combination of thermodenuder data and isothermal dilution data of cooking OA to derive the VBS volatility distribution of the COA and its vaporization enthalpy.

The evolution of its mass concentration was also measured and expressed as mass fraction remaining. Both sets of measurements were carefully corrected for losses. Then the VBS was fitted to either the TD-data only or in the TD-dilution data and the corresponding VBS parameters were derived. The use of both data sets reduced the uncertainty of the corresponding parameters (Louvaris et al., 2017). This algorithm can become even more powerful if it is merged with the Stanier et al. (2008) one so that SOA yield measurements can be combined with thermodenuder data and isothermal dilution data. This work is in progress in **FORTH**.

PSI further developed the hybrid **volatility basis set (VBS)** box model by Ciarelli et al. (2017). The model was developed based on the partitioning model SOAP of the chemical transport model CAMx. SOAP uses the pseudo-ideal solution theory to partition secondary organic species between aerosol and gas phases. By using the measurements of non-traditional volatile organic compounds with a high-resolution proton transfer reaction mass spectrometer and organic aerosol concentration by an aerosol mass spectrometer during wood burning experiments, the box model was able to constrain volatility distribution of different precursor families. To initiate the simulation, PSI classified the measured condensable gases into 6 families (i.e. furans, single-ring aromatics, polycyclic aromatic hydrocarbons (PAHs), oxygenated aromatics, and organic compounds containing more or less than 6 carbon atoms). A genetic algorithm approach was applied to search for the best-fitting volatility distributions, which yield the lowest mean bias and root mean square error between modelled and measured organic aerosol.

The methodology, described here, improved on previous methods (Ciarelli et al., 2017) which only separated condensable gases into 2 components (semi-volatile organic compounds and intermediate-volatile organic compounds) rather than 6 distinct chemical families. The results showed that the simulated organic aerosol mass concentration with optimized parameters agreed well with measurements under different temperature and burning conditions (Figure 1.2.11-18). Furan and oxygenated aromatics generally contribute most to SOA formation, while

the contribution of PAHs is the highest at low temperature (-10 °C). These results will contribute to Deliverable 11.4 (due in month 36).

Development of modelling tools for the use of the EUROCHAMP aerosol-cloud interaction, aerosol chemistry and cloud chemistry results in CTMs (*sub-task 11.2.2*)

TROPOS have conducted developments of condensed chemical schemes for application in higher-scale models. In order to study the complex multiphase chemistry effects of aerosol-cloud-interactions in air quality models, reduced chemical schemes are required for the numerical simulation. Depending complexity of implemented chemical mechanisms, simulations will require a huge amount of CPU time and, therefore, very large computing clusters. Moreover, explicit chemical mechanism schemes grow exponentially in their number of chemical species and reactions depending on the number of hydrocarbons and are, therefore, not applicable in air quality models. Thus, the **TROPOS** started with the development of a software package for the detailed analysis of ordinary differential equation systems (ODEs) derived from multiphase chemical mechanisms, to obtain condensed ODE systems with fewer unknowns, which will reduce the amount of required computing power.

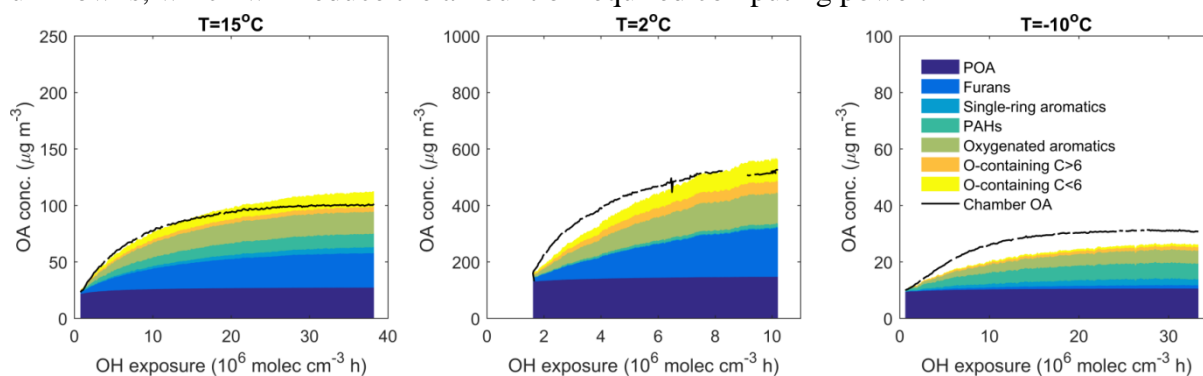


Figure 1.2.11-18: Comparison between simulated organic aerosol concentrations from different precursor families and measured concentrations by smog chamber experiments.

The ISSA method of Mauersberger (2005) was improved to be able to apply complex multiphase reaction mechanisms, with tens of thousands of multiphase reactions, to the reduction procedure. The algorithms of Tarjan (1972) and Johnson (1975) were implemented allowing an efficient calculation of reaction cycles, which are used to further reduce a given mechanism. The improved ISSA method is applied to identify important sets of species and chemical reactions/reaction cycles under different environmental conditions (Mauersberger, 2005). Deleting both redundant species and reactions leads to reduced mechanisms which accelerate the computation of the chemical code within both box-model or higher dimensional CFD simulations. **TROPOS** has performed several applications to both medium (i.e., **RACM+CAPRAM2.4**) and large (i.e., **MCM3.2+CAPRAM4.0**) mechanisms resulting in a first reduction of 40% up to 65% in the number of reactions, respectively (see Table 11.2 for details). The mean deviation of the target species between full and reduced mechanism is less than 10%. The computational costs of the reduced chemical mechanisms are lowered by about 55%. These results constitute Deliverable D11.5 and further mechanism reduction works are still ongoing.

Table 1.2.11-1: Summary of the number of compounds and processes in the full and reduced chemical mechanism (RACM_CAPRAM2.4, MCM32_CAPRAM40) as well as the reductions, and the required CPU times.

Parameter	RACM_CAPRAM2.4			MCM32_CAPRAM40		
	Full	Reduced	Reduction %	Full	Reduced	Reduction %
Number of compounds						
All	250	210	16.00	10199	5620	44.90
Gas phase	109	99	9.17	5941	3265	45.04
Aqueous phase	137	108	21.17	4255	2352	44.72
Number of processes						
All processes	787	515	34.54	23098	7971	65.49
Gas phase	281	223	20.64	14233	5175	63.64
Aqueous phase	328	146	55.49	6525	1626	75.08
Phase transfers	34	28	17.65	318	187	41.20
Dissociations	55	45	18.18	852	398	53.29
Computational costs						
Integration times (CPU time) / s	3.66	2.79	23.77	20.10	8.95	55.48

NCAS-UMAN have implemented a scheme allowing the dynamic partitioning of VBS components to sectional aerosol microphysical representation in the WRF-Chem model. This scheme is explicitly coupled to the cloud physics module allowing co-condensation of semi-volatile organic components and water vapour (Topping et al., 2013).

This has been tested in a number of geographical locations and the development and results are being written up for publication. Fig. 1.2.11-19 shows the difference in CCN and cloud droplets predicted in a domain covering the Southern UK and Northern France in July 2010 and the associated change in radiative forcing (Archer-Nicholls et al., 2016) attributable to these cloud adjustments.

The VBS scheme can be modified to incorporate the emerging outputs from 11.2.1. This will ensure optimum draw-through from

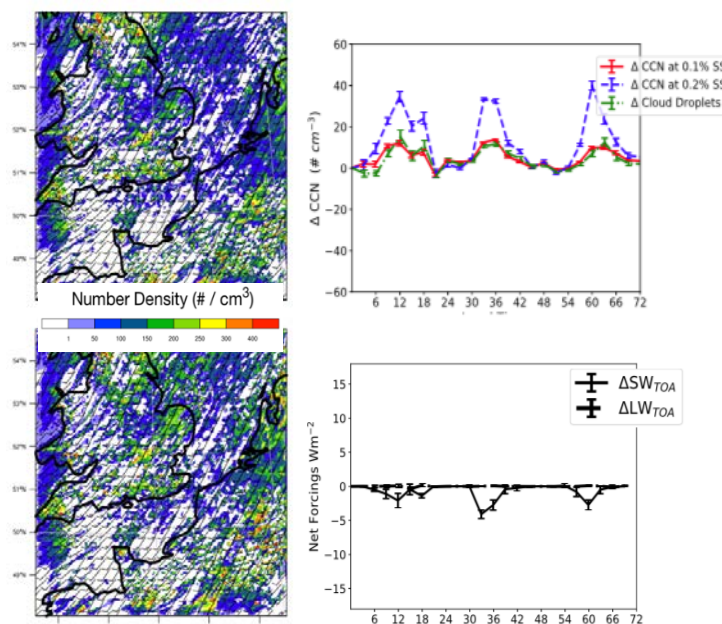


Figure 1.2.11-19: Differences in CCN, cloud properties and radiative forcing predicted to follow from co-condensation of semi-volatile organic vapours.

our chamber-informed understanding of OA volatility to inform large-scale model predictions of climate impact.

Development of modelling tools for the use of other EUROCHAMP results in CTMs (sub-task 11.2.3)

INFN activity at the *ChAMBR*e facility has been mainly addressed to establish the conditions to achieve the WP11 goals. A procedure to prepare, inject and collect viable bacteria in ChAMBR*e* has been set-up (see report on WP10) and published as a regular article (Massabò et al., 2018). The basic equipment to expose bacteria and/or other bioaerosol species to typical atmospheric pollutants, has been almost completed. In particular, O₃ and NO_x concentrations in ChAMBR*e* can be produced and monitored on-line. Such preparatory work has been accompanied by a fluid-dynamic simulation of the atmospheric simulation chamber to single out technical solution to increase the life time of bacteria (Fig. 22). Plans for completion of the study in fall 2018 have been made together the first exploratory experiments with a polluted atmosphere inside the chamber. Further activity to systematically study the correlation between air quality and different bacteria strains has been planned for 2019 to provide the key inputs for the modelling work in WP11.

References for WP11

- Archer-Nicholls, S., Lowe, D., Schultz, D. M. and McFiggans, G. (2016): Aerosol–radiation–cloud interactions in a regional coupled model: the effects of convective parameterisation and resolution, *Atmos. Chem. Phys.*, 16, 5573–5594, 2016
- Ciarelli, G., El Haddad, I., Bruns, E., Aksoyoglu, S., Möhler, O., Baltensperger, U., and Prévôt, A. S. H.: Constraining a hybrid volatility basis-set model for aging of wood-burning emissions using smog chamber experiments: a box-model study based on the VBS scheme of the CAMx model (v5.40), *Geosci. Model Dev.*, 10, 2303–2320, 2017.
- Connolly, P. and Emersic, C. and Field, P. R. A laboratory investigation into the aggregation efficiency of small ice crystals. *Atmos. Chem. Phys.* Vol. 12, pp. 2055–2076, 2012.
- Connolly, P. J. and Mohler, O. and Field, P. R. and Saathoff, H. and Burgess, R. and Choularton, T. and Gallagher, M. Studies of heterogeneous freezing by three different desert dust samples. *Atmos. Chem. Phys.*, vol. 9, pp. 2805–2824, 2009.
- Jenkin, M.E., R. Valorso, B. Aumont, A. R. Rickard, T.J. Wallington; Estimation of rate coefficients and branching ratios for gas-phase reactions of OH with aliphatic organic compounds for use in automated mechanism construction, *Atmos. Chem. Phys. Discuss.*, in review, (2018a).
- Jenkin, M.E., R. Valorso, B. Aumont, A. R. Rickard, T.J. Wallington; Estimation of rate coefficients and branching ratios for gas-phase reactions of OH with aromatic organic compounds for use in automated mechanism construction, *Atmos. Chem. Phys. Discuss.*, in review, 2018b.
- Johnson, D. B.: Finding All the Elementary Circuits of a Directed Graph, *SIAM Journal on Computing*, 4, 77–84, 1975
- Karadima K., V. G. Mavratzas, and S. N. Pandis (2017) Molecular dynamics simulation of local concentration and structure in multicomponent aerosol nanoparticles under atmospheric conditions, *Phys. Chem. Chem. Phys.*, 19, 16681–16692.
- Karadima K., V. G. Mavratzas, and S. N. Pandis (2018) Insights into organic aerosol morphology from an extended molecular dynamics study, *Atmos. Chem. Phys.*, to be submitted.
- Karnezi, E., Riipinen, I. and Pandis, S. N.: Measuring the atmospheric organic aerosol volatility distribution: A theoretical analysis, *Atmos. Meas. Tech.*, 7, 2953–2965, 2014.

- Koop, T. and Luo, B. and Tsias, A. and Peter, T. Water activity as the determinant for homogeneous ice nucleation in aqueous solutions. *Nature*, vol. 406, pp. 611–614, 2000.
- Louvaris, E. E., E. Karnezi, E. Kostenidou, C. Kaltsonoudis, and S. N. Pandis (2017) Estimation of the volatility distribution of organic aerosol combining thermogravimetric and isothermal dilution measurements, *Atmos. Meas. Tech.*, 10, 3909-3918.
- Mauersberger, G.: ISSA (iterative screening and structure analysis) - A new reduction method and its application to the tropospheric cloud chemical mechanism RACM/CAPRAM2.4, *Atmospheric Environment* 39, 39, 4341-4350, 2005
- Niemand, M. and Mohler, O. and Vogel, B. and Vogel, H. and Hoose, C. and Connolly, P. and Klein, H. and Bingemer, H. and DeMott, P. and Skrotzki, J. and Leisner, T. A particle-surface-area-based parameterisation of immersion freezing on desert dust particles. *J. Atmos. Sci.*, vol. 69, pp. 3077-2092, 2012.
- Petters, M. D. and Kreidenweis, S. M. A single parameter representation of hygroscopic growth and cloud condensation nucleus activity. *Atmos. Chem. Phys.*, vol. 7, pp. 1961-1971, 2007.
- Pierce, J. R., Engelhart, G. J., Hildebrandt, L., Weitkamp, E. A., Pathak, R. K., Donahue, N. M., Robinson, A. L., Adams, P. J., and Pandis, S. N.: Constraining particle evolution from wall losses, coagulation, and condensation-evaporation in smog-chamber experiments: optimal estimation based on size distribution measurements, *Aerosol Sci. Tech.*, 42, 1001-1015, 2008.
- Stanier C. O., N. Donahue, and S. N. Pandis (2008) Parameterization of secondary organic aerosol mass fractions from smog chamber data, *Atmos. Environ.*, 42, 2276-2299.
- Tarjan, R., Depth-First Search and Linear Graph Algorithms, *SIAM Journal on Computing*, 1, 146-160, 1972
- Topping, D., Connolly, P. and McFiggans, G.: Cloud droplet number enhanced by co-condensation of organic vapours, *Nat. Geosci.*, 6, 443–446, 2013
- Vereecken, L., B. Aumont, I. Barnes, J.W. Bozzelli, M. J. Goldman, W. H. Green, S. Madronich, M. R. McGillen, A. Mellouki, J. J. Orlando, B. Picquet-Varrault, A.R. Rickard, W. R. Stockwell, T. J. Wallington, W. P. L. Carter; Perspective on Mechanism Development and Structure-Activity Relationships for Gas-Phase Atmospheric Chemistry, *Int. J. Chem. Kinetics*, 2018.
- Wang N., M. Schervish, N. M. Donahue and S. N. Pandis (2018) Multi-generation chemical aging of α -pinene ozonolysis products formed under high NO_x conditions, to be submitted.
- Wang N., S. D. Jorga, J. R. Pierce, N. M. Donahue, and S. N. Pandis (2018) Particle wall-loss correction methods in smog chamber experiments, *Atmos. Meas. Tech. Discuss.*, 2018.

Annex 1: details about scientific outreach activities*Scientific articles***2018**

1. Arthur T. Zielinski, Peter J. Gallimore, Paul T. Griffiths, Roderic L. Jones, Ashwin A. Seshia, and Markus Kalberer. Measuring Aerosol Phase Changes and Hygroscopicity with a Microresonator Mass Sensor. *Analytical Chemistry* 2018 90 (16), 9716-9724. DOI: 10.1021/acs.analchem.8b00114.
2. Amalia Muñoz, Esther Borrás, Milagros Rodenas, Teresa Vera, and Hans Albert Pedersen. Atmospheric Oxidation of a Thiocarbamate Herbicide Used in Winter Cereals. *Environ. Sci. Technol.* 2018, 52, 9136–9144. DOI: 10.1021/acs.est.8b02157.
3. Dario Massabò, Silvia G. Danelli, Paolo Brotto, Antonio Comite, Camilla Costa, Andrea Di Cesare, Jean-François Doussin, Federico Ferraro, Paola Formenti, Elena Gatta, Laura Negretti, Maddalena Oliva, Franco Parodi, Luigi Vezzulli, Paolo Prati. ChAMBRé: a new atmospheric simulation Chamber for Aerosol Modelling and Bio-aerosol Research. *Atmos. Meas. Tech. Discuss.*, <https://doi.org/10.5194/amt-2018-147>.
4. Kelly L. Pereira, Rachel Dunmore, James Whitehead, M. Rami Alfarra, James D. Allan, Mohammed S. Alam, Roy M. Harrison, Gordon McFiggans and Jacqueline F. Hamilton. Technical note: Use of an atmospheric simulation chamber to investigate the effect of different engine conditions on unregulated VOC-IVOC diesel exhaust emissions. *Atmos. Chem. Phys.*, 18, 11073–11096, 2018, <https://doi.org/10.5194/acp-18-11073-2018>
5. Sarah S. Steimer, Aurélie Delvaux, Steven J. Campbell, Peter J. Gallimore, Peter Grice, Duncan J. Howe, Dominik Pitton, Magda Claeys, Thorsten Hoffmann, and Markus Kalberer. Synthesis and characterisation of peroxy-pinonic acids as proxies for highly oxygenated molecules (HOMs) in secondary organic aerosol. *Atmos. Chem. Phys.*, 18, 10973–10983, 2018 <https://doi.org/10.5194/acp-18-10973-2018>.
6. Martin Brüggemann, Nathalie Hayeck, Christian George, Interfacial photochemistry at the ocean surface is a global source of organic vapors and aerosols, *Nature Communications* volume 9, Article number: 2101 (2018), DOI: 10.1038/s41467-018-04528-7
7. Nivedita K. Kumar, Joel C. Corbin, Emily A. Bruns, Dario Massabó, Jay G. Slowik, Luka Drinovec, Griša Močnik, Paolo Prati, Athanasia Vlachou, Urs Baltensperger, Martin Gysel, Imad El-Haddad, and André S. H. Prévôt, Production of particulate brown carbon during atmospheric aging of wood-burning emissions, *Atmos. Chem. Phys.*, <https://doi.org/10.5194/acp-2018-159>.
8. Newland, M. J., Rickard, A. R., Sherwen, T., Evans, M. J., Vereecken, L., Muñoz, A., Ródenas, M., and Bloss, W. J.: The atmospheric impacts of monoterpene ozonolysis on global stabilised Criegee intermediate budgets and SO₂ oxidation: experiment, theory and modelling, *Atmos. Chem. Phys.*, 18, 6095-6120, <https://doi.org/10.5194/acp-18-6095-2018>, 2018.
9. L. Vereecken, B. Aumont, I. Barnes, J.W. Bozzelli, M.J. Goldman, W.H. Green, S. Madronich, M.R. McGillen, A. Mellouki, J.J. Orlando, B. Picquet-Varrault, A.R. Rickard, W.R. Stockwell,

- T.J. Wallington, W.P.L. Carter, Perspective on Mechanism Development and Structure-Activity Relationships for Gas-Phase Atmospheric Chemistry, *International Journal of Chemical Kinetics*, 2018, doi.org/10.1002/kin.21172.
10. Garcia-Santos, V., E. Valor, C. Di Biagio, V. Caselles, Predictive power of the emissivity angular variation of soils in the thermal infrared (8–14 μm) region by two Mie-based emissivity theoretical models, *IEEE Geosci. Rem. Sens. Lett.*, doi: 10.1109/LGRS.2018.2826446, 2018.
 11. A. G. Galon-Negru, R. I. Olariu, and C; Arsene, Chemical characteristics of size-resolved atmospheric aerosols in Iasi, north-eastern Romania: nitrogen-containing inorganic compounds control aerosol chemistry in the area, *Atmos. Chem. Phys.*, 18, 5879–5904, 2018, <https://doi.org/10.5194/acp-18-5879-2018>.
 12. E. L. Simpson, P. J. Connolly, and G. McFiggans, Competition for water vapour results in suppression of ice formation in mixed-phase clouds, *Atmos. Chem. Phys.*, 18, 7237-7250, 2018, doi: 10.5194/acp-18-7237-2018.1
 13. H. Fuchs, S. Albrecht, I.–H. Acir, B. Bohn, M. Breitenlechner, H.-P. Dorn, G. I. Gkatzelis, A. Hofzumahaus, F. Holland, M. Kaminski, F. N. Keutsch, A. Novelli, D. Reimer, F. Rohrer, R. Tillmann, L. Vereecken, R. Wegener, A. Zaytsev, A. Kiendler-Scharr, and A. Wahner. Investigation of the oxidation of methyl vinyl ketone (MVK) by OH radicals in the atmospheric simulation chamber SAPHIR, *Atmos. Chem. Phys. Discuss.*, <https://doi.org/10.5194/acp-2018-265>.
 14. David O. De Haan, Natalie G. Jimenez, Alexia de Loera, Mathieu Cazaunau, Aline Gratien, Edouard Pangui, and Jean-François Doussin, Methylglyoxal Uptake Coefficients on Aqueous Aerosol Surfaces, *J. Phys. Chem. A* 2018, 122, 4854–4860, DOI: 10.1021/acs.jpca.8b00533
 15. Jun Zhou, Peter Zotter, Emily A. Bruns, Giulia Stefenelli, Deepika Bhattu, Samuel Brown, Amelie Bertrand, Nicolas Marchand, Houssni Lamkaddam, Jay G. Slowik, André S. H. Prévôt, Urs Baltensperger, Thomas Nussbaumer, Imad El-Haddad, and Josef Dommen. Particle-bound reactive oxygen species (PB-ROS) emissions and formation pathways in residential wood smoke under different combustion and aging conditions, *Atmos. Chem. Phys.*, 18, 6985-7000, 2018 doi: 10.5194/acp-18-6985-2018.
 16. Yu Wu, Tianhai Cheng, Dantong Liu, James D. Allan, Lijuan Zheng and Hao Chen. Light Absorption Enhancement of Black Carbon Aerosol Constrained by Particle Morphology. *Environmental Science & Technology*, 2018, doi: 10.1021/acs.est.8b00636.
 17. Wiebke Frey, Dawei Hu, James Dorsey, M. Rami Alfarra, Aki Pajunoja, Annele Virtanen, Paul Connolly, and Gordon McFiggans. The efficiency of secondary organic aerosol particles acting as ice-nucleating particles under mixed-phase cloud conditions. *Atmos. Chem. Phys.*, 18, 9393-9409, 2018, <https://doi.org/10.5194/acp-18-9393-2018>

2017

18. Atmospheric degradation of VOCs: Isoprene and its ozonolysis products, a perfluoro-ketone and long chain ketones (REN Yangang), University of Orleans, 2017.
19. Atmospheric chemistry of NO₃ : reactions with a series of organic and inorganic compounds (Li Zhou), University of Orléans, 2017
20. Chiara Giorio, Anne Monod, Lola Brégonzio-Rozier, Helen Langley DeWitt, Mathieu Cazaunau, Brice Temime-Roussel, Aline Gratien, Vincent Michoud, Edouard Pangui, Sylvain Ravier, Arthur T. Zielinski, Andrea Tapparo, Reinhilde Vermeylen, Magda Claeys, Didier Voisin, Markus Kalberer, and Jean-François Doussin. Cloud Processing of Secondary Organic Aerosol from Isoprene and Methacrolein Photooxidation. *J. Phys. Chem. A*, 121 (40), pp 7641–7654, doi: 10.1021/acs.jpca.7b05933, 2017.
21. Ren, Y. G., Grosselin, B., Daele, V., and Mellouki, A.: Investigation of the reaction of ozone with isoprene, methacrolein and methyl vinyl ketone using the HELIOS chamber, *Faraday Discuss.*, 200, 289-311, 10.1039/c7fd00014f, 2017.
22. Di Biagio, C., Formenti, P., Cazaunau, M., Pangui, E., Marchand, N., and Doussin, J. F.: Aethalometer multiple scattering correction Cref for mineral dust aerosols, *Atmos. Meas. Tech.*, 10, 2923-2939, 10.5194/amt-10-2923-2017, 2017.
23. Kangasluoma, J., Hering, S., Picard, D., Lewis, G., Enroth, J., Korhonen, F., Kulmala, M., Sellegri, K., Attoui, M., and Petaja, T. Characterization of three new condensation particle counters for sub-3 nm particle detection during the Helsinki CPC workshop: the ADI versatile water CPC, TSI 3777 nano enhancer and boosted TSI 3010, *Atmospheric Measurement Techniques*, 10, 2271-2281, 10.5194/amt-10-2271-2017, 2017.
24. Bruggemann, M., Hayeck, N., Bonnineau, C., Pesce, S., Alpert, P. A., Perrier, S., Zuth, C., Hoffmann, T., Chen, J. M., and George, C.: Interfacial photochemistry of biogenic surfactants: a major source of abiotic volatile organic compounds, *Faraday Discuss.*, 200, 59-74, 10.1039/c7fd00022g, 2017.
25. Caponi, L., Formenti, P., Massabo, D., Di Biagio, C., Cazaunau, M., Pangui, E., Chevaillier, S., Landrot, G., Andreae, M. O., Kandler, K., Piketh, S., Saeed, T., Seibert, D., Williams, E., Balkanski, Y., Prati, P., and Doussin, J. F. Spectral- and size-resolved mass absorption efficiency of mineral dust aerosols in the shortwave spectrum: a simulation chamber study, *Atmospheric Chemistry and Physics*, 17, 7175-7191, 10.5194/acp-17-7175-2017, 2017.
26. Duncianu, M., David, M., Kartigeyane, S., Cirtog, M., Doussin, J. F., and Picquet-Varrault, B. Measurement of alkyl and multifunctional organic nitrates by proton-transfer-reaction mass spectrometry, *Atmos. Meas. Tech.*, 10, 1445-1463, 10.5194/amt-10-1445-2017, 2017.

27. Liu, D., Whitehead, J., Alfarra, M. R., Reyes-Villegas, E., Spracklen, D. V., Reddington, C. L., Kong, S., Williams, P. I., Ting, Y.-C., Haslett, S., Taylor, J. W., Flynn, M. J., Morgan, W. T., McFiggans, G., Coe, H., and Allan, J. D. Black-carbon absorption enhancement in the atmosphere determined by particle mixing state, *Nature Geoscience*, advance online publication, doi:10.1038/ngeo2901, 2017.
28. Di Biagio C., P. Formenti, Y. Balkanski, L. Caponi, M. Cazaunau, E. Pangui, E. Journet, S. Nowak, S. C., M. O. Andreae, K. Kandler, T. Saeed, S. Piketh, D. Seibert, E. Williams, and J.-F. Doussin. Global scale variability of the mineral dust longwave refractive index: a new dataset of in situ measurements for climate modelling and remote sensing, *Atmospheric Chemistry and Physics*, 17, 3, pp:1901-1929; 2017.
29. Onel L., Brennan A., Gianella M., Ronnie G., Lawry Aguila A., Hancock G., Whalley Lisa, Seakins P.W., Ritchie G. A. D., Heard D. E., An intercomparison of HO₂ measurements by fluorescence assay by gas expansion and cavity ring-down spectroscopy within HIRAC (Highly Instrumented Reactor for Atmospheric Chemistry), *Atmospheric Chemistry Techniques*, <https://doi.org/10.5194/amt-10-4877-2017>; 2017.
30. Allison E. Reed Harris, Mathieu Cazaunau, Aline Gratien, Edouard Pangui, Jean-François Doussin, and Veronica Vaida. ; Atmospheric Simulation Chamber Studies of the Gas-Phase Photolysis of Pyruvic Acid. *The Journal of Physical Chemistry A* 2017 121 (44), 8348-8358, DOI: 10.1021/acs.jpca.7b05139

Oral presentations in an international conference

1. Di Biagio, C., P. Formenti, Y. Balkanski, L. Caponi, M. Cazaunau, E. Pangui, E. Journet, S. Nowak, S. Caquineau, M. Andreae, K. Kandler, T. Saeed, S. Piketh, D. Seibert, E. Williams, and J.-F. Doussin, Global scale variability of the mineral dust shortwave and longwave refractive index: a new dataset of in situ measurements for climate modelling and remote sensing, 2018 Joint 14th iCACGP Symposium and 15th IGAC Science Conference, 25-29 September 2018, Takamatsu, Kagawa, Japan.
2. David M. Bell, Veronika Pospisilova, Amelie Bertrand, Houssni Lamkaddam, Chuan Ping Lee, Ruby Marten, Jay G. Slowik, Andre S.H. Prévôt, Urs Baltensperger, Imad El Haddad, Josef Dommen, Probing the Molecular Composition of Model Systems and Secondary Organic Aerosol during Evaporation, International Aerosol Conference 2018, 2-7 September 2018, St. Louis, USA.
3. Newland, M., G. Rea, J. Wenger, I. Barnes, A. R. Rickard, The photolysis mechanism of monoaromatic ring opening products – unsaturated 1,4 dicarbonyls – from chamber experiments, 25th International Symposium on Gas Kinetics & Related Phenomena, 22-26 July 2018, Lille, France.

4. Di Biagio, C., P. Formenti, Y. Balkanski, L. Caponi, M. Cazaunau, E. Panguì, E. Journet, S. Nowak, S. Caquineau, M. Andreae, K. Kandler, T. Saeed, S. Piketh, D. Seibert, E. Williams, and J.-F. Doussin, Global scale variability of the mineral dust shortwave and longwave refractive index from laboratory chamber experiments, 9th International Workshop on Sand/Duststorms and Associated Dustfall, 22-24 May 2018, Tenerife, Spain.
5. Formenti, P., The ageing of African mineral dust during transport, 9th International Workshop on Sand/Duststorms and Associated Dustfall, 22-24 May 2018, Tenerife, Spain.
6. Di Biagio, C., P. Formenti, L. Caponi, M. Cazaunau, E. Panguì, E. Journet, S. Nowak, S. Caquineau, M. Andreae, K. Kandler, T. Saeed, S. Piketh, D. Seibert, E. Williams, Y. Balkanski, and J.-F. Doussin, Laboratory estimate of the regional shortwave refractive index and single scattering albedo of mineral dust from major sources worldwide, EGU General Assembly, 8-12 April 2018, Wien, Austria.
7. Coll P., Lanone S., Zysman M., Cazaunau M., Doussin J.-F., Derumeaux G., Pini M., Gratien A., Panguì E., Hüe S., Relaix F., Der Vartanian A., Coll I., Foret G., Thavaratnasingam L., Amar A., Mäder M. and Boczkowski J., Pollu-Risk : une plateforme expérimentale innovante pour étudier les impacts sanitaires de la qualité de l'air, colloque francophone de COMbustion et POLLution Atmosphérique, april 2018, Ouarzazate, Maroc.
8. M. Ródenas, C. Gimeno, E. Borrás, T. Vera, T. Gómez, A. Muñoz: Characterizing air quality in different urban sites: Tunnel and school, 11th International Conference on Air Quality Science and Application, 12-16 March 2018, Barcelona, Spain
9. Coll P., Lanone S., Zysman M., Cazaunau M., Doussin J.-F., Derumeaux G., Pini M., Gratien A., Panguì E., Hüe S., Relaix F., Der Vartanian A., Coll I., Foret G., Thavaratnasingam L., Amar A., Mäder M. and Boczkowski J., Pollu-Risk: an innovative experimental platform to study the health impacts of air quality, Air Pollution 2018, june 2018, Naples, Italy
10. Fouqueau A., Cirtog M., Cazaunau M., Panguì E., Doussin J.-F., Picquet-Varrault B. ; Reactivity of γ -terpinene and α -terpinene with NO₃ radical : a comparative kinetic and mechanistic study; 25th Symposium on Gas Kinetics and Related Phenomena, july 2018, Lille, France.
11. Fuchs H., A. Novelli, M. Rolletter, M. Kaminski, Radical concentrations during the oxidation of biogenic VOCs investigated in the atmospheric simulation chamber SAPHIR, Telluride meeting on "Gas phase Atmospheric Chemistry", 23-27 July 2018, Telluride, USA
12. A. Hofzumahaus, Atmospheric Simulation Chamber Experiments: Bridging the Gap Between Laboratory and Field Studies", 25th International Symposium on Gas Kinetics and Related Phenomena, 22-26 July 2018, Lille, France

13. Zysman M., Franco-Montoya M.-L., Der Vartanian A., Cazaunau M., Pini M., Doussin J.-F., Ridoux A., Hüe S., Relaix F., Derumeaux G., Boczkowski J., Coll P. and Lanone S, Atmospheric simulation chamber: a versatile tool to get a comprehensive understanding of Air Quality impacts on Health, ERS International Congress, september 2018, Paris, France
14. Danelli S. G., Massabò D., Gatta E., Parodi F., Comite A., Corno G., Costa C., Di Cesare A., Oliva M., Vezzulli L., Prati P., Bioaerosol Investigation: New Experimental Activity in Chambre, an Atmospheric Simulation Chamber, International Aerosol Conference 2018, Americas Center, St. Louis, Missouri, USA, 2-7 September, 2018.
15. Bejan, I., Barnes, I., Wiesen, P., Kourtchev, I., Wenger, J., Products and Mechanisms for the Atmospheric Oxidation of Dimethylbenzoquinones, The 25th International Symposium on Gas Kinetics and Related Phenomena, pp. 167, Lille, Franța, 22- 26 July 2018.
16. Herrmann, H., Schindelka, J., Mutzel, A., Poulain, L., Berndt, T., Böge, O., Tilgner, A. and Van Pinxteren, D., Aerosol particle organic mass formation: HOMs uptake and cloud processing, in 'International Conference on Aerosol Cycle Sources - Aging - Sinks - Impacts', 21-23 March, University of Lille, France.
17. Herrmann, H., Atmospheric multiphase chemistry: Developments up to now, current work and future directions, in '4th International Workshop on Heterogeneous Kinetics Related to Atmospheric Aerosols', 23-24 September 2018, Takamatsu, Japan.
18. Oesterstroem, F, Seakins, P, Heard, D et al. Kinetic Study of the $\text{CH}_3\text{O}_2 + \text{HO}_2$ Cross-reaction in the Highly Instrumented Reactor for Atmospheric Chemistry in 25th International Symposium on Gas Kinetics, 22nd - 26th July 2018, Lille, France.
19. Herrmann, H., Atmospheric multiphase chemistry: What could be important in China?, in 'Sino-French Joint Workshop on Atmospheric Environment', 10-12 September 2018, Orleans, France.
20. Herrmann, H., Multiphase chemistry and air pollution-related studies of TROPOS-ACD, in 'Bridging Aerosol Chemistry and Health Effects: Challenges and Opportunities for Analytical Chemistry', 19-23 March, Guangzhou, China.
21. Herrmann, H., Recent studies on tropospheric multiphase chemistry: Impact on SOA, 16-18 March 2018, Hong Kong, China.
22. Herrmann, H., Schindelka, J., Mutzel, A., Berndt, T., Böge, O., Tilgner, A., Poulain, L., Van Pinxteren, D. and team, H.-. Multiphase Chemistry Contributions to SOA Formation, in 'Towards a Molecular Understanding of Atmospheric Aerosols', 27-31 August 2018, Bad Honnef, Germany.

23. Di Biagio, C., P. Formenti, Y. Balkanski, L. Caponi, M. Cazaunau, E. Panguì, E. Journet, S. Nowak, S. Caquineau, M. O. Andreae, K. Kandler, T. Saeed, S. Piketh, D. Seibert, E. Williams, O. Boucher, and J.-F. Doussin, Global scale variability of the mineral dust longwave refractive index from laboratory chamber experiments: re-evaluation of its direct radiative effect, AGU General Assembly 2017, 11-15 December 2017, New Orleans, USA.
24. Di Biagio, C., P. Formenti, Y. Balkanski, L. Caponi, M. Cazaunau, E. Panguì, E. Journet, S. Nowak, S. Caquineau, M. O. Andreae, K. Kandler, T. Saeed, S. Piketh, D. Seibert, E. Williams, O. Boucher, and J.-F. Doussin, Re-evaluation of the global dust longwave direct radiative effect from laboratory estimates of the refractive index and model simulations, Goldschmidt 2017, 13-17 August 2017, Paris, France.
25. Albrecht S., A. Novelli, A. Hofzumahaus, S. Kang, Y. Baker, T. Mentel, A. Wahner, H. Fuchs, HO₂ measurements at atmospheric concentrations using a chemical ionization mass spectrometry, oral presentation, AGU General Assembly 2017, 11-15 December 2017, New Orleans, USA.
26. Borrás, E., Vera, T., Ródenas, M., Gómez, T., and Muñoz, A.: Ozone and secondary organic aerosol production by interaction between pesticides and biogenic VOCs. 7th International Conference on Pesticide Behaviour in Soils, Water and Air. 30 August-1 September 2017. York, UK.
27. Herrmann, H., Schindelka, J., Mutzel, A., Poulain, L., Berndt, T., Böge, O., Otto, T., Tilgner, A., and van Pinxteren, D., Aerosol particle organic mass formation: HOMs uptake, multiphase isoprene oxidation and cloud processing, Seminar at NOAA Earth System Research Laboratory-Chemical Science Division, 09 August 2017, Boulder, USA.
28. Herrmann, H., Otto, T., Felber, T., Mutzel, A., Berndt, T., Böge, O., Poulain, L., Tilgner, A., Van Pinxteren, D. and Schindelka, J., Tropospheric Multiphase Chemistry: Gas Phase HOMs Formation, Aqueous Phase Isoprene Oxidation Products and Real Cloud Chemistry, in 'Atmospheric Chemical and Biological Processes: Interactions and Impacts (ATMOCHEMBIO)', 19-21 June 2017, Clermont-Ferrand, France.
29. Herrmann, H., Schindelka, J., Mutzel, A., Berndt, T., Böge, O., Tilgner, A., Poulain, L. and Van Pinxteren, D., Tropospheric aerosol particle organic mass formation: HOMs uptake and cloud processing, in '254th American Chemical Society, Fall National Meeting & Exposition', 20-24 August 2017, Washington, DC, USA.
30. Ródenas, M., Muñoz, A., and EUPHORE Team: The EUPHORE chambers: a shared research platform to study atmospheric processes - 20 years of international cooperation. EGU General Assembly. ENVRI. 23-28 April 2017. Vienna, Austria.
31. Borrás, E., Vera, T., Ródenas, M., and Muñoz, A.: Ozone and secondary organic aerosol production by interaction between an organophosphorous pesticide and a biogenic VOCs mixture. EGU General Assembly 2017. April 23-28 Vienna, Austria.

32. Prati P., Gatta E., Brotto P., Massabò D., Parodi F., Comite A., Costa C., Doussin J.F., Formenti P., Characterization of the ChAMBRe atmospheric simulation chamber, European Aerosol Conference 2017, Zurich, Switzerland, Aug 27, - Sep. 1, 2017.

Oral presentations in a national conference

1. Doussin J.-F. ; Processus de transformations intra-particulaires affectant la composition et les propriétés de l'aérosol atmosphérique; GDR EMIE-suie meeting, may 2018, Lille, France.
2. Mettke, P., Mutzel, A., Boge, O., Herrmann, H., Atmosphärische Multiphasenchemie von Oxidationsprodukten des Isoprens, Umwelt 2018, Munster, Germany, 9-12 September 2018.
3. Coll P., Lanone S., Zysman M., Cazaunau M., Doussin J.-F., Derumeaux G., Pini M., Gratien A., Pangui P., Hüe S., Relaix F., Der Vartanian A., Coll I., Foret G., Thavaratnasingam L., Amar A., Mäder M. and Boczkowski J., Pollu-Risk : une plateforme expérimentale innovante pour étudier les impacts sanitaires de la qualité de l'air, colloque Atmos'Fair, june 2018, Paris, France.
4. Di Biagio, C., P. Formenti, Y. Balkanski, M. Cazaunau, E. Pangui, E. Journet, S. Nowak, S. Caquineau, and J.-F. Doussin, Laboratory estimates of the mineral dust shortwave and longwave refractive index from global sources: a new dataset for climate modelling and remote sensing, Journée Scientifique SIRTa 2018, 15 June 2018, Palaiseau, France, 2018.
5. Herrmann, H., Atmospheric multiphase SOA formation: Isoprene oxidation and cloud processing, in 'Seminar of the Joint Mass Spectrometry Centre and the Virtual Helmholtz Institute HICE-Aerosol and Health: Winter term 2017/2018', 23 January 2018, IOW Rostock, Germany.
6. Danelli S. G., Massabò D., Gatta E., Parodi F., Comite A., Corno G., Costa C., Di Cesare A., Oliva M., Vezzulli L., Prati P., ChAMBRe: studi su bio-aerosol in camera di simulazione atmosferica, VIII Convegno Nazionale sul Particolato Atmosferico (PM2018), Italian Aerosol Society (IAS), Matera, Italy, 22-25 May, 2018.
7. Prati P., Danelli S. G., Massabò D., Parodi F., EUROCHAMP2020 e la camera di simulazione atmosferica ChAMBRe, VIII Convegno Nazionale sul Particolato Atmosferico (PM2018), Italian Aerosol Society (IAS), Matera, Italy, 22-25 May, 2018.
8. Danelli S. G., Massabò D., Gatta E., Parodi F., Comite A., Corno G., Costa C., Di Cesare A., Oliva M., Vezzulli L., Prati P., Experimental activity in ChAMBRe, a new atmospheric simulation chamber, XVII Congresso Nazionale di Chimica dell'Ambiente e dei Beni Culturali, Genova, Italy, 24-27 June, 2018.
9. Danelli S.G., Massabò D., Brotto P., Comite A., Costa C., Di Cesare A., Doussin J.F., Ferraro F., Formenti P., Gatta E., Negretti L., Oliva M., Parodi F., Vezzulli L., Prati P., Studi su bio-aerosol in ChAMBRe, una nuova camera di simulazione atmosferica, 104° Congresso Nazionale della Società Italiana di Fisica, Arcavacata di Rende - Cosenza, Italy, 17 -21 September, 2018.

10. M. Ródenas, A. Muñoz and EUPHORE Team: Air pollution treatment in European urban environments by means of photocatalytic textiles. LIFE MINOX STREET final meeting. 21 March 2018, Madrid, Spain.
11. Cecilia Arsene, C., Olariu, R.I., AI-FORECAST project (PN-III-P4-ID-PCE-2016-0299) between prediction of the aerosol chemical composition and integration of Cernesim's infrastructure in a European context, The XXXV-th Romanian Chemistry Conference, Posters Section, Calimanesti-Caciulata, Valcea, Romania, 02-05 October 2018.
12. Roman, C., Arsene, C., Bejan, I.G., Duncianu, M., Tomas, A., Riffault, V., Olariu, R.I., Rate coefficient of gas-phase O₃ initiated oxidation of C₅-C₆ unsaturated aldehydes, The 9th Scientific Session of Undergraduate, Master and PhD Students, Iasi, Romania Book of Abstracts, pp. 9, communication, 29-30 June, 2018.
13. Rickard, A., "The Master Chemical Mechanism – Strategy for the development of detailed chemical mechanisms", York-Durham Symposium on "Mechanism-Driven Understanding in Complex Molecular Systems", University of Durham, 18th May 2017.
14. Fouqueau A., Cirtog M., Cazaunau M., Pangui E., Doussin J.-F., Picquet-Varrault B. ; Réactivité des composés organiques volatils biogéniques avec le radical NO₃ : étude cinétique et mécanistique par approche expérimentale ; Colloque annuel du GFCP, june 2017, Douai, France.
15. Brotto P., Gatta E., Massabò D., Parodi F., Prati P., Exploring the feasibility of aerosol and bio-aerosol studies by the ChAMBRé atmospheric simulation chamber, 103° Congresso Nazionale della Società Italiana di Fisica, Trento, Italy, 11-15 September, 2017.
16. Petrea-Ioneasa, M, Bejan, I.G., Olariu, R.I., Arsene, C., Gas-Phase Kinetic Study of OH Radical Reactions with Selected Saturated Ketones, 20th Romanian International Conference on Chemistry and Chemical Engineering (RICCCE), Poiana Braşov, România, 6-9 September 2017.
17. Olariu, R.I., Roman, C., Bejan, I.G., Arsene, C., ESC-Q-UAIC chamber, a proper analytical tool for the estimation of infrared absorption cross sections for selected volatile organic compounds in the gas phase, 20th Romanian International Conference on Chemistry and Chemical Engineering (RICCCE), Poiana Braşov, România, 6-9 September 2017.
18. Bejan, I.G., Olariu, R.I., Barnes, I., Wiesen, P., Atmospheric Chemistry of Catechol. Product Studies and Mechanistic Investigations, 20th Romanian International Conference on Chemistry and Chemical Engineering (RICCCE), Poiana Braşov, România, 6-9 September 2017.

Poster in an international conference

1. Lamkaddam H., Gratien A. , Pangui E. , Cazaunau M. ,David M., J-M Polienor, M. Jerome, C. Gaimoz, B. Picquet-Varrault, J-F Doussin, Analysis of gas-phase and particulate reaction products from high-NO_x photooxidation of n-dodecane: Influence of temperature and relative humidity on secondary organic aerosol formation, 10th International Aerosol Conference (IAC 2018), September 2-7, 2018, St. Louis, Missouri, USA, 2018.
2. Fuchs H., S. Andres, B. Bohn, H.-P. Dorn, R. Haeseler, A. Hofzumahaus, F. Holland, X. Li, M. Kaminski, A. Novelli, F. Rohrer, R. Tillmann, R. Wegener, A. Wahner: Investigation of the oxidation of methyl vinyl ketone (MVK) by OH radicals in the atmospheric simulation chamber SAPHIR, 2018 Joint 14th iCACGP Symposium and 15th IGAC Science Conference, 25-29 September 2018, Takamatsu, Kagawa, Japan.
3. Novelli A., B. Bohn, H.-P. Dorn A. Hofzumahaus, F. Holland, X. Li, M. Kaminski, Z. Yu, S. Rosanka, D. Taraborelli, L. Vereecken, F. Rohrer, R. Tillmann, R. Wegener, A. Kiendler-Scharr, A. Wahner and H. Fuchs: Investigation of OH regeneration from isoprene oxidation across different NO_x regimes in the atmosphere simulation chamber SAPHIR, 2018 Joint 14th iCACGP Symposium and 15th IGAC Science Conference, 25-29 September 2018, Takamatsu, Kagawa, Japan.
4. Brauer, P., C. Mouchel-Vallon, M. Newland, K. Murphy, B. Aumont, R. Valorso, M. Camredon, S. Madronich, M. Jenkin, M. Evans, A. R. Rickard, The MAGNIFY project – Updated protocols for ozonolysis and photolysis of organic compounds, 2018 Joint 14th iCACGP Symposium and 15th IGAC Science Conference, 25-29 September 2018, Takamatsu, Kagawa, Japan.
5. Gratien A. , Lamkaddam H., Pangui E. , Cazaunau M. ,David M., J-M Polienor, M. Jerome, C. Gaimoz, B. Picquet-Varrault, J-F Doussin, Analysis of gas-phase and particulate reaction products from high-NO_x photooxidation of n-dodecane: Influence of temperature and relative humidity on secondary organic aerosol formation, 25th Symposium on Gas Kinetics and Related Phenomena, July 2018, Lille, France.
6. Rayez M.-T., Cirtog M., Rayez J.-C., Duncianu M., Fouqueau A., Picquet-Varrault B. ; Reactivity of NO₃ radical with unsaturated aldehydes and terpenes : Theoretical approach for kinetic and mechanistic studies ; 25th Symposium on Gas Kinetics and Related Phenomena, July 2018, Lille, France.
7. Rickard, A. R., M. Newland, P. Brauer, M. Evans, K. Murphy, B. Aumont, R. Valorso, M. Camredon, C. Mouchel-Vallon, S. Madronich, M. Jenkin, Mechanisms for Atmospheric chemistry: GeneratioN, Interpretation and FidelitY – MAGNIFY, 25th International Symposium on Gas Kinetics & Related Phenomena, 22-26 July 2018, Lille, France.

8. Brauer, P., D. Ellis, C. Mouchel-Vallon, M. Newland, K. Murphy, B. Aumont, R. Valorso, M. Camredon, S. Madronich, M. Jenkin, M. Evans, A. R. Rickard, MAGNIFY – Mechanisms for Atmospheric Chemistry: Generation, Interpretation and Fidelity. Royal Meteorological Society Atmospheric Science Conference 2018: Weather, Climate and Air Quality, 3-4 July 2018, York, UK.
9. Chaput, A., King, J., Formenti, P., Di Biagio, C., Chevallier, S., Nowak, S., Pangui, E., Cazaunau, M., Gauvin-Bourdon, P., J-F, Doussin, Wind partitioning in the coast of the namibian desert, International Conference on Aeolian Research (ICARX), 25–29 June 2018, Bordeaux, France, 2018.
10. Oliva M., Danelli S. G., Massabò D., Comite A., Costa C., Di Cesare A., Gatta E., Parodi F., Vezzulli L., Prati P., An atmospheric simulation chamber to investigate dust-borne microbiota composition and viability. DUST 2018, 3rd International Conference on Atmospheric Dust, Bari, Italy, May 29-31, 2018.
11. Roman, C., Arsene ,C., Olariu, R.I., Bejan, I., Gas phase kinetic study of the OH radical initiated oxidation of alkylfurans at atmospheric pressure and 298 ± 2 K., The 25th International Symposium on Gas Kinetics and Related Phenomena, pp. 167, Lille, Franța, 22- 26 July 2018.
12. Brennan, A, Heard, D.E, Seakins, P.W. An inter-comparison of FAGE and CRDS for the detection of HO₂ and CH₃O₂ radicals in a simulation chamber, at 25th International Symposium on Gas Kinetics, 22-26th July 2018, Lille, France.
13. Roman, C., Arsene, C., Bejan, I.G., Olariu, R.I., Temperature dependence kinetic studies by using the newly thermostated ESC-Q-UAIC chamber, The 25th International Symposium on Gas Kinetics and Related Phenomena, pp. 167, Lille, Franța, 22- 26 July 2018.
14. Ródenas, M., Fages, E., Fatarella, E., Herrero, D., Castagnoli, L., Borrás, E., Vera, T., Gómez, T., Catota, M., Carreño, J., Hernández, D., Gimeno, C., López, R., and Muñoz, A.: Can TiO₂-based photocatalytic textiles be used to improve the urban airquality? EGU General Assembly. 23-28 April 2017. Vienna, Austria.
15. Di Biagio, C., P. Formenti, L. Caponi, M. Cazaunau, E. Pangui, E. Journet, S. Nowak, S. Caquineau, M. O. Andreae, K. Kandler, T. Saeed, S. Piketh, D. Seibert, E. Williams, Y. Balkanski, and J.-F. Doussin, Laboratory estimate of the regional shortwave refractive index and single scattering albedo of mineral dust from major sources worldwide, AGU General Assembly 2017, 11-15 December 2017, New Orleans, USA, 2017.
16. Vera, T., Borrás, E., Ródenas, M., Gómez, T., and Muñoz, A., 2017. Atmospheric degradation of thiocarbamate herbicides under atmospheric conditions. 7th International Conference on Pesticide Behaviour in Soils, Water and Air. 30 August-1 September 2017. York, UK.

17. Massabò D., Gatta E., Brotto P. and Prati P., Exploring the feasibility of aerosol and bio-aerosol studies by the ChAMBRé atmospheric simulation chamber, International conference on ATMOSpheric CHEMical and BIOlogical processes: interactions and impacts (ATMOCHEMBIO) Conference, Clermont-Ferrand, France, June 19-21, 2017.
18. Ródenas, M., Hernández, D., Gómez, T., López, R., and Muñoz, A., 2017. Urban air quality measurements using a sensor-based system. EGU General Assembly, 23-28 April 2017, Vienna, Austria.
19. Muñoz, A., Ródenas, M., Borrás, E., Vera, T., and Calatayud, V.: Use of the European Photo-Reactor (EUPHORE) for testing the depolluting capacity of representative combinations of urban vegetation. Green Infrastructure: Nature Based Solutions for Sustainable and Resilient Cities: 4-7 April 2017, Orvieto, Italy.
20. Borrás, E., Ródenas, M., Vera, T., and Muñoz, A.: Particulate matter formation from photochemical degradation of currently used herbicides. International Conference on Aerosol Cycle Sources. Aging-sinks-Impact (ICAC 2017), 21-23 March 2017, Lille, France.
21. Borrás, E., Ródenas, M., Vera, T., and Muñoz, A.: Secondary organic aerosol production by interaction between an organophosphorous pesticide and biogenic vocs mixtures. International Conference on Aerosol Cycle Sources. Aging-sinks-Impact (ICAC 2017), 21-23 March 2017, Lille, France.
22. M. Ródenas, E. Borrás, T. Vera, T. Gómez, M. Catota, D. Hernández, A. Muñoz: Removal of nitrogen oxides and other gas-phase organic pollutants by using photocatalytic textiles. Simulations performed at the EUPHORE chambers, 3rd ACTRIS-2 General Meeting, 1-2 February 2017. Granada, Spain.
23. Borrás, E., Ródenas, M., Gimeno, C., Vera, T., Gómez, T., Hernández, D., Salazar, M., and Muñoz, A.: Comparison of gaseous inorganic and organic pollutants trends in the presence and in the absence of photocatalytic textiles at urban locations. Active and passive campaigns. 3rd ACTRIS-2 General Meeting. 1-2 February 2017. Granada, Spain.
24. Muñoz, A., Borrás, E., Ródenas, M., Vera, T., and Pedersen, H. A.: Atmospheric degradation of thiocarbamate herbicides under atmospheric conditions. 3rd ACTRIS-2 General Meeting, 1-2 February 2017. Granada, Spain.
25. Olariu R.I., Marin S. L., Roman C., Bejan I.G., Arsene C., Gas-phase kinetic study of OH radical reactions with selected alkylaromatic compounds, Atmospheric Chemical and Biological Processes: Interactions and Impacts (ATMOCHEMBIO), Clermont-Ferrand, Franța, 19-21 Iunie, 2017.

Poster in a national conference

1. P. Formenti, C. Di Biagio, Y. Balkanski and J.-F. Doussin, Atmospheric simulation study of the optical properties of desert aerosols and their modifications during the life cycle, Colloque de Bilan et de Prospective du programme LEFE, 28-30 Mars 2018, Clermont-Ferrand, France.
2. Cirtog M., A. Fouqueau, M. Cazaunau, E. Pangui, X. Landsheere, P. Zapf, G. Siour, M-T. Rayez, J-C. Rayez, J-F. Doussin, B. Picquet-Varrault ; Reactivity of NO₃ radicals with BVOC in the atmosphere : experimental and theoretical approach for kinetic and mechanistic study ; Colloque de Bilan et de Prospective du programme LEFE, 28-30 Mars 2018, Clermont-Ferrand, France.
3. Gratien A., H. Lamkaddam, E. Pangui, M. Cazaunau, C. Gaimoz, J-M. Polienor, S. La, M. Camredon, B. Aumont, J-F. Doussin, Atmospheric oxidation of n-dodecane: fundamental studies and parameterization of SOA formation (Dodec-AOS), Colloque de Bilan et de Prospective du programme LEFE, 28-30 Mars 2018, Clermont-Ferrand, France.
4. Galon (Negru), A.G., Olariu, R.I., Arsene, C., Investigation on new atmospheric particles formation and growth in Iasi, north-eastern Romania, The XXXV-th Romanian Chemistry Conference, Posters Section, Calimanesti-Caciulata, Valcea, Romania, 02-05 October 2018.
5. Roman, C., Arsene, C., Bejan I.G., Olariu R.I., Rate coefficient of the gas-phase atmospheric OH radical initiated oxidation of 2-methoxyphenol, The XXXV-th Romanian Chemistry Conference, Posters Section, Calimanesti-Caciulata, Valcea, Romania, 02-05 October, 2018.
6. Roman, C., Arsene, C., Olariu, R.I., Bejan, I.G., Kinetic study of the gas-phase oh radical initiated oxidation of 2-methylfuran in atmospheric conditions, The XXXV-th Romanian Chemistry Conference, Posters Section, Calimanesti-Caciulata, Valcea, Romania, 02-05 October, 2018.
7. Rusu, A.M., Roman, C., Arsene, C., Bejan, I.G., Olariu, R.I., Gas chromatography-mass spectrometry (GC-MS) analysis of gaseous methylglyoxal after derivatization and solid phase extraction, The XXXV-th Romanian Chemistry Conference, Posters Section, Calimanesti-Caciulata, Valcea, Romania, 02-05 October, 2018.
8. Rusu, A.M., Arsene, C., Bejan, I.G., Olariu, R.I., Development of a new method for carbonyls analysis in the atmosphere by using solid phase derivatization coupled with GC/Ion Trap MS technique, The 9th Scientific Session of Undergraduate, Master and PhD Students, Poster Section, Iasi, Romania Book of Abstracts, pp. 37, 29-30 June, 2018.
9. Roman, C., Arsene ,C., Olariu, R.I., Bejan, I., Rate coefficient of the gas-phase OH initiated oxidation of 2,5-dimethylfuran at 298±2 K, The 9th Scientific Session of Undergraduate, Master and PhD Students, Poster Section, Iasi, Romania Book of Abstracts, pp. 37, 29-30 June, 2018.
10. Roman, C., Arsene, C., Bejan, I.G., Olariu, R.I., FT-IR gas-phase products study of OH radicals initiated photooxidation of phenol, Abstracts for Faculty of Chemistry Conference , 25 (2), pp. 325, poster, Iasi, Romania, 26-28 October, 2017.

11. Coll P., Cazaunau M., Franco-Montoya M.-L., Mäder M., Ridoux A., Pangui E., Zysman M., Appan L., Colin de Verdière S., Doussin J.-F., Gratien A., J. Boczkowski J. and Lanone S., POLLURISK - A pollution platform to evaluate health effects of complex atmospheres, Joint INSERM/JSPS (Japan Society for the Promotion of Science) meeting. Paris, France, 2017.
12. Roman, C., Bejan, I.G., Arsene, C., Olariu, R.I., Gas-Phase FT-IR Kinetic Study of the OH Radicals with Phenol, The 8th Scientific Session of Undergraduate, Master and PhD Students (SCSSMD), Poster Section, 25 (1), pp. 103, Iasi, Romania, 30 Iunie, 2017

PhD thesis

1. Fouqueau A. : Réactivité des terpènes avec le radical nitrate: étude expérimentale cinétique et mécanistique en chambre de simulation, University of Paris-East at Créteil, in progress.
2. S. Danelli: Correlation between bacteria viability and air quality: systematic studies by an atmospheric simulation chamber, University of Genoa, in progress.
3. V. Vernocchi: Interaction between airborne nanoparticles and electromagnetic radiation: investigation of possible climatological effects by an atmospheric simulation chamber, University of Genoa, in progress.

Master thesis

1. Amar A. ; Qualité de l'Air et Impacts sanitaires : Etudes d'impacts de la pollution atmosphérique en phase gazeuse et particulaire, University of Paris Diderot, june 2018.
2. Dufresnes M. ; Caractérisation de CESAM dans le cadre du projet EUROCHAMP 2020, University of Paris-East at Créteil, june 2018.
3. Castellano, J.C. : Smart Sensor: Mejora de un prototipo de bajo consume y largo alcance para la medición de contaminantes atmosféricos. U. Valencia. September, 2018



Integration of European Simulation Chambers for Investigating Atmospheric Processes. Towards 2020 and beyond